REPUBLIC OF TURKİYE
ADANA ALPARSLAN TÜRKEŞ SCIENCE AND TECHNOLOGY UNIVERSITY

GRADUATE SCHOOL
ELECTRICAL AND ELECTRONIC ENGINEERING DEPARTMENT

DESIGN AND ANALYSIS OF ACTIVE DISTURBANCE REJECTION CONTROL TECHNIQUES WITH EXPERIMENTAL APPLICATIONS

DEHA EKER

M.Sc.

ADANA 2023

REPUBLIC OF TURKİYE
ADANA ALPARSLAN TÜRKEŞ SCIENCE AND TECHNOLOGY UNIVERSITY

GRADUATE SCHOOL
ELECTRICAL AND ELECTRONIC ENGINEERING DEPARTMENT

DESIGN AND ANALYSIS OF ACTIVE DISTURBANCE REJECTION CONTROL TECHNIQUES WITH EXPERIMENTAL APPLICATIONS

DEHA EKER

M.Sc.

THESIS ADVISOR
ASSOC. PROF. DR. NECDET SİNAN ÖZBEK

ADANA, 2023

DECLARATION OF CONFORMITY

In this thesis study, which was prepared following the thesis writing rules of Adana Alparslan Türkeş Science and Technology University Institute of Graduate School, I declare that I provide all the information, documents, evaluations and results in accordance with scientific ethics and moral codes without resorting to any means or assistance that would be contrary to scientific ethics and traditions. I also declare that I refer to all of the articles I used in this study with appropriate references and accept all moral and legal consequences if a situation is found contrary to my statement regarding my work.

21/12/2023

[Signature]

Deha EKER

ÖZET

DENEYSEL UYGULAMALAR İLE AKTİF BOZUCU BASTIRMA KONTROL TEKNİKLERİNİN TASARIMI VE ANALİZİ

Deha EKER

Yüksek Lisans, Elektrik-Elektronik Mühendisliği Anabilim Dalı

Danışman: Doçent Dr. Necdet Sinan ÖZBEK

Aralık 2023, 96 sayfa

Bu tez, bir dizi deneysel uygulama ile aktif bozucu bastırma kontrol tekniklerinin tasarımını ve analizini incelemeyi amaçlamaktadır. Bu çalışmanın temel amacı, çeşitli ileri kontrol stratejilerinin gerçek dünya senaryolarında nasıl etkin bir şekilde uygulanabileceğini ve performanslarının nasıl sistematik bir şekilde değerlendirilebileceğini keşfetmektir. Tez, aktif bozucu bastırma yöntemlerinin geliştirilmesi ve deneysel doğrulama sürecini ayrıntılı bir şekilde incelemektedir. Bu yöntemlerin pratik kullanılabilirliğini ve etkinliğini anlamak için detaylı bir şekilde tasarım, parametre ayarlama ve farklı senaryolarda test edilmesi planlanmıştır. Deney platformu olarak endüstriyel uygulamalarda sayısız alanda kullanılan elektromekanik sistem seçilmiştir. Sistemin matematiksel ve parametrik modeli gerçek zamanlı sistem tanılama deneyleri ile elde edilmiştir.

Bu araştırmanın temel katkılarından biri, endüstriyel süreçlerde doğrusal aktif bozucu bastırma kontrolünün uygulanabilirliği ve etkinliği hakkında aydınlatıcı bilgiler sunmasıdır. Çalışma, değerlendirme için çeşitli performans metriklerini kullanılarak, geçici durum performansının ve sürekli durum hatalarının incelenmesine odaklanmıştır.

Bu tezin önemli bir diğer yönü, kesir dereceli doğrusal bozucu bastırma yöntemlerinin tanıtılması ve deneysel doğrulamasını içermesidir. Bu yenilikçi yaklaşım ve deneysel doğrulama, bilgi sınırlarını genişletmekte ve mühendislik uygulamaları ile kontrol sistemlerinin geliştirilmesine katkıda bulunmaktadır. Sonuç olarak, bu yüksek lisans tezi, mühendislik uygulamaları ve kontrol sistemleri alanındaki gelişmiş bir araştırma çabasını temsil etmektedir.

Anahtar Kelimeler:. Gözleyici Tabanlı Kontrol, Aktif Bozucu Bastırma Kontrolü, Lineer Aktif Bozucu Bastırma Kontrolü, Dahili Model Kontrolü

ABSTRACT

DESIGN AND ANALYSIS OF ACTIVE DISTURBANCE REJECTION CONTROL TECHNIQUES WITH EXPERIMENTAL APPLICATIONS

Deha EKER

M.Sc., Department of Electrical and Electronic Engineering
Supervisor: Assoc. Prof. Dr. Necdet Sinan ÖZBEK

December 2023, 96 pages

This thesis is intended to explore the design and analysis of active disturbance rejection control techniques through a series of experimental applications. The fundamental objective of this study is to investigate how various advanced control strategies can be effectively applied in real-world scenarios and how their performances can be systematically assessed. The thesis meticulously examines the development and experimental validation process of active disturbance rejection methods. The practical utility and effectiveness of these methods are planned to be comprehensively understood through detailed design, parameter tuning, and testing in various scenarios. As the experimental platform, electromechanical system has been chosen which is widely used in numerous industrial applications. The mathematical and parametric model of the system has been obtained through real-time system identification experiments.

One of the primary contributions of this research is to provide enlightening insights into the applicability and effectiveness of linear active disturbance rejection control in industrial processes. The study is focused on the examination of transient state performance and steady-state errors, employing various performance metrics for evaluation.

Another significant aspect of this thesis is the introduction and experimental validation of fractional-order linear disturbance rejection methods. This innovative approach and its experimental verification are expected to expand the boundaries of knowledge and contribute to the improvement of engineering applications and control systems. In conclusion, this master thesis represents an advanced research endeavor in the field of engineering applications and control systems.

Keywords: Active Disturbance Rejection Control, Internal Model Control, Linear Active Disturbance Rejection Control, Observer-Based Control.

Dedication

This thesis is dedicated to my beloved parents, who have been my source of inspiration, continually provide moral, emotional, and financial support.
To my love who have been always there for me when I was struggled.

ACKNOWLEDGMENTS

I would like to thank my supervisor Assoc. Prof. Dr. Necdet Sinan ÖZBEK to for his valuable guidance and moral support during this thesis study.

I would like to thank also Prof. Dr. İlyas EKER for allowing me to use the control laboratory and meaningful advices for this journey.

I would like to thank my friends for supporting me by the end of thesis study.

TABLE OF CONTENTS

LIST OF FIGURES

LIST OF TABLES

LIST OF ABBREVIATIONS

ADR	: Active Disturbance Rejection
ADRC	: Active Disturbance Rejection Control
DOB	: Disturbance Observer-based
DOBC	: Disturbance Observer-based Control
EID	: Equivalent Input Disturbance
EIDC	: Equivalent Input Disturbance Control
ELADRC	: Error Based Linear Active Disturbance Rejection Control
ESO	: Extended State Observer
IMC	: Internal Model Control
LADRC	: Linear Active Disturbance Rejection Control
LESO	: Linear Extended State Observer
LSEF	: Linear State Error Feedback
SMC	: Sliding Mode Control
TD	: Tracking Differentiator
TDF	: Two Degree of Freedom
PD	: Proportional-Derivative
PID	: Proportional-Integral-Derivative

1. INTRODUCTION

1.1. A Brief Review of Control Systems

The evolution of control systems spans a rich historical narrative, reflecting the ever-growing quest for precision, efficiency, and adaptability in managing dynamic systems across various fields. The journey begins with classical control theories, evolving through a variety of paradigms, ultimately culminating in contemporary methodologies like Linear Active Disturbance Rejection Control (LADRC).

At the dawn of the control theory discipline, classical control systems, primarily based on proportional-integral-derivative (PID) controllers, laid the foundation for understanding and regulating system behavior. These early systems aimed to maintain stability and regulate performance by responding to system errors. However, they were limited in addressing uncertainties and disturbances that inherently exist in real-world systems.

As technology progressed and systems became more complex, the limitations of classical control methods became apparent (Shi et al., 2023). This led to the emergence of more sophisticated control strategies, such as state-space control and observer-based control. These advancements introduced the concept of system states and the use of observers to estimate unmeasurable internal states, revolutionizing the capability to design more adaptable and robust control systems.

LADRC represents a significant leap in the evolution of control methodologies. It addresses a fundamental challenge that has persisted throughout the history of control systems—the effective management of disturbances. LADRC introduces an innovative and active approach to handle disturbances by incorporating a disturbance observer and a compensation mechanism within the control loop. Unlike traditional methods that often struggle with disturbances, LADRC actively estimates and counteracts disturbances in real-time, significantly enhancing the system's robustness against external influences.

The integration of LADRC into the broader landscape of control systems signifies a paradigm shift towards actively addressing disturbances, uncertainties, and variations that were previously challenging to manage effectively. LADRC represents a novel approach that transcends the traditional methods by dynamically estimating and compensating for disturbances, thereby substantially improving control performance in electromechanical systems.

In summary, the historical journey of control systems reflects a continuous quest for more effective methodologies to manage complex systems. The emergence of LADRC stands as a testament to this evolution, offering a groundbreaking approach to address disturbances, aligning with the overarching goal of achieving more robust and adaptive control strategies in the ever-evolving landscape of control theory and practice.

1.2. Observer-Based Control Methods

Observer-based control methods stand as a cornerstone in the landscape of modern control theory. Their importance lies in their capability to infer and estimate unmeasurable or difficult-to-measure system states, which are crucial for devising precise and effective control strategies. These methods serve as invaluable tools in addressing the challenges posed by complex systems where direct measurement of all internal states might be unfeasible or costly.

The essence of observer-based control lies in its ability to provide estimates of unobservable states, enabling control systems to operate effectively without direct access to these internal variables. Such methods utilize state observers or estimators, which are based on available system inputs and outputs, predict the unmeasured states crucial for control design.

In modern control paradigms, particularly in complex or high-dimensional systems such as advanced mechatronic systems, robotics, and power systems, observer-based control

techniques play a vital role. They facilitate the development of robust and adaptable control strategies by enabling a deeper understanding and utilization of the system's internal dynamics.

The practical implications of observer-based control are profound. They offer the means to design control systems that are robust in the face of uncertainties, disturbances, and unmeasured states, thus enhancing system performance and stability. Furthermore, these methods contribute significantly to real-time implementation, enabling adaptive and responsive control actions, especially in applications where precise and agile control is imperative.

There have been three main disturbance rejection control methods studied and improved by the control engineers, which are Disturbance Observer-Based Control (DOBC), Equivalent Input Disturbance Control (EIDC), and ADRC (Active Disturbance Rejection Control) (Du, Cao, She, & Fang, 2020). The recent and most studied control technique among mentioned techniques is ADRC for its simplicity and applicability. It is certain that it will be used more often in modern control engineering and industrial applications because there is always model mismatch and unknown dynamics that lead to unexpected outcomes in real systems.

1.2.1. Equivalent Input Disturbance Control

Equivalent Input Disturbance (EID) is a concept that focuses on modeling and compensating for disturbances by treating them as equivalent inputs directly into the control system. The idea is to analyze the effect of disturbances as if they were additional inputs to the system. EID aims to compensate for these equivalent disturbances, considering their impact on the control system as if they were part of the control input.

EID approach is firstly proposed by Jin-Hua She (She, Fang, Ohyama, Hashimoto, & Wu, 2008) to deal with the drawbacks of DOBC control method. Needlessness of priori information of the disturbance and inverse dynamics of the plant are the key advantages of EID. Moreover, it does not require the differentiation of the measured outputs. (She et al., 2008). Disturbances are

almost completely rejected in both the transient and steady-state responses (She, Xin, & Pan, 2011).

The way of imposing the disturbance is not necessarily from the control input channel in EID. Instead, a slight change in plant model results in an approach which tends to attenuate the disturbance as in Figure 1.1 and Figure 1.2.

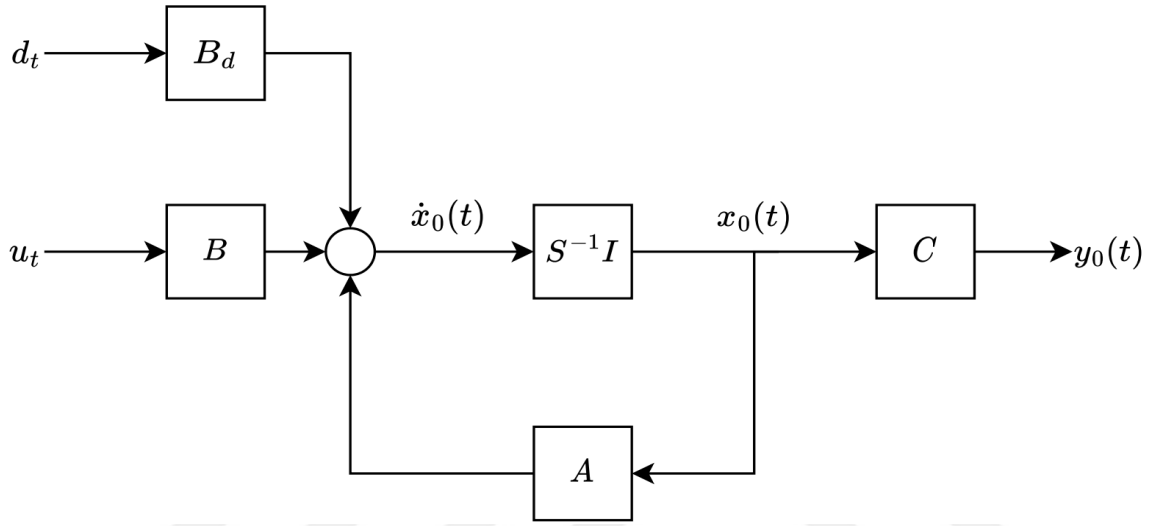

Figure 1.1. The Regular Plant Model.

Consider the linear time-invariant plant model as:

$$\dot{x}_0(t) = Ax_0(t) + Bu(t) + B_d d(t)$$
$$y_0(t) = Cx_0(t) \tag{1.1}$$

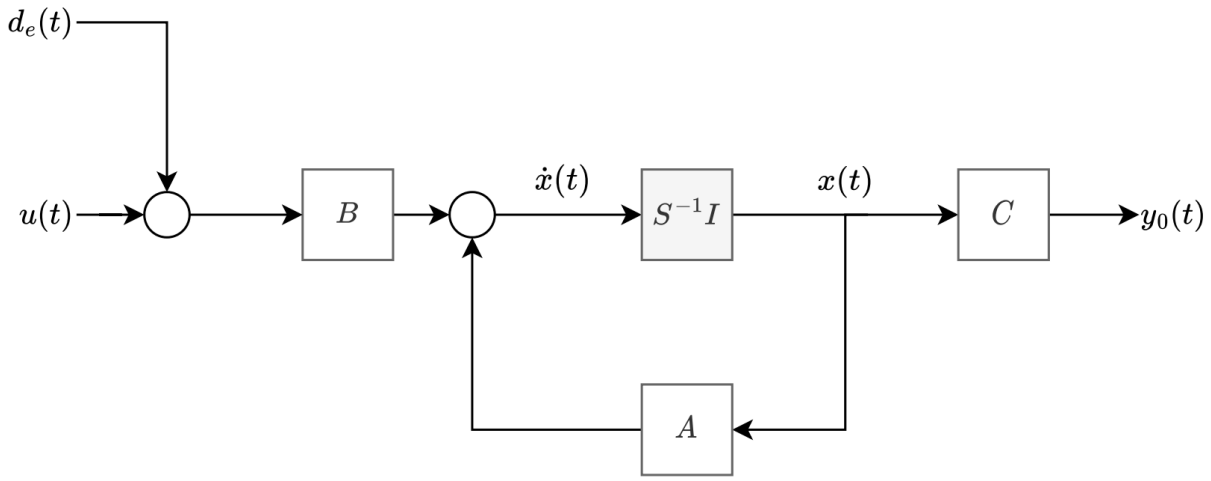

Figure 1.2 The Regular Plant with EID.

It has been already proven in (She et al., 2008) that plant with an exact disturbance as in above equation can be shifted to EID form with the disturbance denoted as $d_e(t)$. The prerequisites of demonstration of EID form are to be observable and controllable of the plant and no zeros on the imaginary axis are existed. The reproduced form of the plant is:

$$\begin{aligned} \dot{x}(t) &= Ax(t) + B|u(t) + d_e(t)| \\ y(t) &= Cx(t) \end{aligned} \tag{1.2}$$

where $x \in R^n$, $u \in R$ and $y \in R$ are the system state, the input and output of the plant respectively, with the equivalent input disturbance variable $d_e(t)$. $A \in R^{n \times n}$, $B \in R^n$, and $C \in R^{1 \times n}$ are the constant system matrices.

Since the reference input signal is precisely known, an internal model can be devised and implemented:

$$\begin{aligned} \dot{x}_R(t) &= A_R x_R(t) + B_R|r(t) - y(t)| \\ y(t) &= Cx(t) \end{aligned} \tag{1.3}$$

It allows the perfect tracking performance in a more regulated form. For the state observer:

$$\dot{\hat{x}}(t) = Ax(t) + Bu_f(t) + LC|y(t) - \hat{y}(t)|$$
$$\hat{y}(t) = C\hat{x}(t) \tag{1.4}$$

where $\hat{x} \in R^n$, $u_f \in R$, and $\hat{y}$ are the state, the input and the ouput of the observer and L is the observer gain matrice. The state error can be defined:

$$\Delta x(t) = \hat{x}(t) - x(t) \tag{1.5}$$

Substitution of the equation (1.5) into the (1.2) and the estimation of $d_e(t)$ becomes:

$$\hat{d}_e(t) = B^+ LC|\Delta x| + u_f(t) - u(t) \tag{1.6}$$

where $B^+ = (B^T B)^{-1} B^T$

Figure 1.3 shows the structure and components that generates the EID approach. A low pass filter $F(s)$ is used to filter the disturbance variable and $\hat{d}(t)$. Choosing the appropriate filter where ω_r is the highest angular frequency band for disturbance rejection as:

$$|F(j\omega)| \approx 1, \forall\omega \in [0, \omega_r] \tag{1.7}$$

As a result, the adverse effect of $d_e(t)$ is expected to compansate via the filtered version of it. Then, the block diagram of EID approach should be redrawn and extacted the transfer function from $d_e(t)$ to y.

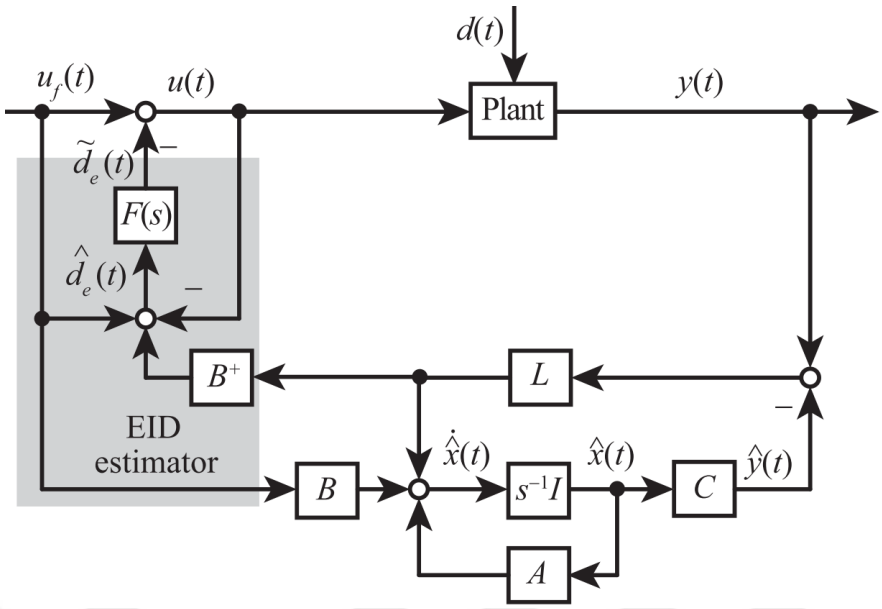

Figure 1.3. The Complete Block Diagram of EID Control Method. (Du et al., 2020)

The new transfer function can be acquired as:

$$G_{yde}(s) = G_{FF}(s)G_P(s) \tag{1.8}$$

The variables on the right hand side are:

$$G_{FF}(s) = \frac{1 - F(s)}{1 + F(s)B^{+}LC[sI - (A - LC)]^{-1}B} \tag{1.9}$$

$$G_P(s) = C(sI - A)^{-1}B \tag{1.10}$$

With the applicable and efficient filter design the transfer function $G_{yde}(s)$ get closes to zero, which means that EID is rejected from the system and there is no transfer to the output. $G_{FF}(s)$ represents the feedforward function used to diminish the unwanted effect caused by $d_e(t)$.

Figure 1.4. shows the alternative representation of EID method involving only the state space representation of plant and the estimation block.

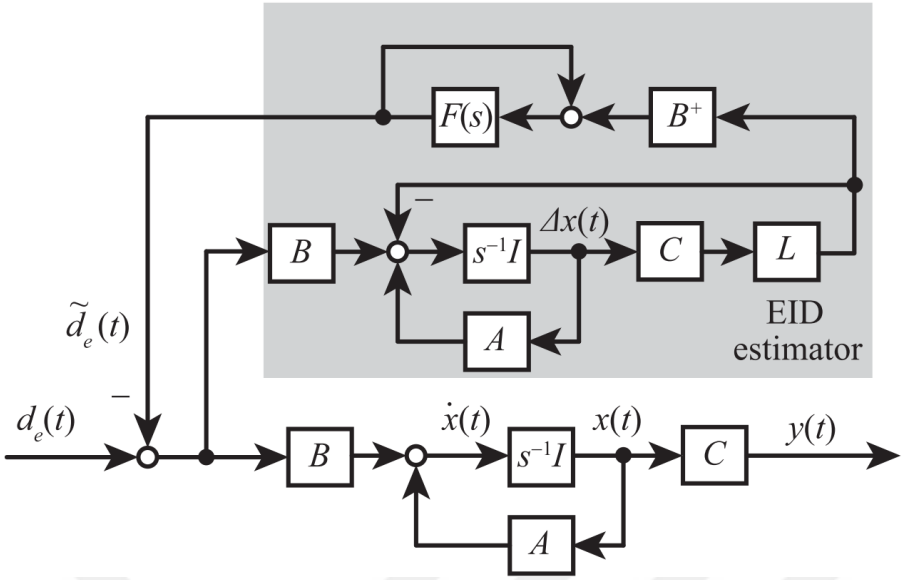

Figure 1.4. The Complete Block Diagram of EID Control with the Other Form. (Du et al., 2020)

1.2.2. Disturbance Observer-Based Control

Disturbance observer-based control was introduced with the for the sake of overcoming the unknown perturbations and disturbances. For instance, industrial robotic manipulators, servo systems, maglev suspension systems encapsulate the need of controller precision to deal with external disturbances, torque variations and pivot frictions. In addition, the performances of the controller, belongs to the mechanical systems, are subject to the effects of internal model parameter perturbations results from the changes of operation conditions (S. Li, Yang, Chen, & Xisong, 2014). Therefore, the development of new control algorithms with the ability of strong disturbance attenuation is helpful for practitioners to design robust systems.

To illustrate briefly, DOBC method is analyzed without system stability. The structure of DOBC is shown in Fig 1.5. Consider a single input single output linear minimum phase system:

$$G(s) = G_n(s) + \Delta G(s) \tag{1.11}$$

where $G(s)$ is the the plant dynamics with uncertainty, $G_n(s)$ is the nominal plant dynamics, $\Delta G(s)$ is unknown uncertainty. The next step is to extract the transfer function from disturbance to the output.

$$G_{yd}(s) = \frac{[1 - Q(s)]G(s)}{1 + Q(s)\Delta G(s){G_n}^{-1}(s)} \tag{1.12}$$

The transfer function from $u(t)$ to $y(t)$ is

$$G_{yu}(s) = \frac{G(s)}{G_n(s) + \Delta G(s)Q(s)} G_n(s) \tag{1.13}$$

So, the disturbance supression is dependent on the bandwidth of the filter $Q(s)$. It should be close to one in order to make purified the system from uncertainty.

$$Q(s) \approx 1, G_{yd} = 0, G_{yu} = G_n(s) \tag{1.14}$$

As a result, the disturbance may be discarded while designing the system's feedback controller for a nominal plant as long as the condition above is valid.

The crucial part of the DOBC is the low-pass filter $Q(s)$ and plays a key role. The variation of low-pass filter has an effect on disturbance rejection performance as well as the implementation of DOBC. The order of the filter should be more or the same with the relative degree of the plant model. Performance and robustness of DOBC systems can be improved via changing the bandwidth of the filter just as $Q(s){G_n}^{-1}(s)$ term providing that the practical conditions are available.

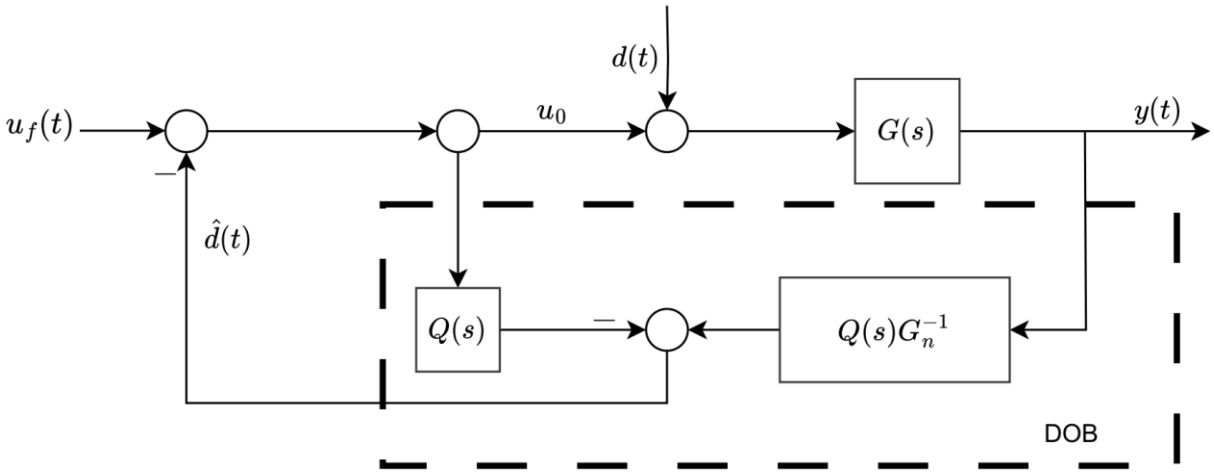

Figure 1.5. The Block Diagram of Disturbance Observer-Based Control

1.2.3. Active Disturbance Rejection Control

ADRC is a control strategy that actively estimates and rejects disturbances in real-time by introducing a disturbance estimator and a compensator into the control loop. It uses an extended state observer to estimate the system state, including disturbances, and then generates a control action that explicitly accounts for these estimated disturbances. ADRC focuses on identifying and rejecting disturbances dynamically, continuously adjusting the control action to counteract the effects of disturbances.

ADRC differs from traditional control methods by its ability to actively estimate and compensate for both known and unknown disturbances in real-time. This approach has gained popularity due to its versatility, simplicity, and adaptability in dealing with uncertain and time-varying systems. ADRC structure is shown in the Figure 1.6 and the key components of ADRC can be listed:

1. **Tracking Differentiator (TD):** The tracking differentiator, which is the initial component of the relative algorithm, seeks to eliminate the influence of the reference signal's derivative. The reason for this is that the derivative component in a PID

controller is rarely employed in the control loop due to its sensitivity to high frequency noise; instead, TD is used to mitigate this impact. (Feng & Guo, 2017)

2. **Extended State Observer (ESO):** The ESO is a crucial component of ADRC. It acts as a dynamic compensator by estimating the system's state variables and disturbances simultaneously. The estimated disturbance information is then used to generate control actions that compensate for the disturbance effects. (Han, 2009)

3. **Controller:** The controller generates control commands based on the estimated disturbance information and the system's desired reference signals. It is responsible for maintaining the system's output close to the desired setpoint while actively compensating for disturbances. The tracking controller can be designed using various control techniques such as PD (Proportional-Derivative), state feedback, sliding mode control or other advanced control methods. (Herbst, 2013)

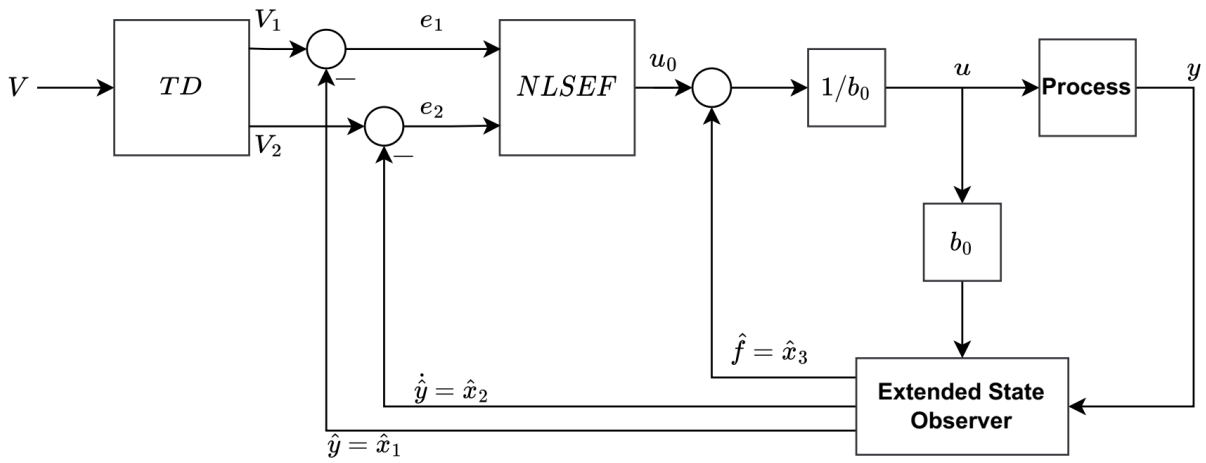

Figure 1.6. The Block Diagram of Active Disturbance Rejection Control Method

In Figure 1.6, “TD” represents Tracking Differentiator, “NLSEF” represents the “Nonlinear State Error Feedback”-can be named as controller- , “V” represents system input signal to be differentiated, V_1 is the desired trajectory and V_2 is its derivative, e_1 and e_2 are the error signals

between the ouput of the TD and estimated states, u is the control signal, y is the output signal and b_0 is the tuning parameter.

The core idea behind ADRC is to estimate the effects of disturbances in the system. These disturbances can be external factors, measurement noise, or model inaccuracies that can significantly affect system performance. ADRC uses mathematical models and algorithms to estimate the disturbances in real-time. The benefits of ADRC are as follows:

1. **Robustness:** ADRC is known for its robustness in the presence of various disturbances and uncertainties. It can handle both known and unknown disturbances, making it suitable for real-world applications where disturbances are difficult to predict.

2. **Improved Performance:** By actively estimating and compensating disturbances, ADRC can significantly improve the closed-loop performance of control systems. It allows better tracking of reference signals and disturbance rejection.

3. **Simplicity:** ADRC is relatively simple to implement and does not require extensive knowledge of the system's dynamics. It can be applied to a wide range of systems with minimal model-based design.

4. **Adaptivity:** ADRC can adapt to changing system dynamics and disturbances over time, making it suitable for applications where the environment or system characteristics are not constant.

1.3. Background and Motivation of Thesis

PID controllers are still the dominant in industrial implementations although its primitivity and drawbacks. That is why, observer-based control methods are the alternative methods proposed in the literature aims to make the dominance of PID in the industry to decrease. The replaced control method instead of PID should have those properties:

1. The solid and fixed control structure which should be easy to implement in practical application.
2. Not to many tuning parameters which are directly connected to the performance of closed-loop system. Moreover, the tuning should not posses the complexity.
3. Prediction and estimation error between the output signal and the reference signal in real time causes the system to be avoided from the unwanted outcomes.

ADRC comes with the solution of those issues. So, the supremacy of the ADRC, is the main validation point of this thesis. With the simplified version which does not have the bunch parameters that ADRC used in tuning, (Gao, 2003) Because of TD and LADRC has been recently popular control strategy. This thesis aims to explain the different versions of LADRC algorithms along with the design and application processes. The results of the real time experimental implementations on electromechanical system were compared through some performance metrics. Hence, the effect of LADRC on real time applications can be assessed.

1.4. Objectives and Contribution of Thesis

This study aims to address crucial challenges in the field of control systems, particularly focusing on electromechanical system. The primary objectives of this thesis, which are multifaceted, incorporating both theoretical advancements and practical implementations to enhance control methodologies, are summarized as follows:

1. Investigate and analyze the theoretical foundations of disturbances affecting electromechanical systems to develop a robust framework for disturbance rejection. Explain the observer-based control methods and why they are essential for modern control.
2. Establish a comprehensive understanding of LADRC principles for electromechanical systems.

3. Explore and refine the integration of LADRC with electromechanical systems, emphasizing its advantages and limitations.
4. Offer practical insights and guidelines for the application of LADRC in real-world electromechanical systems, including but not limited to robotics, mechatronics, and motor control.
5. Provide a roadmap for industry practitioners and researchers to implement and adapt LADRC to enhance the control of electromechanical systems in diverse applications.
6. Provide a foundation for further research and development in the realm of control systems for electromechanical devices, encouraging ongoing advancements and innovation in the field.

The main contributions of the thesis are summarized as follows:

1. Real-time identification of an electromechanical system is conducted through process reaction curve techniques.
2. LADRC based algorithms are designed to mitigate disturbances in electromechanical systems in the the control framework for real-time applications, considering system-specific constraints and requirements.
3. The designed control strategies are implemented on practical electromechanical systems to evaluate their performance and efficacy.
4. Extensive experimental investigations are conducted to validate the proposed LADRC methods under various operating conditions and disturbances.
5. The performance of the LADRC is compared with existing control techniques to demonstrate its superiority in mitigating disturbances in electromechanical systems.

This thesis is envisioned to significantly contribute to the advancement of control methodologies for electromechanical systems, particularly through the development and validation of the LADRC framework. The findings and outcomes are anticipated to be beneficial for both academic research and practical industrial applications, offering new perspectives and strategies to tackle disturbances in such systems effectively.

2. LITERATURE REVIEW

2.1. Review of Active Disturbance Rejection Control Method

Active Disturbance Rejection Control (ADRC) emerges as a potent and adaptive control strategy, demonstrating the capacity to markedly elevate the performance and robustness of control systems across diverse applications. Its distinctive capability to actively estimate and compensate for disturbances distinguishes it from conventional control methods, rendering it an appealing option for contemporary control engineering.

It was first proposed by Han (Han, 2009) and from that point it evolves in both theoretical and experimental aspects. It reveals that PID control will eventually lose its appeal due to diminishing utility. Furthermore, it introduces a novel problem-solving methodology and mindset regarding the application of ADRC to diverse engineering challenges.

The ADRC can be combined with numerous control strategy such has Fuzzy Control and Backstepping Control. Studies have reported applications of Fuzzy Control in underwater biometric vehicle system, (R. Wang, Wang, Wang, Tang, & Tan, 2018) underactuated underwater vehicle system (A. Li et al., 2019), exoskeleton system (Z. Li, Guan, Li, & Xu, 2020), networked control system (Y. W. Wang, Zhang, Dong, & Yu, 2020), robotic arm system (X. A. Li, Sun, Guo, & Liu, 2021), medium and high voltage distribution system (Xuesong Zhou, Cui, & Ma, 2021), magnetic levitation system (Ouyang, Fan, Liu, & Li, 2021), aircraft anti-skid breaking system (Z. Zhang et al., 2021) and quadrotor system (Z. Wang & Zhao, 2022).

The evolution of ADRC are now undeniable truth for literature. Sliding Mode Control (SMC) is one of the applicable methods which can be combined or be part of the elements of ADRC. For example, one of the alternative approach for observer design is utilizing the Sliding Mode apprıoach for electromechanical systems as in Figure 2.1 (Qiu, Xiao, & Wang, 2015). Using the sigmoid function instead of sign function with constant boundary layers and Kalman filter,

weakens the chattering and observer error when compared the conventional sliding mode observer. The output of the proposed observer is combined with ADRC to increase the efficiency of speed regulation. Other example demonstrates the compound control of ADRC with SMC is a solution of the performance problem of path following problem of underactuated surface ships (Li et al., 2016). The model free advantage of ADRC is utilized and heading angle following performance is upgraded to certain level with easily tuning. In (Alonge, Cirrincione, D'Ippolito, Pucci, & Sferlazza, 2017), the induction motor system have been included the work of centre. Rotor flux and speed of induction motor were controlled by ADRC to aim to deal with internal and external disturbances, which are estimated and disrupted by means of two LESO.

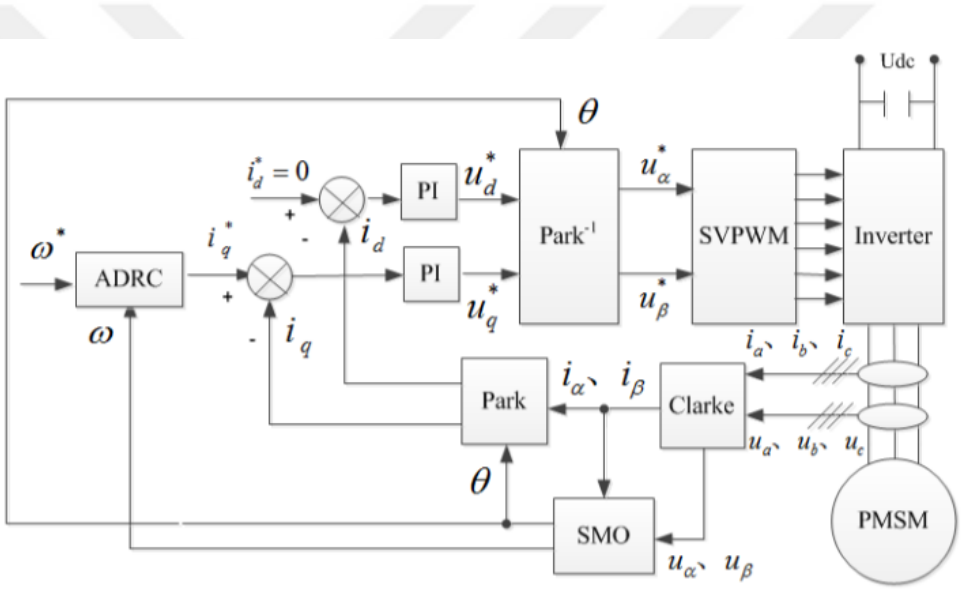

Figure 2.1. The Usage of Sliding Mode Observer With ADRC (Qiu et al., 2015)

The estimation errors of the total disturbance and parameter fluctuations, which are not included in the endogenous disturbances and cannot be assessed by the ESO, are the root source of the issues that ADRC cannot solve. Hence, the robustness of the controlled system is provided with the help of SM component which is used in the control law. The superiority of the proposed method over conventional ADRC was supported with both simulation study and experimental application.

Wearable exoskeletons have garnered increased attention in research recently because of their many uses, which include easing the burden of intensive rehabilitation, assisting quadriplegic or paraplegic individuals in regaining movement, enabling healthy individuals to lift large objects, and supplying extra force for walking. The significant challenge in this field is how to control exoskeletons to maximize their potential. In (C. F. Chen et al., 2019), ADRC with Fast Terminal SMC are combined to improve the performance lower limb exoskeleton by means of disturbance estimation with finite-time convergence. The paper demonstrates that ADRC is not enough to provide fast convergence so the reason behind the usage of both method collectively is to control the system fast and accurate way. The drum water level systems include strong disturbance, nonlinearity and variation of the operating conditions. Because the SMC has the advantages of quick response and robustness, this paper (Pu, Ren, & Su, 2019) introduces that it can be collectively incorporated in to closed loop control system with the LESO. For modelling and reconstruction, the LESO uses the systems's total disturbance as the extended state. This allows the estimation of the equivalent disturbance of the system. The combination of two methods is applied to as SMC based on LESO to the control of drum water level. Performance of the controller exceeds compared with the conventional LADRC when external disturbance and model parameter mismatch exist in the system. Unmanned surface vessels are one of the application areas which uses SMC and ADRC combined. The maneuvering problems arises while unmanned surface vessels are sailing in the ocean. They need to launch swiftly and travel steadily in an emergency case. Although, the SMC is combined with adaptive theory and backstepping control methology in (X. Chen, Liu, Hu, Wang, & Dong, 2017), the instant and frequent changes in switching function makes the control state is effected negatively because of high frequency oscilations. Hence, as in Figure 2.2. (Dong, Huang, & Zhuang, 2020) proposes a new strategy, which combines Levant Tracking Differentiator that is a nonlinear differentiator allows to extract input signals and their differentials with efficacy, ESO and Sliding Mode Control which uses power exponential approaching law to construct the new piecewise function. The method presented in the paper manifests that the Levant TD reduces the alterations of the rudder angle and lessens the wear of the steering gear. Marine current turbine energy systems attracts attention. because of searching alternative energy sources of the

humanity, the predictability and availability. Marine current turbines face challenges in operating and maintaining mechanical sensors due to the extreme underwater conditions they

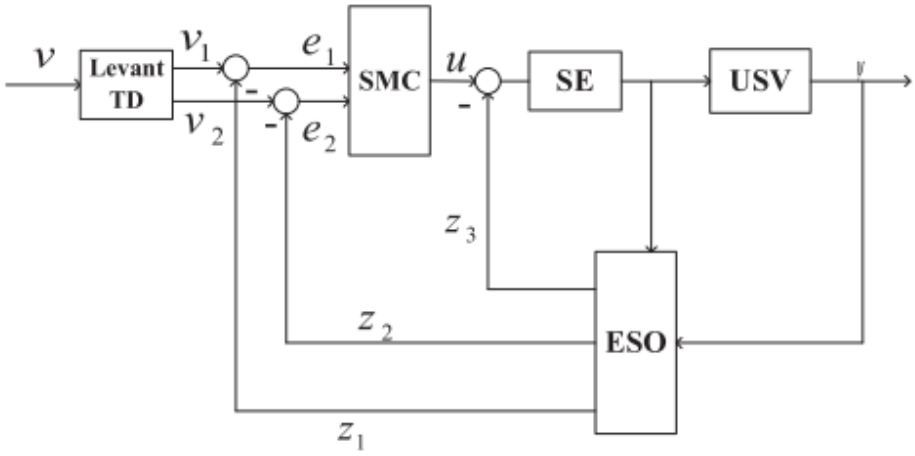

Figure 2.2. The Combination of Levant TD, SMC And ESO (Dong et al., 2020)

encounter. Hence, implementing a sensorless control approach is completely justified in order to enhance the dependability of electrical energy output in the system. To overcome this issue, In the beginning, an examination has been conducted on the influence of the swell effect on the velocity of the marine current, which can result in disruptions to the MCT system. Afterwards, an ADRC controller was developed to enhance the anti-interference capability of the MCT system. Subsequently, Smith predictor based time-delay compensation sliding mode observer is implemented to eliminate system time delay (Xiangyang Zhou, Wang, & Diallo, 2022). Permanent Magnet Sycronous Motors (PMSM) needs to posses good tracking performance for the current control in industry. Even if, model predictive control (X. Zhang, Hou, & Mei, 2017) is a solution in many ways such that has the ability to determine and forecast future voltages, the predictions of model predictive control comes with high computational costs. That is why, in order to improve the performance of the current control ADRC based SMC was proposed in (Qu, Qiao, & Qu, 2021) and the proposed technique was validated by experimental results for 200W salient pole PMSM drive system as in Figure 2.3. The article introduces a new active-disturbance-rejection-based sliding-model current controller (ADR-SMCC) for field oriented based control PMSM drives to enhance their disturbance rejection ability and current tracking

performance. The ADR-SMCC combines an SMCC with ESO to achieve fast current tracking performance. The ESO's real-time disturbance estimate mitigates the influence of disturbances on current tracking performance, making the ADR-SMCC more robust to system disturbances than PI current control, SMCC and the disturbance observer sliding mode current control.

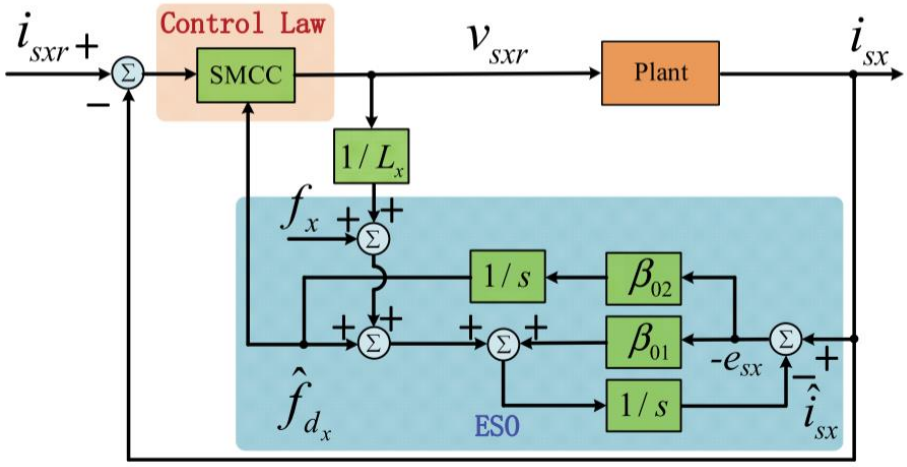

Figure 2.3. The Block Diagram of the Plant Controlled by the ADR-SMCC Scheme (Qu et al., 2021)

Sliding mode ESO combined with SMC in way that constittutes a structure that applies ADRC with sliding mode components to the fractional order systems in (Djeghali, Bettayeb, & Djennoune, 2021). Several studies have focused on developing the ADRC specifically for linear and nonlinear fractional-order systems. Nevertheless, the application of the sliding mode technique in the design of ADRC for fractional-order systems has not been implemented thus far. This study aims to introduce a sliding mode active disturbance rejection controller for stabilizing and tracking nonlinear fractional-order systems that have uncertainties and external disturbances as in Figure 2.4.

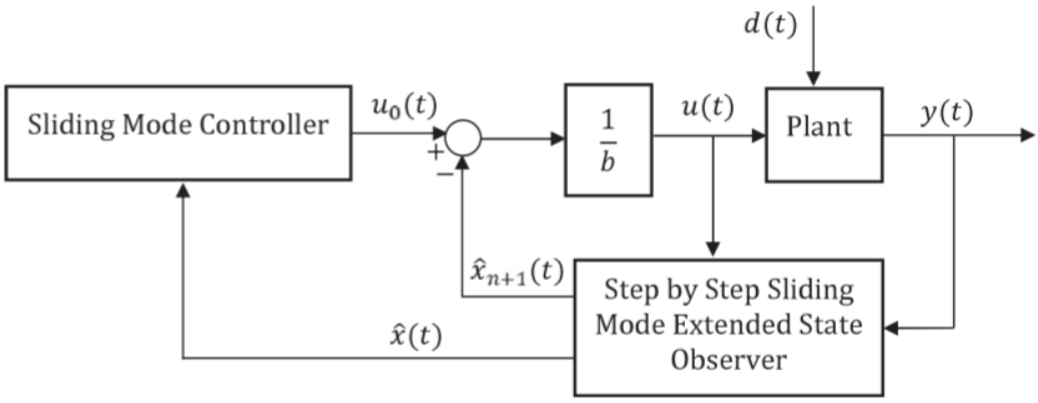

Figure 2.4. The Block Diagram of the Proposed Scheme for Fractional Order System. (Djeghali et al., 2021)

The more applicable form of ADRC is referred to as LADRC, which avoids the use of nonlinear functions seen in ADRC. Applying to various control systems is significantly easier due to the requirement of fewer parameters compared to ADRC. Since its proposal by Gao (Gao, 2003), the approach has been recognized as an acceptable alternative control methodology for over two decades (D. Eker, Özbek, & Çelik, 2022)(D. Eker & Özbek, 2021). For example, a generalized version of LADRC is proposed in (R. Zhou & Tan, 2015) to account for additional plant information, such as the presence of extra dynamics in the controlled plant. To optimize, the suggested configuration is transformed into an Internal Model Control (IMC) framework. Consecutively, the generalized version of LADRC with Smith predictor is investigated for time delayed systems in (B. Zhang, Tan, & Li, 2020). After that, (Cui, Tan, Li, Wang, & Wang, 2020) proposes a new tuning method for LADRC via relay feedback to initialize the parameters of LADRC and tested simulatively. Then, reduced-order ESO is combined with LADRC is proposed in (Fu & Tan, 2020) to improve the control performance of LADRC. In (R. Zhou, Fu, & Tan, 2021), the question that where the linear control is sufficient, is it possible to apply LADRC in any strictly proper linear controller was tried to answered. It is inevitable that LADRC method will draw more attention by the researchers and control engineers. Hence, it became the primary subject of investigation in this thesis.

3. BACKGROUND OF SELECTED CONTROL METHODS

3.1. Linear Active Disturbance Rejection Control

Linear Active Disturbance Rejection Control (LADRC) offers a range of notable advantages that make it a compelling choice in control system design and practical applications. Its inherent robustness against diverse disturbances and system uncertainties ensures reliable performance even in noisy environments. LADRC excels in tracking desired trajectories with precision, making it ideal for applications where maintaining control in the face of disturbances is crucial. What sets LADRC apart is its ability to function without the need for a precise mathematical model of the system, simplifying the control design process. This ease of parameter tuning is especially valuable in experimental and practical settings (R. Zhou et al., 2021). Additionally, the incorporation of an Extended State Observer (ESO) for real-time disturbance estimation and compensation further enhances its effectiveness. LADRC's adaptability to various system types, suitability for both linear and nonlinear systems, and ability to reduce control effort make it a versatile and advantageous choice for control system engineers and researchers across numerous industries, seeking to elevate the performance and resilience of their systems (Fu & Tan, 2021).

Bearing these observations in mind, the LADRC method, is considered a due to the ease of parameter selection which provides to the designer in experimental applications.

Rather than the conventional approaches as PID, LADRC does not need all the parameters of the plant in order to control the system. That is why despite conventional control approaches, the control scheme derives the information required to regulate the plant through using the ESO rather than the plant's model. The following second order system is taken into consideration in order to effectively express the LADRC scheme:

$$\ddot{y} = -a\dot{y} - by + w + bu \tag{3.1}$$

where y is the output of the plant, u is the input of the plant, b is the system parameter and w is the external disturbance. The coefficients of y and $\dot{y}$ may not be known, but it is useful to get some prior knowledge of the plant model while constructing the LARDC controller. So, the information of $b \approx b_0$ is used as:

$$\ddot{y} = -a\dot{y} - by + w + (b - b_0)u + b_0 u \tag{3.2.a}$$

$$\ddot{y} = f + b_0 u \tag{3.2.b}$$

The idea is cover all the internal unknown dynamics and external disturbance as total disturbance, which is denoted as f, and convert the system to double integral plant. Fundementally, an ESO should practically be implemented so that the estimation of f, which is denoted as $\hat{f}$, is possible to use in the control law. Moreover, the impact of f on the control loop can be compansated and remaining part to be handled for the controller is the process with nearly double integrating behaviour. With the usage of $\hat{f}$, the control signal becomes:

$$u = (-\hat{f} + u_0)/b_0 \tag{3.3}$$

After that, it is mandatory to define state equation form of (3.1) as:

$$\begin{aligned} \dot{x}_1 &= x_2 \\ \dot{x}_2 &= x_3 + b_0 u \\ \dot{x}_3 &= h \\ y &= x_1 \end{aligned} \tag{3.4}$$

The point is the augmented state is added as $x_3 = f$. Hence, $\dot{x}_3 = \dot{f} = h$ is denoted as unknown disturbance which can be estimated by a state observer-based on the state space model below:

$$\dot{x} = Ax + Bu + Eh \tag{3.5.a}$$

$$y = Cx \tag{3.5.b}$$

where,

$$A = \begin{bmatrix} 0 & 1 & 0 \\ 0 & 0 & 1 \\ 0 & 0 & 0 \end{bmatrix}$$
$$B = [0 \quad b_0 \quad 0]^T$$
$$E = [0 \quad 0 \quad 1]^T \tag{3.6}$$
$$C = [1 \quad 0 \quad 0]$$

LESO, which is a special form of ESO, for (3.5) now can be designed as:

$$\dot{z} = Az + Bu + L(y - \hat{y})$$
$$\hat{y} = Cz \tag{3.7}$$

L can be named as observer gain vector, which can be determined using pole placement method. With the estimated variables, $z = \hat{x}$, ESO equation can be written as where $L = [l_1 \quad l_2 \quad l_3]^T$:

$$\begin{bmatrix} \hat{x}_1 \\ \hat{x}_2 \\ \hat{x}_3 \end{bmatrix} = \begin{bmatrix} 0 & 1 & 0 \\ 0 & 0 & 1 \\ 0 & 0 & 0 \end{bmatrix} \begin{bmatrix} \hat{x}_1 \\ \hat{x}_2 \\ \hat{x}_3 \end{bmatrix} + \begin{bmatrix} 0 \\ b_0 \\ 0 \end{bmatrix} u + \begin{bmatrix} l_1 \\ l_2 \\ l_3 \end{bmatrix} (y - \hat{y}) \tag{3.8.a}$$

$$\begin{bmatrix} \hat{x}_1 \\ \hat{x}_2 \\ \hat{x}_3 \end{bmatrix} = \begin{bmatrix} -l_1 & 1 & 0 \\ -l_2 & 0 & 1 \\ -l_3 & 0 & 0 \end{bmatrix} \begin{bmatrix} \hat{x}_1 \\ \hat{x}_2 \\ \hat{x}_3 \end{bmatrix} + \begin{bmatrix} 0 \\ b_0 \\ 0 \end{bmatrix} u + \begin{bmatrix} l_1 \\ l_2 \\ l_3 \end{bmatrix} y \tag{3.8.b}$$

According to equation above, it can be deduced that $\hat{x}_1 = \hat{y}$, $\hat{x}_2 = \dot{\hat{y}}$ and $\hat{x}_3 = \hat{f}$. Using the variables which are guessed by ESO, a modified PD controller as in Figure 3.1 without the derivative part of the reference signal causes second order closed loop controlled system to exist:

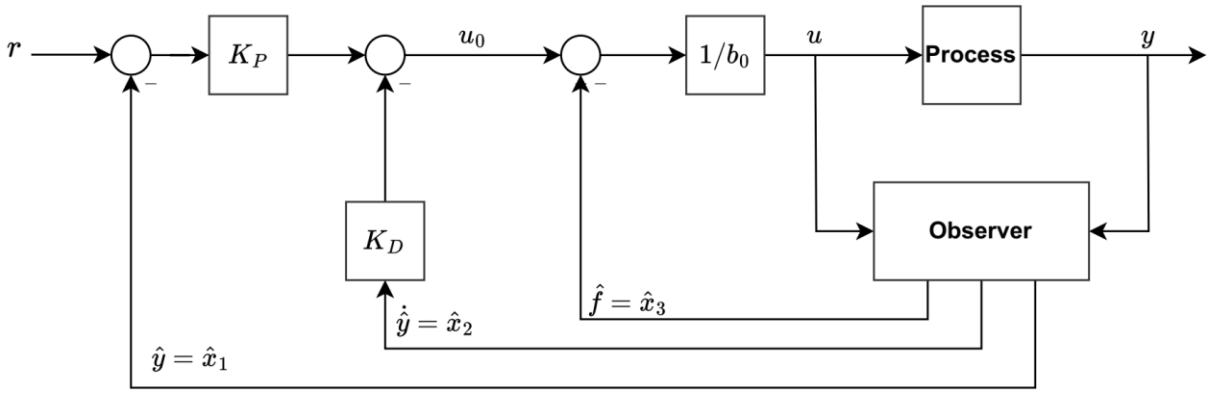

Figure 3.1. The Block Diagram of PD Based LADRC Method.

$$u = \frac{(-z_3 + u_0)}{b_0} \tag{3.9.a}$$

$$u_0 = K_P(r - \hat{x}_1) - K_D\hat{x}_2 \tag{3.9.b}$$

Provided that the ESO makes sufficient estimates of states such that $\hat{x}_1 = \hat{y} \approx y$, $\hat{x}_2 = \dot{\hat{y}} \approx \dot{y}$ and $\hat{x}_3 = \hat{f} \approx f$, equation (3.9.a) can be substitued into (3.2.b) (Herbst, 2013):

$$\ddot{y} = \left(f - \hat{f}\right) + u_0 \approx u_0 \approx K_P(r - \hat{x}_1) - K_D\hat{x}_2 \tag{3.10}$$

where r represents the setpoint. One of the key point is that $K_D.\hat{x}_2$ is utilized instead of $K_D.(\dot{r} - \hat{x}_2)$ in order that the control signal does not include the differentiation of the setpoint. It provides a closed loop pure second order transfer function without a zero. Setpoint signal equals:

$$\frac{1}{K_P}\ddot{y} + \frac{K_P}{K_D}\dot{y} + y = r \tag{3.11}$$

3.1.1. Tuning of Linear Active Disturbance Rejection Control

The selection of controller gains are not strictly restricted, means any second order dynamics can be used to determine the K_P and K_D. Practically, these two parameters are linked with controller bandwidth and damping ratio, denoted as w_C and δ.

$$K_D = 2\delta w_C \, , K_P = {w_C}^2 \tag{3.12}$$

The parameter w_C is related the question that how the controller can be optimized for each application and how the engineer eloborates deep in the system so that gets the most reliable performance. Hence, w_C can be expressed as the measure of performance, which corresponds better disturbance rejection and better setpoint following as it's value gets higher.

Practically, it is assumed beneficially to tune closed loop system as critically damped behaviour and 2% settling time so that negative real double pole is obtained. Since the damping ratio is one:

$$\begin{aligned} K_D &= 2w_C \\ K_P &= {w_C}^2 \\ w_C &= \frac{6}{T_S} \end{aligned} \tag{3.13}$$

The coefficient that stands above the fraction which identifies w_C depends on the desired closed loop transfer function and proof is presented at the Appendix A.

After the controller gains were determined, the gains of ESO should be specified. One way to do this is to placing all observer poles at one location. So, there is another parameter, denoted as w_O and named observer bandwidth, emerged to regulate observer dynamics. The LESO has three observer poles and should be placed $-w_O$ equivalently:

$$\theta(s) = s^3 + l_1 s^2 + l_2 s + l_3 = (s + w_O)^3$$
$$l_1 = 3w_O, l_2 = 3{w_O}^2, l_3 = {w_O}^3 \quad (3.14)$$

The equations are easily extended up to n^{th} order LESO. The parameters of LESO are the functions of w_O and the real question, in particular, is how the observer bandwidth should be optimized. Moreover, as the LESO tracks the states with expected speed, it will be better for the system to eliminate unwanted noises and internal disturbances. It, requires a relation between the controller bandwidth and the observer bandwidth.

$$w_O = (3 \dots 10).wc \quad (3.15)$$

The coeffcient of the equation above demostrates that observer bandwidth should be faster than controller bandwidth so that the compensation of uncertainties is possible.

3.2. Error Based Linear Active Disturbance Rejection Control

This version of the LADRC scheme deploys the LESO in conjunction with a linear state feedback controller. However, it's worth noting that the system's state vector encompasses the feedback error and its successive time derivatives. (Madonski et al., 2023).

The objective is to make system output y track the reference signal r by manipulating the input signal u. The less trajectory tracking error $e \triangleq r - y$ results in the less presence of unknown system dynamics and unpredictable external disturbance. In order to utilize this method, reference signal should satisfies:

- The signal itself and its consecutive reference time derivatives are unknown.
- Its consecutive time derivatives exist for all $t \geq 0$ and are bounded.
- The signal itself should be bounded.

The following single input single output plant model is introduced first:

$$y^{(n)} = \sum_{i=0}^{n-1} a_i\, y^{(i)} + bu + d \tag{3.16}$$

where n is the order of the plant, y is the output, u is the control input, a_i are unknown plant parameters, d is the external disturbance and b is partially known plant gain. The approach of the presented method leads to the system into more compact form:

$$y^{(n)} = f + b_0 u \tag{3.17}$$

where f is the total disturbance. The definition of tracking error makes the plant model into:

$$e^{(n)} = f_e - b_0 u \tag{3.18}$$

where f_e can be defined total disturbance in error domain and the expansion of f_e is:

$$f_e = r^{(n)} - \sum_{i=0}^{n-1} a_i\, r^{(i)} + \sum_{i=0}^{n-1} a_i\, e^{(i)} - \Delta b u - d \tag{3.19}$$

The derivation and approach of ADRC allows to represent $b = b_0 + \Delta b$ where $b_0 \neq 0$. Hence, the estimation of uncertainties are made to possible to demonstrate. In LADRC, the reference signal and its derivatives are not part of the total disturbance, while in this approach they becomes the part of the term, f_e. For a second order system the equations above turns into:

$$\ddot{y} = a_0 y + a_1 \dot{y} + bu + d \tag{3.20}$$

$$\ddot{e} = f_e - b_0 u \tag{3.21}$$

$$f_e = \ddot{r} - a_0 r - a_1 \dot{r} + a_0 e + a_1 \dot{e} - \Delta b u - d \tag{3.22}$$

The following part of E-LADRC involves the derivations for second order system (H. Zhang, 2017). The states of the system for a second order system can be written in terms of error signal as where $e \triangleq r - y$.

$$\begin{aligned} x_1 &= e = r - y \\ x_2 &= \dot{r} - \dot{y} = \dot{x}_1 \\ x_3 &= f_{e(2)} \end{aligned} \tag{3.23}$$

Where $f_{e(2)} = \ddot{r} - f$. Then x_2 can be rewritten as:

$$\dot{x}_2 = f_{e(2)} = \ddot{r} - \ddot{y} = \ddot{r} - (f + bu) = \ddot{r} - f - bu = x_3 - bu \tag{3.24}$$

The plant's form can be expressed as:

$$\begin{aligned} \dot{x}_1 &= x_2 \\ \dot{x}_2 &= x_3 - bu \\ \dot{x}_3 &= \dot{f}_{e(2)} \end{aligned} \tag{3.25}$$

The block diagram of the error based LADRC structure is shown in Figure 3.2. The main difference with the LADRC structure depicted in Figure 3.1, is the feedback controller which involves not the multiplication of estimaton of the states but the estimation of errors. So the control signal can be written as:

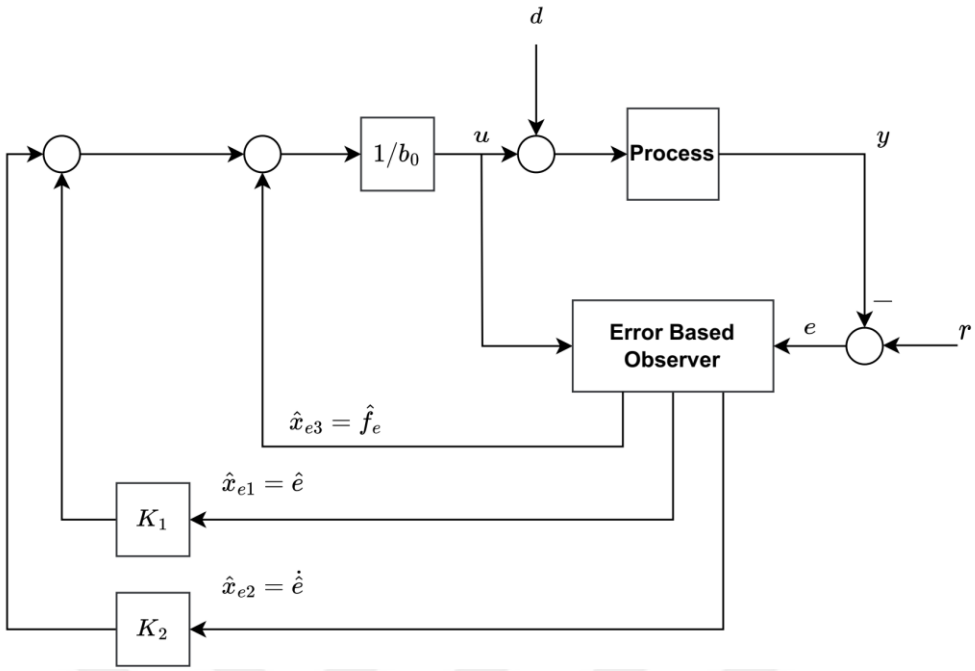

Figure 3.2. The Block Diagram of Error Based LADRC Method

$$u = \frac{(f_{e(2)} + u_0)}{b_0} \tag{3.26.a}$$

$$u_0 = K_1\hat{x}_{e1} + K_2\hat{x}_{e2} \tag{3.26.b}$$

Provided that the output variables of the error based observer are perfectly designed such that $\hat{x}_{e1} = \hat{e} \approx e$, $\hat{x}_{e2} = \dot{\hat{e}} \approx \dot{e}$ and $\hat{x}_{e3} = \hat{f}_{e(2)} \approx f_{e(2)}$, the goal of the ELADRC is to minimize observer estimation which equals $e - \hat{e}$.

$$\begin{aligned} \dot{\hat{x}}_e &= A\hat{x}_e - bu_e + L(e - \hat{e}) \\ \hat{e} &= Cx_e \end{aligned} \tag{3.27}$$

where,

$$A = \begin{bmatrix} 0 & 1 & 0 \\ 0 & 0 & 1 \\ 0 & 0 & 0 \end{bmatrix}$$
$$b = [0 \quad b_0 \quad 0]^T$$
$$L = [l_1 \quad l_2 \quad l_3]^T \tag{3.28}$$
$$C = [1 \quad 0 \quad 0]$$

It can be seen clearly that error based ESO is almost the same with the one which LADRC involves. However, the term related with the control signal, $b.u_e$, has a negative sign in front. Moreover, the input of LESO is the output signal y while the input is the tracking error e in error based ESO. With the use of eq. 3.26, the system model reduces its dynamics to idealized integral form which is denoted as $\ddot{e} = -u_0$.

In the tuning procedure, the error-based LADRC method employs the same tuning methodology as the conventional LADRC structure, relying on both the controller bandwidth and observer bandwidth. For practitioners, using identical controller gains and observer gains can be beneficial in comprehending the relationship between and assessing both methods.

3.3. Linear Active Disturbance Rejection Control via IMC

The following linear system is considered to demonstrate the entire scheme (Tan & Fu, 2016):

$$Y(s) = G(s)U(s) + D_e(s)D(s) \tag{3.29}$$

where:

$$G(s) = \frac{b_m s^m + \cdots + b_1 s + b_0}{a_n s^n + a_{n-1} s^{n-1} + \cdots + a_1 s + a_0} \tag{3.30}$$

$$D_e(s) = \frac{c_h s^h + \cdots + c_1 s + c_0}{a_n s^n + a_{n-1} s^{n-1} + \cdots + a_1 s + a_0} \tag{3.31}$$

$Y(s), U(s)$ and $D(s)$ are representation of Laplace transform of system variables which correspond output, input and disturbance singly. $D_e(s)$ and $G(s)$ are the transfer functions of the external disturbance and the controlled plant.

$p = n - m$ where p the relative order of the controlled plant is sufficient for designer who establishes the ADRC control scheme over the controlled plant. The form of differential equation of the whole system can be written as:

$$\begin{aligned} &a_n y^{(n)}(t) + a_{n-1} y^{(n-1)}(t) + \cdots + a_1 \dot{y}(t) + a_0 y(t) = \\ &b_m u^{(m)}(t) + \cdots + b_1 \dot{u}(t) + b_0 u(t) + \\ &c_h d^{(h)}(t) + \cdots + c_1 \dot{d}(t) + c_0 d(t) \end{aligned} \tag{3.32}$$

The idea is to treat all of the uncertainties and disturbances as ‘lumped’ disturbance. That is why the whole equation can be arranged as:

$$y^{(p)}(t) = bu(t) + f(t) \tag{3.33}$$

where f is the total amount of internal and external disturbance with the unknown dynamics and $b = {}^{b_m}/_{a_n}$ where b is the gain of the controlled plant. The next step is to estimate the states of the controlled system with the ‘lumped’ disturbance which is unknown. To do so, an ESO should be implemented to the control structure.

$$
\begin{aligned}
z_1 &= y \\
z_2 &= \dot{y} \\
&\vdots \\
z_p &= y^{(p-1)} \\
z_{p+1} &= f
\end{aligned}
\tag{3.34}
$$

The fact that the assumption of extra state being differentiable made the expression $\dot{f} = h$. It will be used in:

$$
\begin{aligned}
\dot{z} &= A_e z + B_e u + E_e h, \\
y &= C_e z
\end{aligned}
\tag{3.35}
$$

where $z = \begin{bmatrix} z_1 & z_2 & \dots & z_p & z_{p+1} \end{bmatrix}^T$. Full form of system matrices are shown in below as:

$$
\begin{aligned}
A_e &= \begin{bmatrix} 0 & 1 & 0 & \cdots & 0 \\ 0 & 0 & 1 & \cdots & 0 \\ \vdots & \vdots & \vdots & \ddots & \vdots \\ 0 & 0 & 0 & \cdots & 1 \\ 0 & 0 & 0 & \cdots & 0 \end{bmatrix} \\
B_e &= [0 \quad 0 \quad \dots \quad b \quad 0]^T_{(p+1)\times 1} \\
E_e &= [0 \quad 0 \quad \dots \quad 0 \quad 1]^T_{(p+1)\times 1} \\
C_e &= [1 \quad 0 \quad 0 \quad \dots \quad 0]_{1\times(p+1)}
\end{aligned}
\tag{3.36}
$$

An observer should be constructed so that the estimated states can join the control loop as negative feedback. The aim of that process is to reduce the error at the output with the usage of estimated states within the control scheme.

$$
\begin{aligned}
\hat{\dot{z}} &= A_e \hat{z} + B_e u + L_0 (y - \hat{y}) \\
\hat{y} &= C_e \hat{z}
\end{aligned}
\tag{3.37}
$$

where L_0 is the observer gain vector.

$$L_0 = \begin{bmatrix} \beta_1 & \beta_2 & \cdots & \beta_p & \beta_{p+1} \end{bmatrix} \tag{3.38}$$

According to how effective design of the observer, the control scheme's efficacy varies.

It should be remembered that $\hat{z}_{p+1}(t) \cong f(t)$.

$$u(t) = \frac{u_0(t) - \hat{f}(t)}{b} \tag{3.39}$$

The dynamics of the plant changes after the submission of $u(t)$ into the plant equation as below.

$$\begin{aligned} y^{(p)}(t) &= b\left(\frac{u_0(t) - \hat{f}(t)}{b}\right) + f(t) \\ y^{(p)}(t) &= u_0(t) - \hat{f}(t) + f(t) \end{aligned} \tag{3.40}$$

Dependency of the design quality of ESO makes the plant an integral system which the order of the integral is p. That makes the system:

$$y^{(p)}(t) \approx u_0(t) \tag{3.41}$$

Now, the regulation of system response should be satisfactory. Hence, the controller design is based on state feedback:

$$u_0(t) = k_1\big(r(t) - y(t)\big) + k_2\big(\dot{r}(t) - \dot{y}(t)\big) + \cdots + k_p(r^{(p-1)}(t) - y^{(p-1)}(t)) \tag{3.42}$$

The value $r(t)$ related to the equation is the reference signal. It is assumed that the observer is perfectly operates, which means that the approximations of system states converges the real system states at close level. The term $u_0(t)$ substituted for the purpose of obtaining the control law:

$$u(t) = \frac{k_1\big(r(t) - \hat{z}_1(t)\big) + k_2\big(\dot{r}(t) - \hat{z}_2(t)\big) + \cdots + k_p\left(r^{(p-1)}(t) - \hat{z}_p(t)\right)}{b} - \frac{z_{p+1}(t)}{b} = K_O(\hat{r}(t) - \hat{z}(t)) \tag{3.43}$$

As $\hat{z}_1(t)$ through $\hat{z}_p(t)$ are outputs of ESO and approximately equal output $y(t)$ through $y^{(p-1)}(t)$, they are replaced into (3.14). The extended reference signal is expressed as $\hat{r}(t)$ which involves the reference signal and its derivates with the order up to $p-1$.

$$\hat{r}(t) = [r(t) \quad \dot{r}(t) \quad \cdots \quad r^{(p-1)}(t) \quad 0]^T \tag{3.44.a}$$

$$K_O = [k_1 \quad k_2 \quad \cdots \quad k_p \quad 1]/b \tag{3.44.b}$$

As a summary, the state – space form of the complete LADRC is:

$$\dot{\hat{z}}(t) = A_e\hat{z}(t) + B_e u(t) + L_O(y(t) - C_e\hat{z}(t))$$
$$\dot{\hat{z}}(t) = (A_e - L_O C_e)\hat{z}(t) + B_e u(t) + L_O y(t) \tag{3.45.a}$$

$$u(t) = K_O\big(\hat{r}(t) - \hat{z}(t)\big) \tag{3.45.b}$$

Even though various tuning methods are possible to apply, “bandwidth parametrization” method is used due to its simplicity. Obviously, two sets of parameters should be tuned: K_O, named as controller gain for the plant, and L_O, named as observer gain matrix for ESO. There two parameters are dependent on the controller bandwidth, w_C, and the observer bandwidth, w_O.

3.3.1 The Relation Between IMC and LADRC

The Laplace transform should be used initially to establish a link and dependency between LADRC and IMC (Tan & Fu, 2016). The result is:

$$s\hat{Z}(s) = A_e\hat{Z}(s) + B_eU(s) + L_O(Y(s) - C_e\hat{Z}(s)) \quad (3.46.a)$$

$$s\hat{Z}(s) = (A_e - L_OC_e)\hat{Z}(s) + B_eU(s) + L_OY(s) \quad (3.46.b)$$

$$U(s) = K_O\left(\hat{R}(s) - \hat{Z}(s)\right) \quad (3.46.c)$$

where $\hat{Z}(s)$ is the Laplace transform of $\hat{z}(t)$, and $\hat{R}(s)$ is the Laplace tranform of $\hat{r}(t)$. $\hat{R}(s)$ can be represented as:

$$\hat{R}(s) = [1 \quad s \quad s^2 \quad \dots \quad s^p \quad 0]^T R(s) \quad (3.47)$$

where $R(s)$ is the Laplace transform of the reference signal $r(t)$. Substitute 3.17.c into the equation 3.17.a :

$$s\hat{Z}(s) = (A_e - L_OC_e)\hat{Z}(s) + B_eK_O\left(\hat{R}(s) - \hat{Z}(s)\right) + L_OY(s) \quad (3.48.a)$$

$$s\hat{Z}(s) = (A_e - L_OC_e + B_eK_O)\hat{Z}(s) + B_eK_O\hat{R}(s) + L_OY(s) \quad (3.48.b)$$

3.19.b should be solved for $\hat{Z}(s)$ and be isolated so that the final $\hat{Z}(s)$ term can be obtained:

$$(sI - A_e + L_OC_e - B_eK_O)\hat{Z}(s) = B_eK_O\hat{R}(s) + L_OY(s) \quad (3.49)$$

The term in paranthesis which stands the left side of $\hat{Z}(s)$ represents a matrice. Thus, taking the inverse of the term then multiply from left side brings about the isolated form of $\hat{Z}(s)$:

$$\hat{Z}(s) = (sI - A_e + L_OC_e - B_eK_O)^{-1}B_eK_O\hat{R}(s) + \cdots \\ (sI - A_e + L_OC_e - B_eK_O)^{-1}L_OY(s) \quad (3.50)$$

Substitute $\hat{Z}(s)$ into $U(s) = K_O(\hat{R}(s) - \hat{Z}(s))$:

$$U(s) = K_O[\hat{R}(s) - (sI - A_e + L_O C_e - B_e K_O)^{-1} B_e K_O \hat{R}(s) - \cdots \\ (sI - A_e + L_O C_e + B_e K_O)^{-1} L_O Y(s)] \tag{3.51}$$

Expansion of the equation above is needed by multiplying all terms with K_O:

$$U(s) = K_O \hat{R}(s) - K_O(sI - A_e + L_O C_e - B_e K_O)^{-1} B_e K_O \hat{R}(s) - \cdots \\ K_O(sI - A_e + L_O C_e + B_e K_O)^{-1} L_O Y(s) \tag{3.52}$$

$K_O \hat{R}(s)$ term should be placed in common paranthesis as below:

$$U(s) = [1 - K_O(sI - A_e + L_O C_e + B_e K_O)^{-1} B_e] K_O \hat{R}(s) - \cdots \\ K_O(sI - A_e + L_O C_e + B_e K_O)^{-1} L_O Y(s) \tag{3.53}$$

Due to the complexity of the expressions in the equation, there is a need to simplify the equation as:

$$U(s) = C_1(s) F_r(s) R(s) - C_2(s) Y(s) \tag{3.54.a}$$

$$C_1(s) = 1 - K_O(sI - A_e + L_O C_e + B_e K_O)^{-1} B_e \tag{3.54.b}$$

$$C_2(s) = K_O(sI - A_e + L_O C_e + B_e K_O)^{-1} L_O \tag{3.54.c}$$

$$F_r(s) = K_O[1 \quad s \quad s^2 \quad \ldots \quad s^p \quad 0]^T \tag{3.54.d}$$

For the case of analysis and tuning, it should be demonstrated that the equiavalence of TDF-IMC. The key point is that the conventional LADRC structure can be changed into the TDF-IMC as in Figure 3.3 structure:

$$P_0 = C_e(sI - A_e)^{-1} B_e \tag{3.55}$$

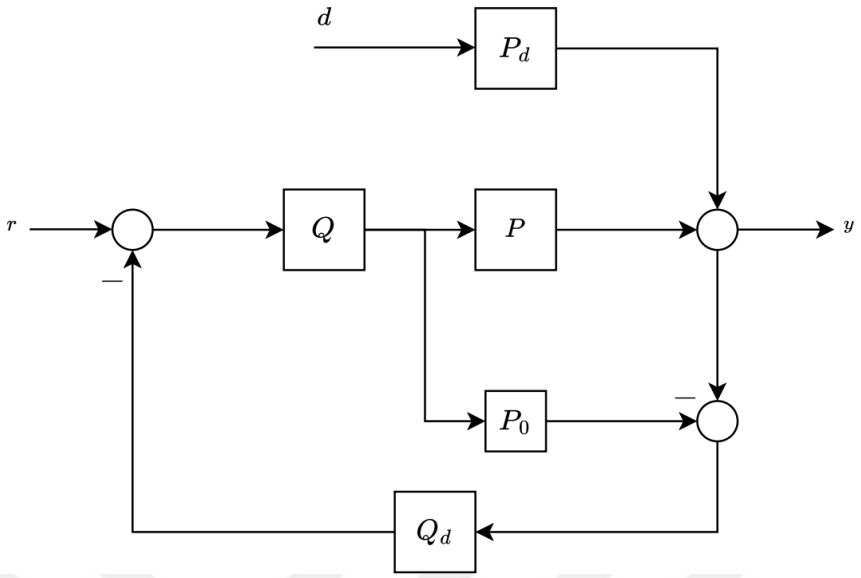

Figure 3.3. The Block Diagram of LADRC With IMC Structure

The set point tracking IMC controller, and the disturbance-rejection IMC controller are respectively:

$$Q = (1 - K_0(sI - A_e + B_e K_0)^{-1} B_e) F_r(s) \quad (3.56.a)$$

$$Q_d = K_0(sI - A_e + L_0 C_e)^{-1} L_0 / F_r(s) \quad (3.56.b)$$

The proof for P_0, Q and Q_d are discussed at Appendix B section.

3.3.2 Tuning of Linear Active Disturbance Rejection with IMC

The bandwidth parametrization methods includes parameters that are observer bandwidth and control bandwidth. In this section, the main components of LADRC-IMC structure will be demonstrated in the form of transfer function.

There are three steps for the design procedure of TDF-IMC structure:

1. Decompose the plant model P_0 in two parts; the invertible part P_M (minimum phase) and the allpass part P_A (non-minimum phase with unity magnitude part).

$$P_0(s) = P_M(s).P_A(s) \tag{3.57}$$

2. Design a setpoint tracking IMC controller where λ is a tuning parameter such that the desired setpoint response is $\frac{1}{(\lambda s+1)^r}$ and r is the relative degree of $P_M(s)$.

$$Q(s) = {P_M}^{-1}(s)\frac{1}{(\lambda s+1)^r} \tag{3.58}$$

3. Design a disturbance - rejecting IMC controller $Q_d(s)$ as :

$$Q_d(s) = \frac{a_m s^m + \cdots + a_1 s + 1}{(\lambda_d s+1)^{r_d}} \tag{3.59}$$

where m is the number of poles of $P_0(s)$ that $Q_d(s)$ should need to cancel and λ_d is a tuning parameter for the disturbance rejection filter $\frac{1}{(\lambda_d s+1)^{r_d}}$ with order $r_d \geq m$. Suppose $p_1, \dots, p_m$ are the poles to be canceled, then $a_1, \dots, a_m$ should satisfy the condition:

$$\left(1 - P_0(s)Q(s)Q_d(s)\right)|_{s=p_1,\dots,p_m} = 0 \tag{3.60}$$

For LADRC, it is noticeable that the nominal plant in TDF-IMC for a pth-order LADRC is simply a pth-order integral model. That is why the plant model can be expressed as:

$$P_0 = C_e(sI - A_e)^{-1}B_e = \frac{b}{s^p} \tag{3.61}$$

Hence the plant model is invertible, setpoint-tracking controller for LADRC can be designed as:

$$\tilde{Q} = \frac{s^p}{b} \times \frac{1}{(\lambda s + 1)^p} \tag{3.62}$$

And the disturbance rejecting IMC controller for LADRC is:

$$\tilde{Q}_d = \frac{a_p s^p + \cdots + a_1 s + 1}{(\lambda_d s + 1)^{p+1}} \tag{3.63}$$

The order of disturbance rejecting filter is chosen $p + 1$ so that it becomes related to the order of ESO for pth-order LADRC.

The expansion of $1 - P_0 \tilde{Q} \tilde{Q}_d$ can be written as:

$$P_0 \tilde{Q} \tilde{Q}_d = \frac{a_p s^p + \cdots + a_1 s + 1}{(\lambda_d s + 1)^p (\lambda_d s + 1)^{p+1}} \tag{3.64.a}$$

$$1 - P_0 \tilde{Q} \tilde{Q}_d = \frac{(\lambda_d s + 1)^p (\lambda_d s + 1)^{p+1} - (a_p s^p + \cdots + a_1 s + 1)}{(\lambda_d s + 1)^p (\lambda_d s + 1)^{p+1}} \tag{3.64.b}$$

The expansion of $1 - P_0 \tilde{Q} \tilde{Q}_d$ shows that the numerator of the expression must have p zeros at the origin to cancel the poles of P_0 because P_0 is a pth-order integral model. That is why, a_i terms are the coefficients of s^i in the expansion of the polynomial term, $(\lambda_d s + 1)^p (\lambda_d s + 1)^{p+1}$. The further derivations in (Tan & Fu, 2016) proves that:

$$w_C = \frac{1}{\lambda}, w_O = \frac{1}{\lambda_d} \tag{3.65}$$

The key point is the bandwidths of LADRC are the inverse of two time constants. The controller bandwidth w_C, in LADRC structure is the inverse of the time constant λ and the observer bandwidth w_O, in LADRC structure is the inverse of the time constant λ_d.

The following procedure should be applied for tuning LADRC via IMC:

- Determine the order p of LADRC.
- Determine the desired tracking performance of the closed loop system by choosing λ.
- Estimate the gain b for the controlled plant. If the plant model is given, it is optional that b can be computed using the model.
- Determine the disturbance-rejection filter constant λ_d, so that the closed loop is stable and has the desired disturbance rejection performance.
- Let $w_C = \frac{1}{\lambda}$ and $w_O = \frac{1}{\lambda_d}$

The adjustments above leads to guaranteed tracking performance and then improves the disturbance rejection capability with the trade-off for robustness by tuning λ_d or b. In order to make the system more robust two possible choices can be followed:

- Increase the gain b
- Increase the time constant λ_d

3.4. Fractional-Order Linear Active Disturbance Rejection Control (FOLADRC)

In the realm of control engineering, the quest for ever more accurate and robust control strategies continues unabated. Engineers and scientists have tirelessly explored various methodologies to address the complexities of modern control systems. Fractional order systems and fractional order calculus have been studied by many researchers in the past two decades thanks to the expressing ability of the real world more detailed. Hence, it caused emerging new idea whether it can be a part of the controller structure. An innovation that has garnered significant attention and relevance in recent years is the Fractional Order Linear Active Disturbance Rejection (FOLADRC).

Control systems are essential components in countless industries, from aerospace and automotive to manufacturing and healthcare. The primary objective of any control system is to regulate the behavior of a dynamic process, ensuring it follows a desired trajectory or setpoint while rejecting external disturbances. Traditional control techniques, such as Proportional-Integral-Derivative (PID) controllers, have long been employed to achieve this objective. However, as systems become more complex, nonlinear, and uncertain, the need for more advanced control strategies becomes apparent. FOLADRC is a novel control technique that brings a fresh perspective to the field. It combines the power of fractional calculus, active disturbance rejection control, and linear control to deliver enhanced performance and robustness. One of the approaches come up with the idea which could be incorporated with the observer structure in (Pacheco, Duarte-Mermoud, Aguila-Camacho, & Castro-Linares, 2017). This paper proves that a single input single output, integer order system states can be tracable with fractional order Luenberger observer which is also a part of LADRC.

The fractional order observer should be initially examined using the preliminaries for fractional calculus. The premise of fractional calculus is that a key component of the generalization that it suggests is the extension of differointegral operators to non-integer orders. Fractional calculus is an extension of the classical calculus, where differentiation and integration of non-integer order are considered. Instead of dealing exclusively with integer orders, fractional calculus encompasses a broader spectrum of orders, including non-integer values. This extension allows engineers to capture more complex dynamics and better model certain physical phenomena. In FOLADRC, fractional calculus plays a pivotal role in defining the fractional order controller, which exhibits unique properties compared to classical integer order controllers.

The two primary reasons for employing fractional calculus in the field of control engineering are as follows: The first reason is that fractional-order models, in contrast to integer models, offer a more accurate representation of the dynamics inherent in complex systems. The second objective is to surpass the performance of filter structures and integer-order control systems.

FOLADRC has found applications in various fields, including but not limited to: 1) Aerospace: FOLADRC can enhance the stability and maneuverability of aircraft, making it invaluable in flight control systems. 2) Robotics: Robotic systems benefit from FOLADRC's ability to track desired trajectories while compensating for external forces. 3) Process Control: Industries such as chemical processing and manufacturing leverage FOLADRC to improve the precision and efficiency of their control systems. 4) Biomedical Engineering: FOLADRC aids in the precise control of medical devices and patient-specific therapies.

The non-integer order differintegration can be expressed in a standardised manner as:

$$ {}_aD_t^{\beta} = \begin{cases} \dfrac{d^{\beta}}{dt^{\beta}} & Re(\beta) > 0 \\ 1 & Re(\beta) = 0 \\ \displaystyle\int_a^t (d\tau)^{(-\beta)} & Re(\beta) < 0 \end{cases} \tag{3.66} $$

where $\beta \in R$ denotes the order of the operator, and D_t^{β} stands for the fractional integrodifferential operation. The parameters a and t specify the bound of the operation. The definitions known as Caputo and Riemann-Liouville are widely used definitions for fractional operators (Monje et al., 2010). The Caputo type fractional derivative can be demostrated as:

$$ D^{\beta} f(t) = \frac{1}{\Gamma(n-\beta)} \int_0^t \frac{f(\tau)}{(t-\tau)^{\beta+n+1}} d\tau \tag{3.67} $$

where $\Gamma(n) = \int_0^{\infty} t^{z-1} e^{-t} dt$ is given with integer order n, $n-1 \leq \beta \leq n$. Further; $\beta = 1$, $\beta \leq 0$, $\beta \geq 0$, gives a first-order derivative, fractional-integration, and fractional-differentiation, respectively. The Riemann-Lionville equation (RL) definition is used in this study to explain fractional differentiation as follows:

$$ {}_{t_0}D_t^{\beta} f(t) = \frac{1}{\Gamma(n-\beta)} \frac{d^n}{dt^n} \int_0^t \frac{f(\tau)}{(t-\tau)^{\beta+n+1}} d\tau \tag{3.68} $$

Furthermore, the Riemann-Liouville (RL) integration may be defined:

$$ {}_{t_0}I_t^{\beta} f(t) = {}_{t_0}D_t^{-\beta} f(t) = \frac{1}{\Gamma(\beta)} \int_{t_0}^t \frac{f(\tau)}{(t-\tau)^{1-\beta}} d\tau \tag{3.69} $$

Active Disturbance Rejection Control (ADRC) is a control technique that emerged to address the challenges posed by disturbances in control systems. ADRC models disturbances as dynamic entities and employs an extended state observer (ESO) to estimate these disturbances in real-time. By doing so, it decouples the control system from the disturbances, making it highly robust and adaptable to varying operating conditions. FOLADRC borrows the concept of ADRC and integrates it with fractional calculus to achieve disturbance rejection with even greater precision and efficiency.

At the heart of FOLADRC lies the fractional order controller, which is responsible for shaping the control input based on the error and its fractional derivatives. The FOLADRC framework can be summarized in the following steps: I) System Modeling: Begin by modeling the plant dynamics and disturbances. This typically involves deriving the fractional order transfer function of the system. II) Fractional Order Controller Design: Determine the fractional order controller based on the system's characteristics and control objectives. This step involves selecting the fractional order (e.g., 0.8, 1.5) and tuning controller parameters. III) Extended State Observer (ESO): Implement an ESO to estimate and compensate for disturbances in real-time. The ESO observes both the system states and the fractional derivatives of the disturbances. IV) Feedback Control: Combine the output of the fractional order controller with the ESO's disturbance estimate to generate the control input to the system. V) Performance Assessment: Evaluate the control system's performance in terms of tracking accuracy, disturbance rejection, and robustness. Fine-tune the controller parameters if necessary.

A fractional-order observer is designed, featuring a rigorous theoretical proof of its convergence guarantees. A series of comprehensive simulations is conducted to juxtapose its performance against the conventional integer-order Luenberger state observer. The results highlight notable advantages associated with the proposed fractional-order observer, specifically in terms of enhanced error convergence speed and superior resilience to high-frequency disturbances.

3.4.1. Fractional-order Luenberger observer

While classical observer theory is well-established and extensively researched, the investigation of observers with orders that do not precisely match those of the observed system remains an underexplored area, constituting the primary contribution of this paper. More specifically, this paper delves into the exploration of Fractional-Order (FO) observers for linear, Integer-Order (IO), and Single-Input Single-Output (SISO) dynamic systems with known parameters. This study reveals several notable advantages of the proposed FO observer over the traditional IO Luenberger observer, particularly in terms of error convergence rates and the mitigation of high-frequency disturbances.

Designing Fractional-order State Observers for Integer-Order Linear Systems involves adapting fractional-order calculus concepts to estimate the unmeasured states of a dynamic system that can be described by integer-order linear equations. The ESO in FOLADRC is designed to estimate both the states of the system and the fractional derivatives of the disturbances. It uses an extended state vector to capture these estimates.

State Estimation: The ESO employs a dynamic model of the system to estimate the internal states, typically based on the system's fractional order transfer function.

Disturbance Estimation: The ESO also estimates the disturbance, including its fractional derivatives, by comparing the predicted system output with the actual output.

Let's contemplate the Linear Time-Invariant (LTI), Single-Input Single-Output (SISO), Integer-Order (IO) system (3.5) with well-defined parameters. We also have the observer presented in (3.7), which shares the same structure as the conventional Luenberger state observer but incorporates Fractional-Order (FO) derivatives.

A schematic diagram of the fractional-order observer is presented in Figure 3.4.

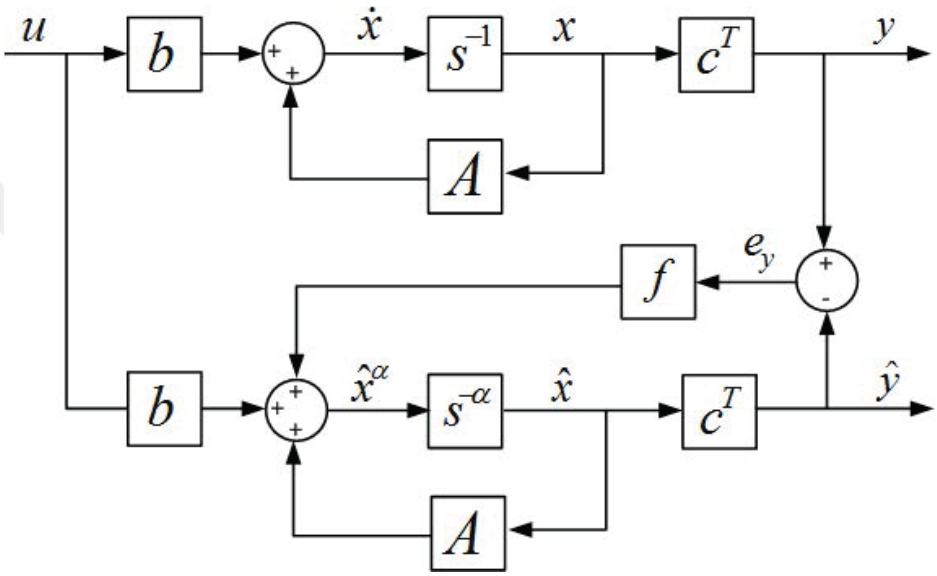

Figure 3.4. The Block Diagram of Fractional-Order Luenberger Observer

The expression (3.70) gives the Laplace domain representation of an integer-order system and (3.71) corresponds to the FO Luenberger observer.

$$X(s) = (sI - A)^{-1}(bU(s) + x_0) \tag{3.70}$$

$$\hat{X}(s) = [s^{\alpha}I - (A - fc^{T})]^{-1}(bU(s) + fc^{T}X(s) + \sum_{k=1}^{m}(\hat{x}_0{}^{(k-1)}\, s^{\alpha-k})) \tag{3.71}$$

The subtraction of (3.70) from (3.71) yields the Laplace domain representation of the state estimation error dynamics, as depicted in (3.73).

$$E_x(s) = \left[(sI - A)^{-1} - \left(s^{\alpha}I - (A - fc^T)\right)^{-1}(I + fc^T(sI - A)^{-1})\right]bU(s) + \left[(sI - A)^{-1} - \left(s^{\alpha}I - (A - fc^T)\right)^{-1}\right]x_0 + \left(s^{\alpha}I - (A - fc^T)\right)^{-1}\sum_{k=1}^{m}(\hat{x}_0{}^{(k-1)}\, s^{\alpha-k}) \quad (3.72)$$

From equation (3.72), it is evident that the dynamics of the estimation error are influenced by the system input $u(t)$, which prevents its asymptotic convergence to zero for arbitrary inputs and initial conditions. Furthermore, the expression of the estimation error involves multiple orders of derivatives, making (3.72) a system of non-commensurate order. Consequently, due to the challenge in factorizing (3.72) and analyzing it in terms of the estimation error $e_x(t)$, we will assess the stability of (3.72) by individually considering each term.

The selection of the α value in the design of the Fractional-Order (FO) observer is not unique, and it is primarily contingent upon the anticipated performance requirements of the observer. For instance, if the objective is to achieve rapid convergence in state estimation, a lower α value within the range of [0.3, 0.9] would be preferred. Conversely, if the goal is to mitigate the impact of external perturbations on state estimation, an α value greater than [0.9 1.1] will significantly diminish the effects of the disturbance with a frequency of 10 rad/sec. In general, the choice of the α value is closely tied to the selection of an appropriate performance criterion.

4. THE EXPERIMENTAL SETUP

This section presents the setups for real-time experiments conducted to validate the proposed control strategies. The systems utilized in experimental applications comprise an electromechanical system.

4.1. Electromechanical System

Electromechanical systems find widespread application in various industrial sectors, including robot control, manufacturing processes, and automotive applications. Moreover, these systems serve as essential platforms for testing innovative control strategies and facilitating control system education. To evaluate the proposed control algorithms, an electromechanical system is utilized, comprising a direct current (DC) motor connected to a tachogenerator via a shaft. The shaft is equipped with several sensors and transducers, representing the load on the shaft. Figure 4.1 illustrates a schematic representation of the system.

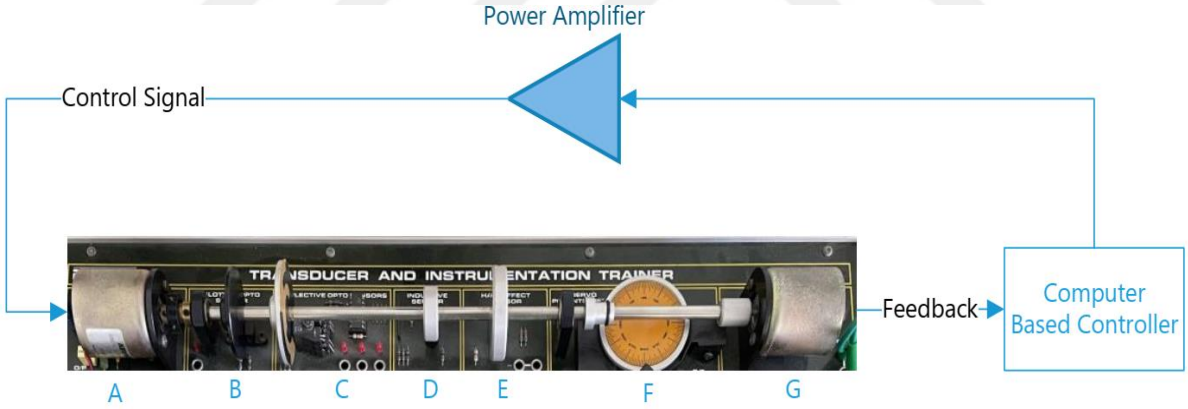

Figure 4.1. Electromechanical System.

The sensors and transducers given in Figure 4.1 are presented as in Table 4.1.

Table 4.1. Sensors and transducers with electromechanical system

Label	Equipment	Label	Equipment
A	DC motor	E	Hall effect sensor
B	Slotted optos sensor	F	Servo potentiometer
C	Reflective opto sensor	G	Tachogenerator
D	Inductive sensor	E	Hall effect sensor

As depicted in Figure 4.1, a DC motor system is mounted on a DIGIAC 1750 control training set. The motor propels a shaft equipped with various sensors, transducers, and a tachogenerator. The slotted-opto transducer is utilized to measure shaft speed during the experiments. Additionally, the tachogenerator, generating voltage in accordance with the shaft speed, serves as a speed transducer.

4.2. Modeling of the Electromechanical System

The modeling and control of electromechanical systems have garnered significant attention in the control community due to their prevalence in a wide array of applications. Direct Current (DC) motors, in particular, find application in various industrial control scenarios, including disk motion control, liquid pumping, and position control of robotic manipulators (İ. Eker, 2004). Moreover, DC motors offer several advantages such as easy position/speed regulation, a simple structure, and low maintenance requirements. A multitude of studies are dedicated to the position and velocity control of DC motors, aiming to achieve set-point regulation, tracking accuracy, robustness, and energy efficiency.

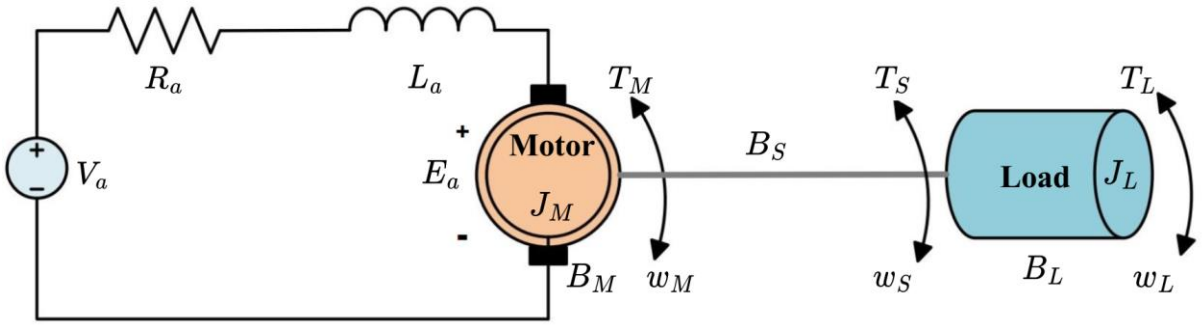

Figure 4.2. The Representation of Electromechanical System.

The schematic diagram of the system is presented in Figure 4.2, and the corresponding parameters are outlined in Table 4.2.

Table 4.2. DC motor parameters

Parameter		**Parameter**	
V_a	Armature voltage	R_m	Viscous friction
L_a	Armature inductance	K_m	Torque coefficient
R_a	Armature resistance	T_m	Generated motor torque
i_a	Armature current	T_D	External load disturbance
T_S	Nonlinear friction	T_f	Transmitted shaft torque
J_M, J_L	Moments of inertia	ω_M, ω_L	Rotational speeds

The dynamic equations of the electromechanical system are provided as follows:

$$V_a = L_a \frac{d}{dt} i_a(t) + R_a i_a(t) + K_m \omega_m(t) \tag{4.1}$$

$$J_m\left(\frac{d}{dt}\omega_m(t)\right) = T_m(t) - T_s(t) = R_m\omega_m(t) - T_f(\omega_m) \tag{4.2}$$

$$T_s(t) = k_s(\theta_m(t) - \theta_L(t) - B_s(\omega_m(t) - \omega_L(t)) \tag{4.3}$$

$$\frac{d}{dt}\theta_m(t) = \omega_m(t), \qquad \frac{d}{dt}\theta_L(t) = \omega_L(t) \tag{4.4}$$

where DC motor parameters are given in Table 4.2.

Model of the nonlinear friction $T_f(\omega)$ can be considered as an asymmetrical characteristic as:

$$T_f(\omega) = \left(a_0 + a_1 e^{-a_2|\omega|}\right)sgn1(\omega) + \left(a_3 + a_4 e^{-a_5|\omega|}\right)sgn2(\omega) \tag{4.5}$$

where $a_1 \ldots a_5$ are positive constants and $a_0 \neq a_3$, $a_1 \neq a_4$, $a_2 \neq a_5$ and the signum functions are defined as:

$$\begin{aligned} sgn1(\omega) &= \begin{Bmatrix} 1 & if & \omega \geq 0 \\ 0 & if & \omega \leq 0 \end{Bmatrix} \\ sgn2(\omega) &= \begin{Bmatrix} 0 & if & \omega \geq 0 \\ -1 & if & \omega \leq 0 \end{Bmatrix} \end{aligned} \tag{4.6}$$

Figure 4.3 illustrates the block diagram of the system. The model incorporates certain parameters, such as friction and mechanical structure resonance, which require additional clarification. Determining the precise values of all these parameters is a laborious task. Additionally, the presence of parametric uncertainties can result in performance degradation in tracking tasks. Therefore, ADRC methods are preferred to effectively manage these uncertainties.

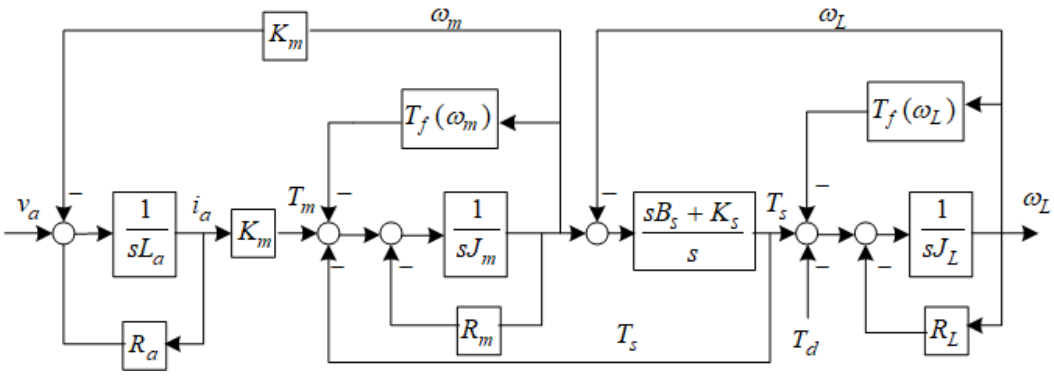

Figure 4.3. Block Diagram of the Electromechanical System.(Özbek, 2018)

It is clear that constructing a precise parametric model of the actual system is a time-consuming operation. Thus, the goal is to use real-time identification techniques to create a model that describes the electromechanical system. Furthermore, the parameter uncertainties degrade tracking task performance.

The specifications of the DC motor are outlined in Table 4.3, with the parameters derived from a series of experiments. The input voltage applied to the motor and the corresponding output voltage of the tachogenerator are measured and summarized in Table 4.4.

Table 4.3. DC motor systems parameters

Armature Resistance	6.2 Ω
No load current	120 mA
Stall current	1.93 A
Starting torque	7 Ncm/A
Torque constant	3.5 Ncm/A
Efficiency	70%-80%
Shaft speed at no load	2400 rpm (max)

Table 4.4. DC motor system responses to different input signals

Shaft Speed (rpm)	Tachagenarator output voltage (V)
600	2.37
800	3.03
900	3.39
1200	4.48
1500	5.52
1800	6.71

Obtaining parameters for dynamical equations poses a significant challenge, and control designers consistently require an accurate model to achieve satisfactory closed-loop control performance. However, the intricate nature of most physical systems makes the development of precise models a tedious task. Consequently, an appropriate approximated model must be derived using various system identification techniques. In this study, the identification problem is approached as linear time-invariant (LTI) to obtain a suitable model. The model's validity is assessed by comparing the actual system output with the predicted model output, aiming to ensure that the model generates responses akin to measured output responses (İ. Eker, 2004)(Kara & Eker, 2004). System identification, a critical aspect for control engineers, is defined as the art of constructing mathematical models of dynamic systems based on observed input-output data. Numerous innovative system identification tools have been developed thus far. In the current work, an interactive software tool, highlighted in (Ozbek & Eker, 2015), is employed.

The process reaction curve serves as a widely accepted tool for elucidating the characteristic properties of a system under diverse conditions. Moreover, various dynamic properties,

including rise time, settling time, and time constant, can be directly derived from the system. To establish the plant model, the armature of the DC motor is stimulated with a step input of 5.20 V magnitude, and the resulting shaft speed is measured in revolutions per minute (RPM). The output voltage generated by the tachogenerator is recorded at 4.48 V, approximately corresponding to a shaft speed of 1200 RPM. This information is then used to approximate a second-order model as follows:

$$G(s) = \frac{644.1}{s^2 + 118.69s + 783.57} \tag{4.7}$$

4.3. Data Acquision Process for Experimental Setup

Data transmission from the experimental setup to the computer is facilitated through the National Instrument 6229 M Series data acquisition card (DAQ). All calculations and controller design processes are carried out using Matlab/Simulink. The specifications of the DAQ board for the electromechanical system are detailed in Table 4.5.

Table 4.5. National Instrument NI 6229 M Series DAQ board.

Analog Input	**Channels**	**32 SE/16Diff**
	Sampling Rates	250 kS/s (kilo samples per second)
	Resolution	16 bits
	Unipolar Input (V)	0~10,0~5,0~1,0~0.2
	Bipolar Inputs	±10,5,1,0.2
Analog Output	Channels	4
	Resolution	16 bits
Digital I/O	Digital Input Channels	16

	Digital Output Channels	32
General	Bus	PCI/PXI
Timer/Counter	Resolution	32 bits
	Time Base	80 MHz, 20MHz, 0.1 MHz
	Channels	2

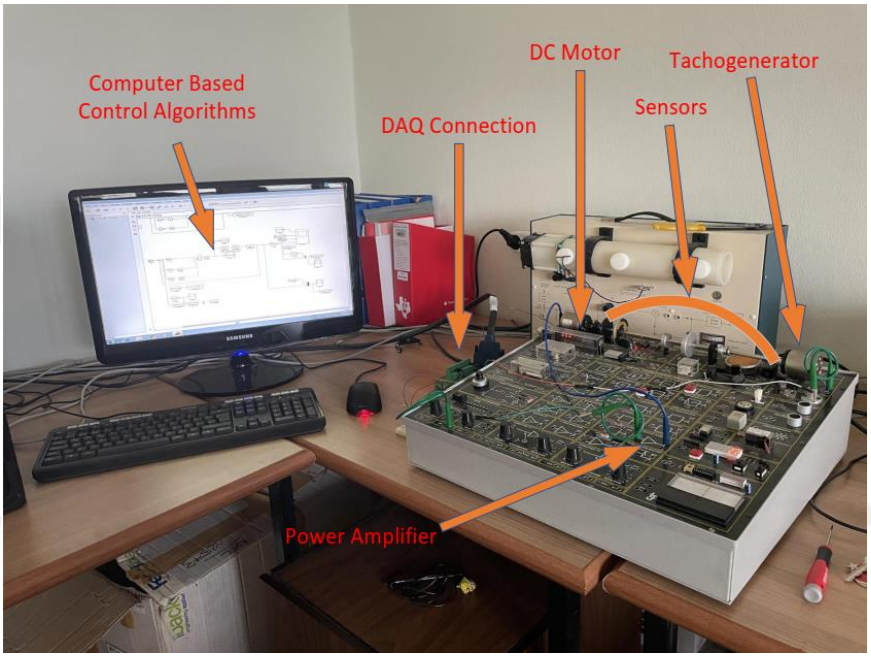

Figure 4.4. The Scene of the Laboratory.

A snapshot of the laboratory environment is depicted in Figure 4.4, where the DC motor is linked to various sensors and the tachogenerator through the shaft.

The simulations and experimental realizations are conducted using the Matlab/Simulink software platform. The controller output is applied within the range of [0V,12V], considering the operating limits of the actual electromechanical system. A sampling interval of 5ms is set, and the output position of the DC motor is acquired through the tachogenerator. Figure 4.5 illustrates the experimental setup, wherein the actual plant is connected to the PC via a PCI

terminal using a multifunction data acquisition (DAQ) board. RS232 series communication is employed for real-time applications.

Real-Time Workshop is utilized to generate C++ source code. Subsequently, the code is compiled to produce an executable program that functions as a controller. Concurrently, Real-Time Windows Target, facilitating interaction with the hardware device through I/O, allows bidirectional control of data flow between the controller and the real system. This application offers several advantages. For example, the control designer need not worry about the communication mechanism of the actual control system while constructing the control scheme using Simulink® tools.

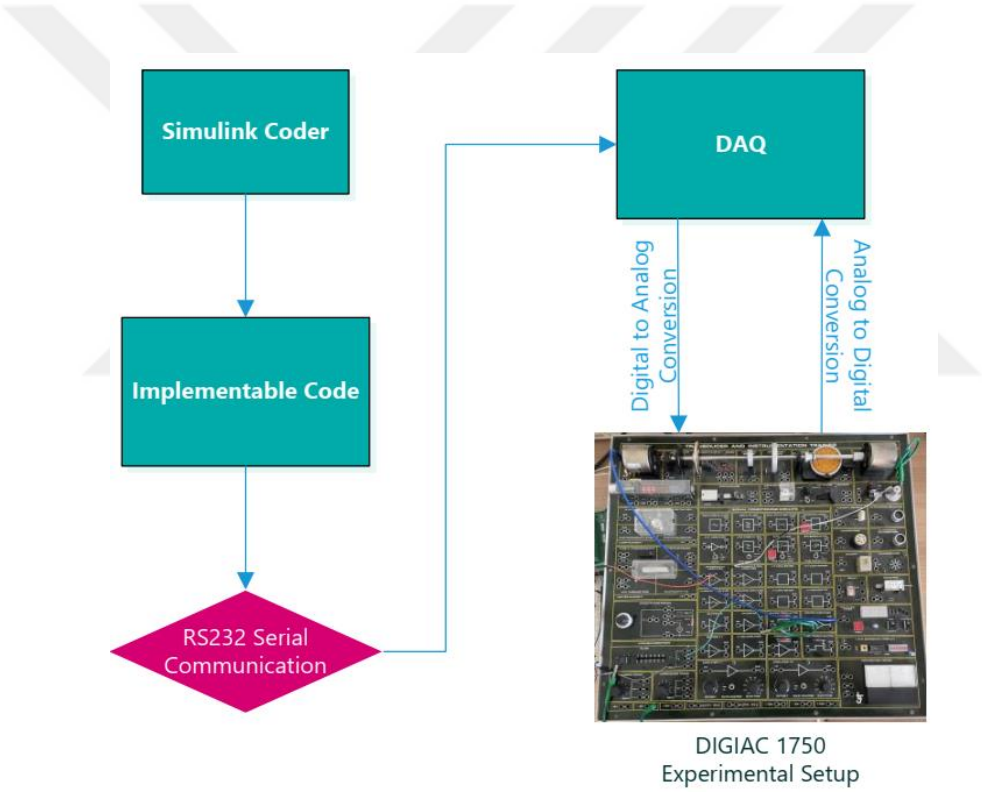

Figure 4.5. Experimental Environment.

5. RESULTS AND DISCUSSION

This chapter includes the test results of real time experimental applications. Aforementioned methods in previous chapter contains the methods, which applied to the system to be controlled in experimental study as follows:

- LADRC
- ELADRC
- LADRC with IMC
- FOLADRC

In order to demonstrate the the superiority and comparison between the studied control methods; three types of test was applied to electromechanical system:

- Step Response Test
- Disturbance Rejection Test
- Tracking Test

The rise time, settling time and overshoot values were also investigated and examined in the applied control methods. The low pass filter $s/(s+90)$ was used in order to improve the performance of the applied control techniques.

5.1. LADRC Applications and Results

LADRC controller was chosen first to apply to the system to be controlled. LADRC has six different parameters as mentioned before which are T_s, w_C, w_O, β, K_P and K_D. These parameters were determined first then applied to the electromechanical system. The calculation of the parameters was carried out just before the experiment, and the experimental process was carried out with these parameters.

5.1.1. Step Test

The parameters are calculated to be $T_s = 0.5\ sec$, $w_C = 12$, $w_O = 120$, $\beta = 210$, $K_P = 144$ and $K_D = 24$. A low pass filter is used at the output of the system to be controlled in order to constitute the feedback signal. The result of transient response is shown in the Figure 5.1 and the whole response signal is shown in Figure 5.2. Also, the control signal in corformity with the total step response is given in the Figure 5.3 and the error signal that corresponds with the total step response is given in the Figure 5.4.

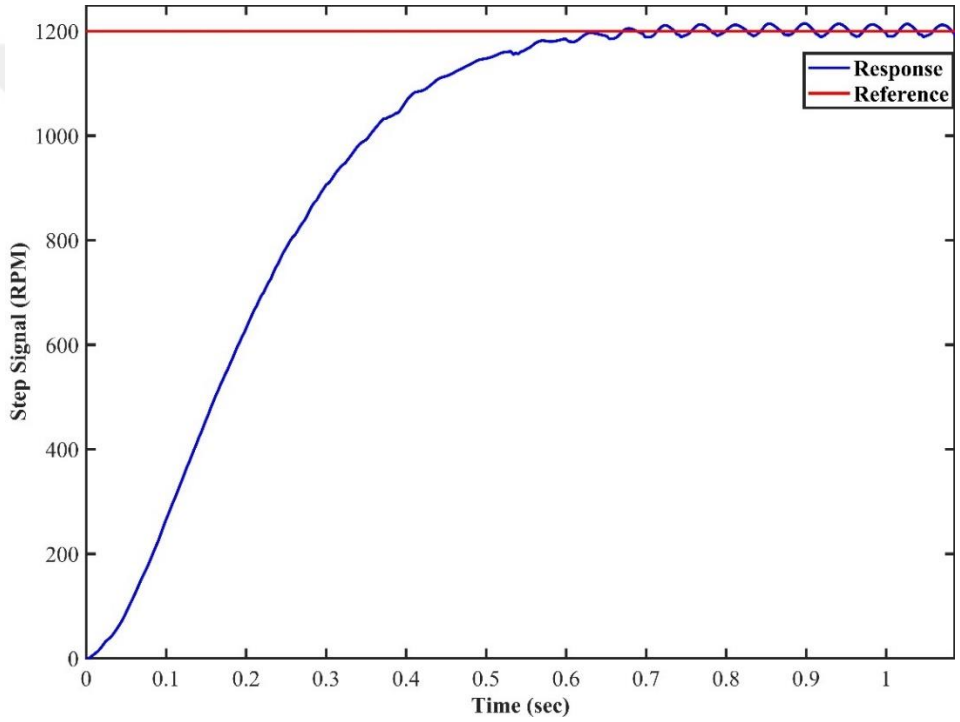

Figure 5.1. The Transient Performance of LADRC

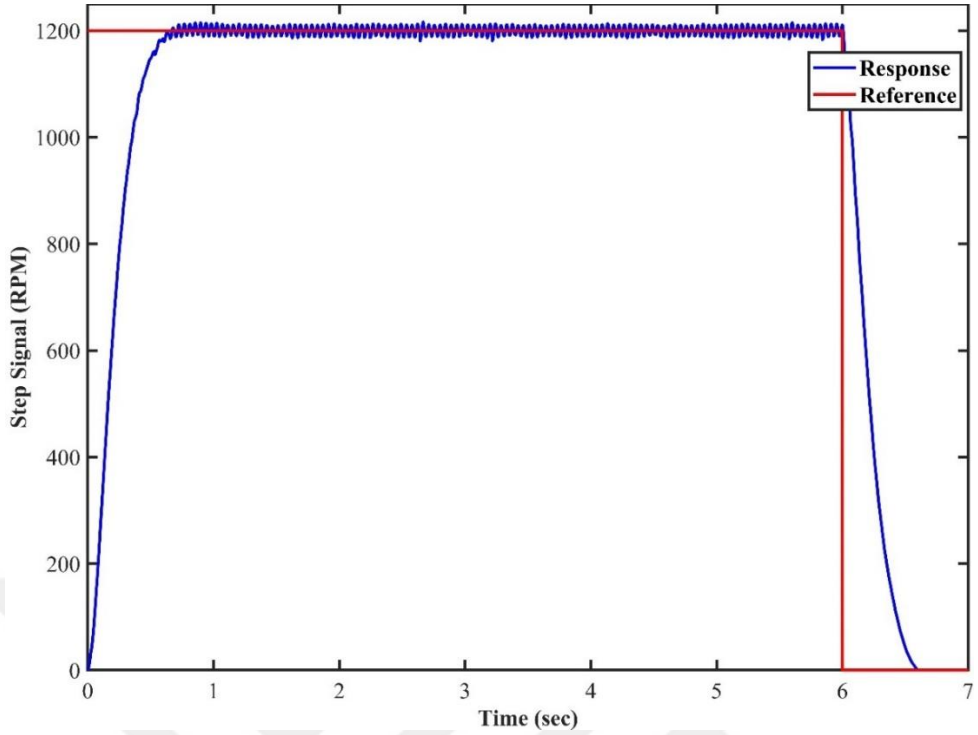

Figure 5.2. The Step Signal Graph of LADRC

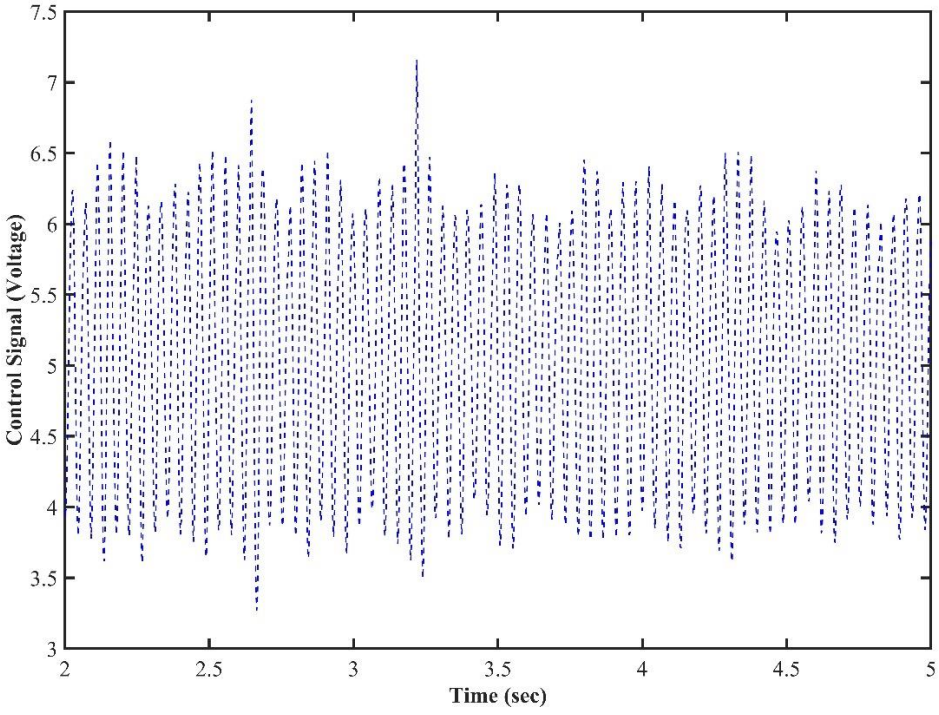

Figure 5.3. The Control Signal Graph of LADRC

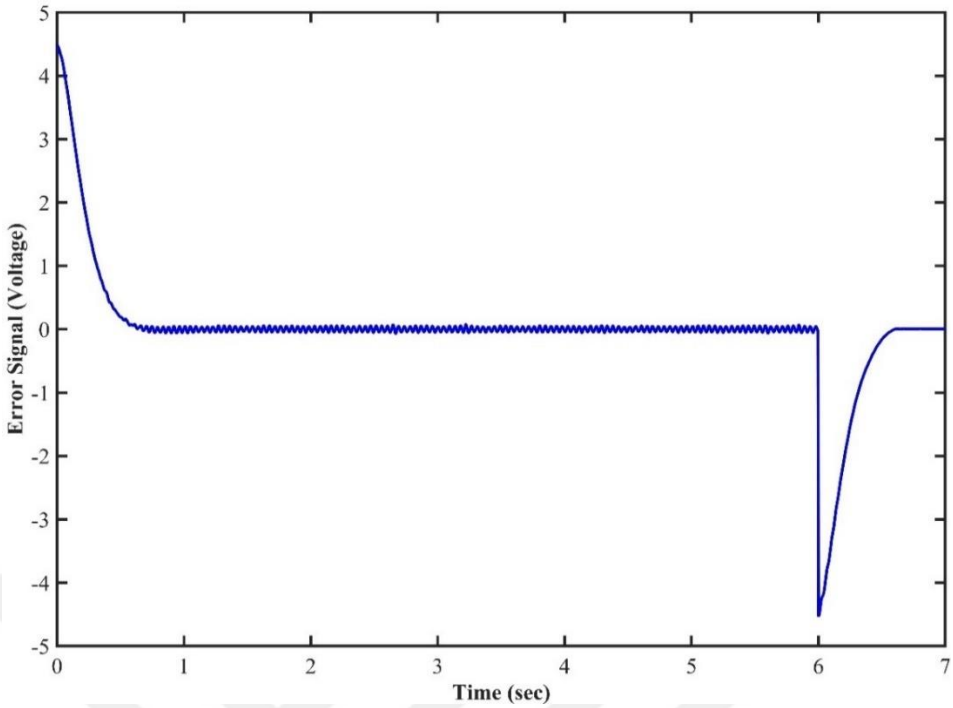

Figure 5.4. The Error Signal Graph of LADRC

No overshoot is observed on the system output signal of the applied LADRC algorithm. Moreover, the tabulated results include rise time, settling time, overshoot and output deviation are demonstrated in Table 5.1.

Table 5.1. The transient values correspond to LADRC

	Rise Time	Settling Time	Overshoot	Output Deviation
LADRC	0.363 sec	0.561 sec	No overshoot	±8.0 rpm

5.1.2. Disturbance Rejection Test

Input disturbance was applied to the system as an addition of 0.22 V, which is 5% of 4.48 V, from the control input channel. As a result, the performance graph of disturbance rejection capability of LADRC was observed. A voltage of 0.22V is applied to the system for a duration of 3 seconds, starting at 3 seconds. The result are shown in the Figure 5.5 with the control signal in the Figure 5.6 and error signal in the Figure 5.7.

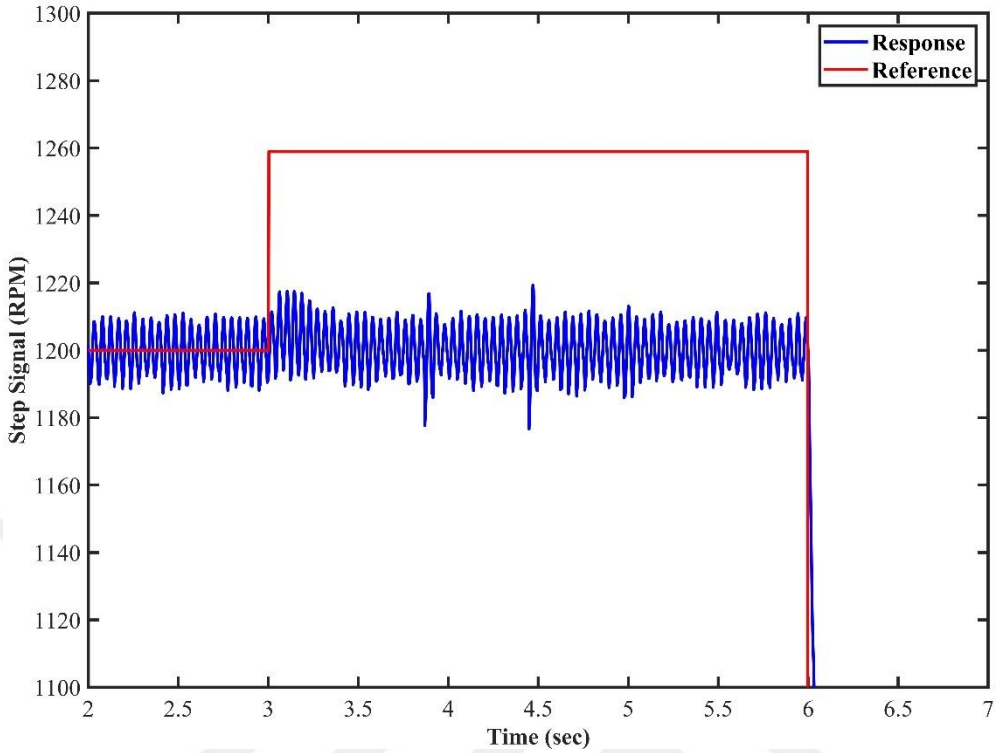

Figure 5.5. The Disturbance Rejection Performance of LADRC

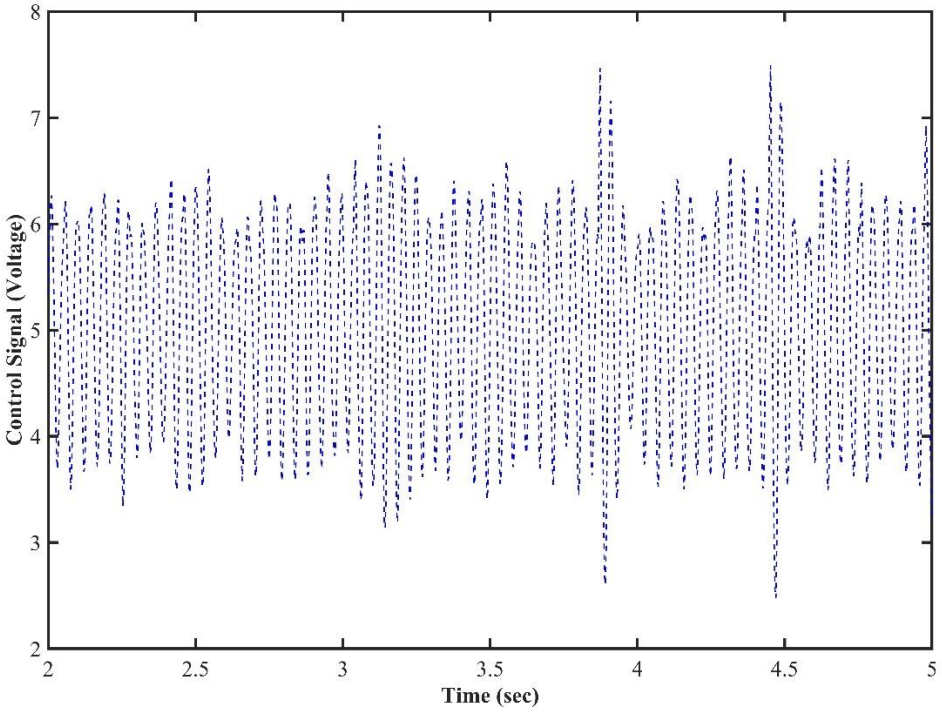

Figure 5.6. The Control Signal Graph of LADRC When Input Disturbance Exists

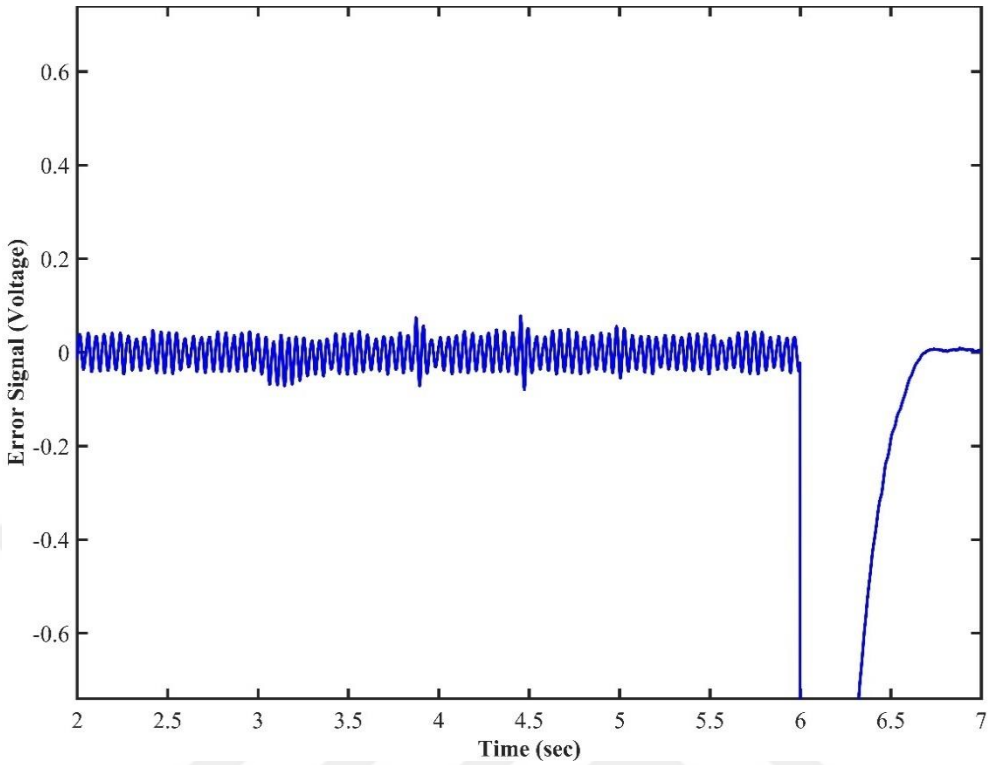

Figure 5.7. The Error Signal Graph of LADRC When Input Disturbance Exists

5.1.3. Tracking Test

Tracking performance can be defined as the capability of the controlled system to follow the changable set point reference signals. For this study, the reference set point signals vary for certain durations between 1000 rpm and 1400 rpm. The results of the tracking performance of LADRC is shown in the Figure 5.8 with control signal in the Figure 5.9 and error signal in the Figure 5.10. At 1000 rpm and 1400 rpm, the output deviation is reduced to ± 5 rpm.

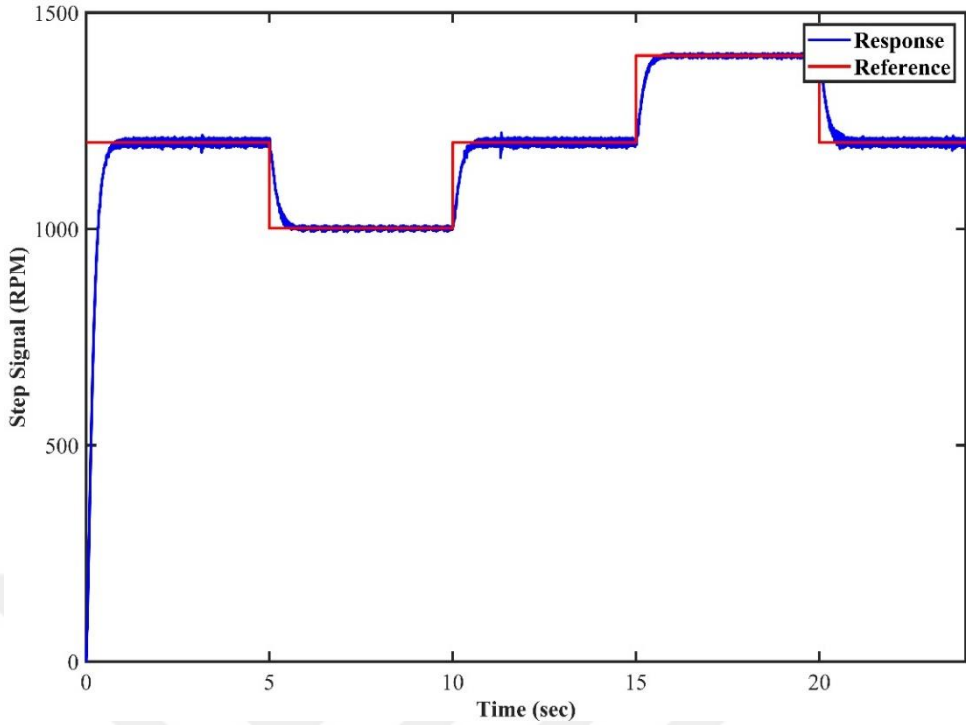

Figure 5.8. The Tracking Performance of LADRC

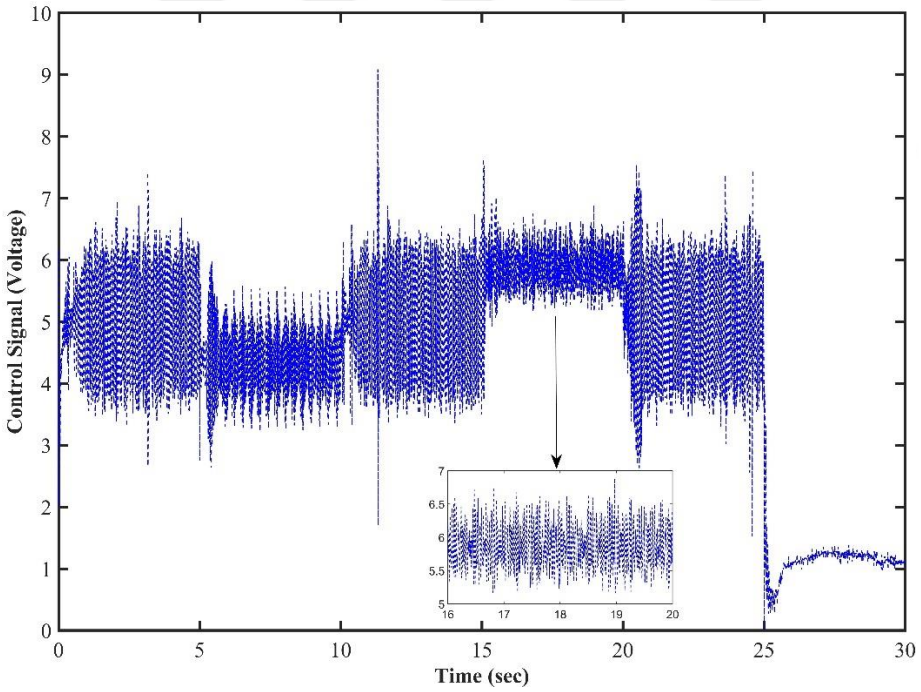

Figure 5.9. The Control Signal of Tracking Test of LADRC

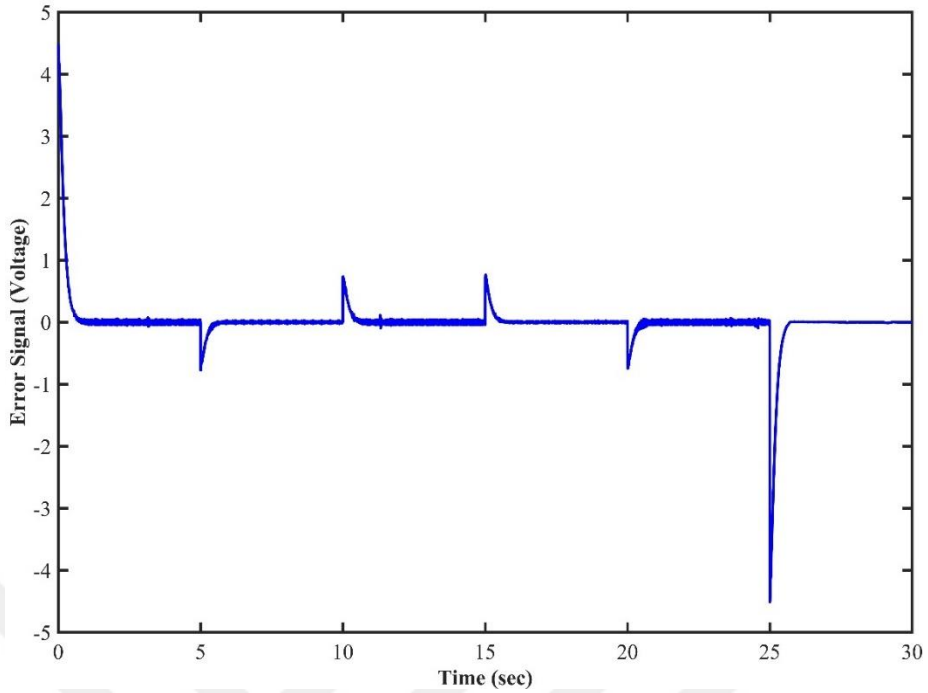

Figure 5.10. The Error Signal of Tracking Test of LADRC

5.2. Error Based LADRC Applications and Results

ELADRC controller was chosen second to apply to the system to be controlled. ELADRC possesses the same parameters as mentioned before which are T_s, w_C, w_O, β, K_P and K_D. These parameters were determined first then applied to the electromechanical system. The calculation of the parameters was carried out just before the experiment, and the experimental process was carried out with these parameters.

5.2.1. Step Test

The parameters are calculated to be $T_s = 0.5\ sec$, $w_C = 12$, $w_O = 120$, $\beta = 210$, $K_P = 144$ and $K_D = 24$. A low pass filter is used at the output of the system to be controlled in order to constitute the feedback signal. The result of step response is shown in the Figure 5.11 and the transient response of the corresponding step signal is shown Figure 5.12. Also, the control signal in corformity with the total step response is given in the Figure 5.13 and the error signal that corresponds with the total step response is given in the Figure 5.14.

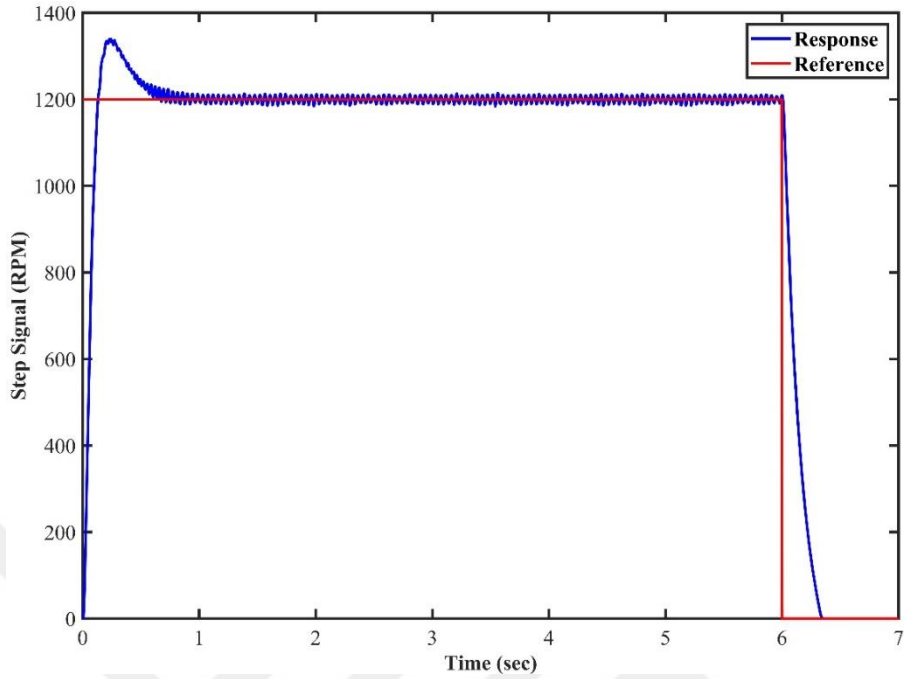

Figure 5.11. The Step Response of ELADRC

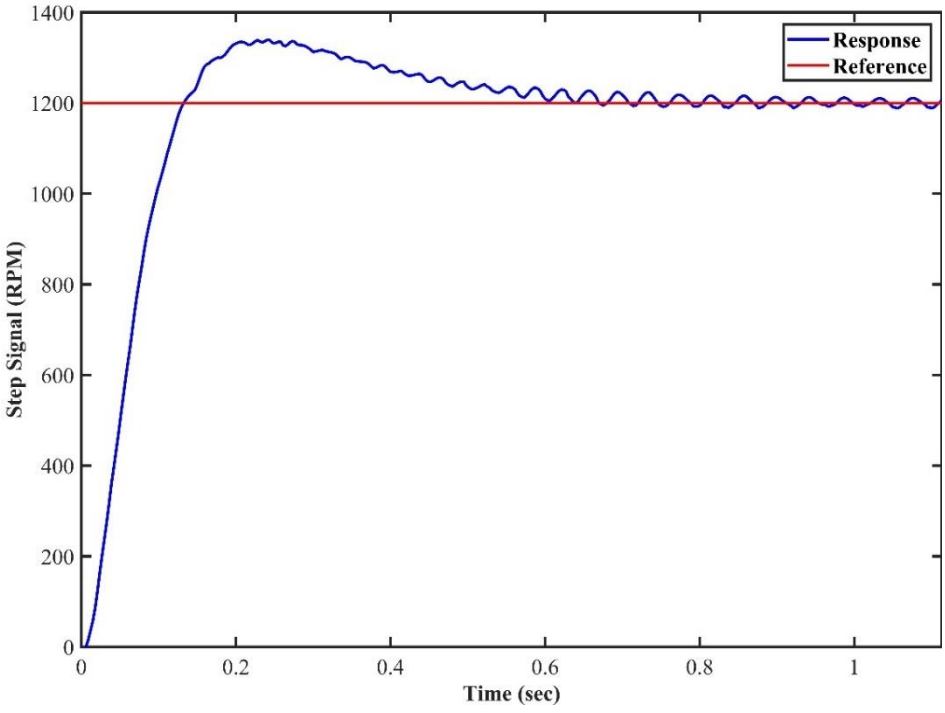

Figure 5.12. The Transient Response of ELADRC

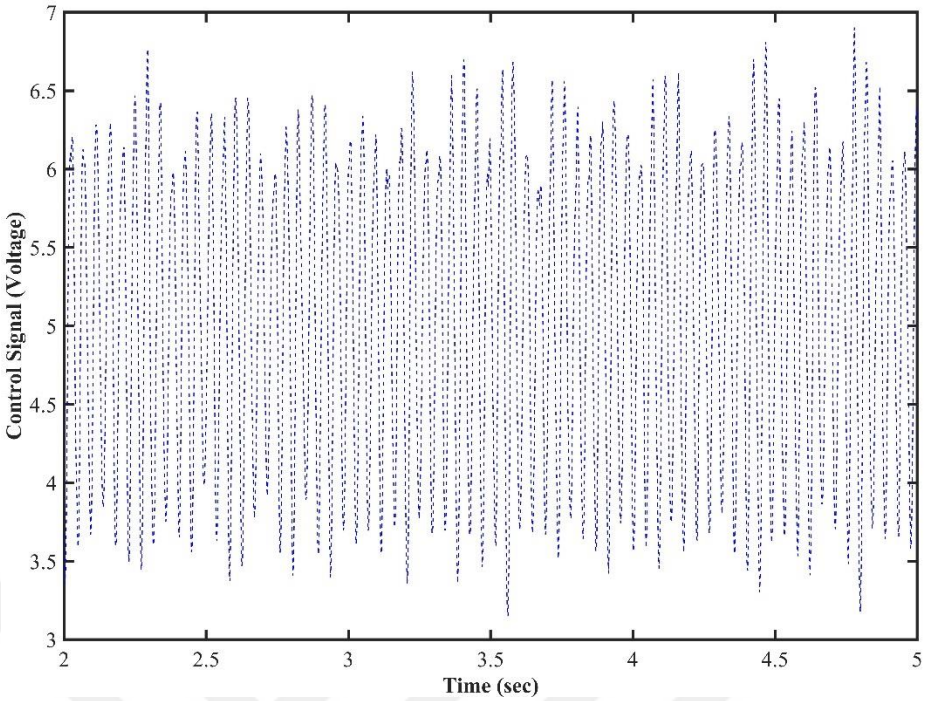

Figure 5.13. The Control Signal of ELADRC

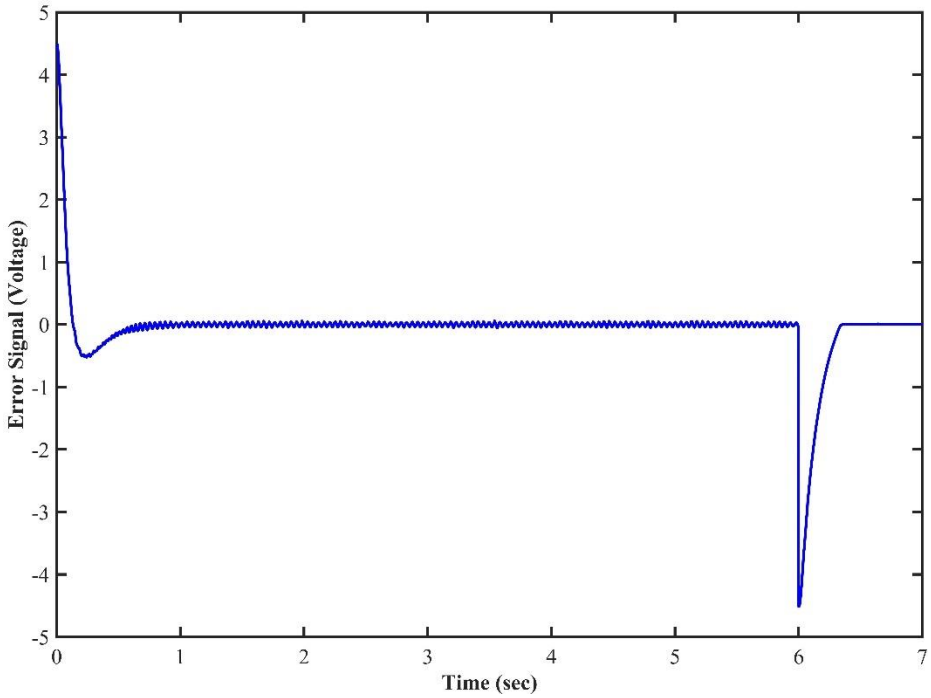

Figure 5.14. The Error Signal of ELADRC

According to the transient profile of ELADRC graph, an overshoot is observed at the output of system. The rise time, settling time, overshoot and output deviation values are given in the Table 5.2.

Table 5.2. The transient values correspond to ELADRC

	Rise Time	Settling Time	Overshoot	Output Deviation
ELADRC	0.09 sec	0.561sec	% 11.5	±8.4 rpm

5.2.2. Disturbance Rejection Test

Input disturbance was applied to the system as an addition of 0.22 V, which is 5% of 4.48 V, from the control input channel. As a result, the performance graph of disturbance rejection capability of ELADRC was observed. A voltage of 0.22V is applied to the system for a duration of 3 seconds, starting at 3 seconds. The result are shown in the Figure 5.15 with the control signal in the Figure 5.16 and error signal in the Figure 5.17.

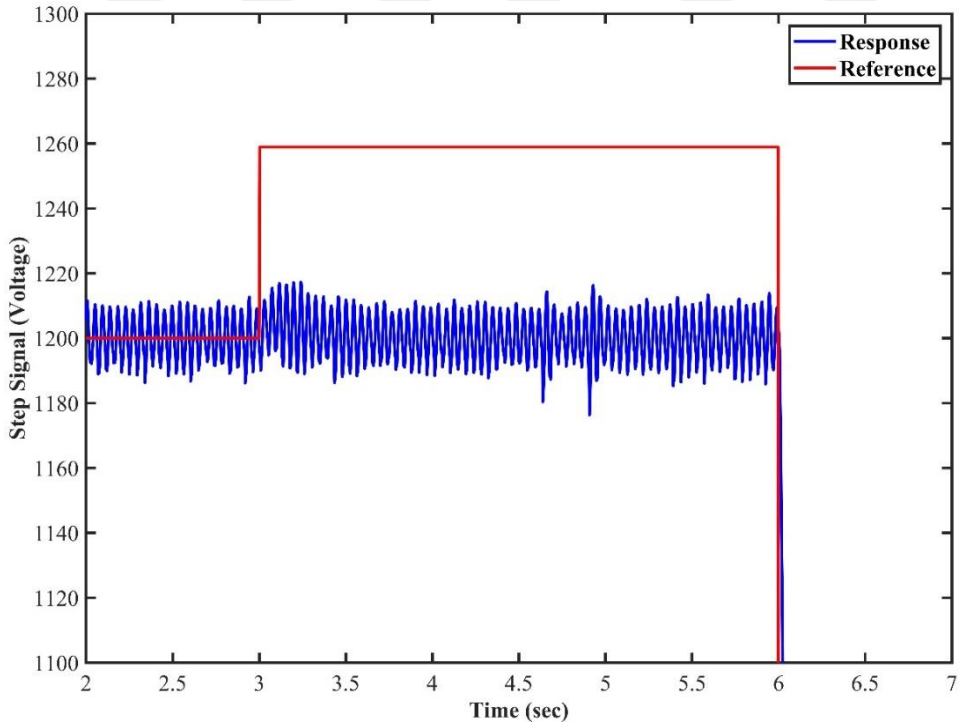

Figure 5.15. The Step Signal of ELADRC While Input Disturbance Exists

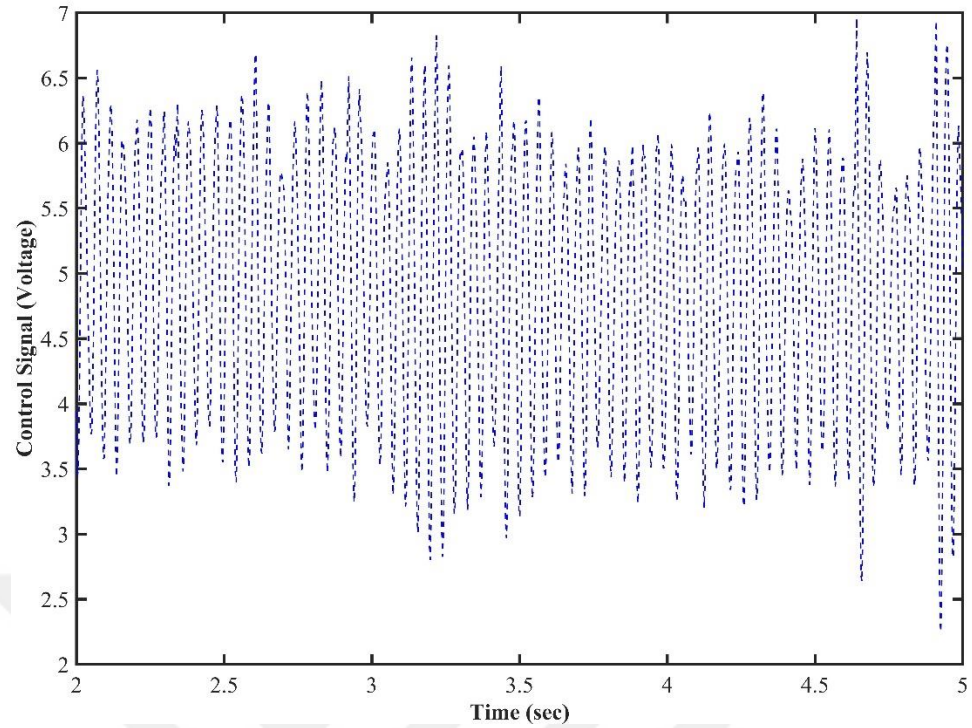

Figure 5.16. The Control Signal of ELADRC While Input Disturbance Exists

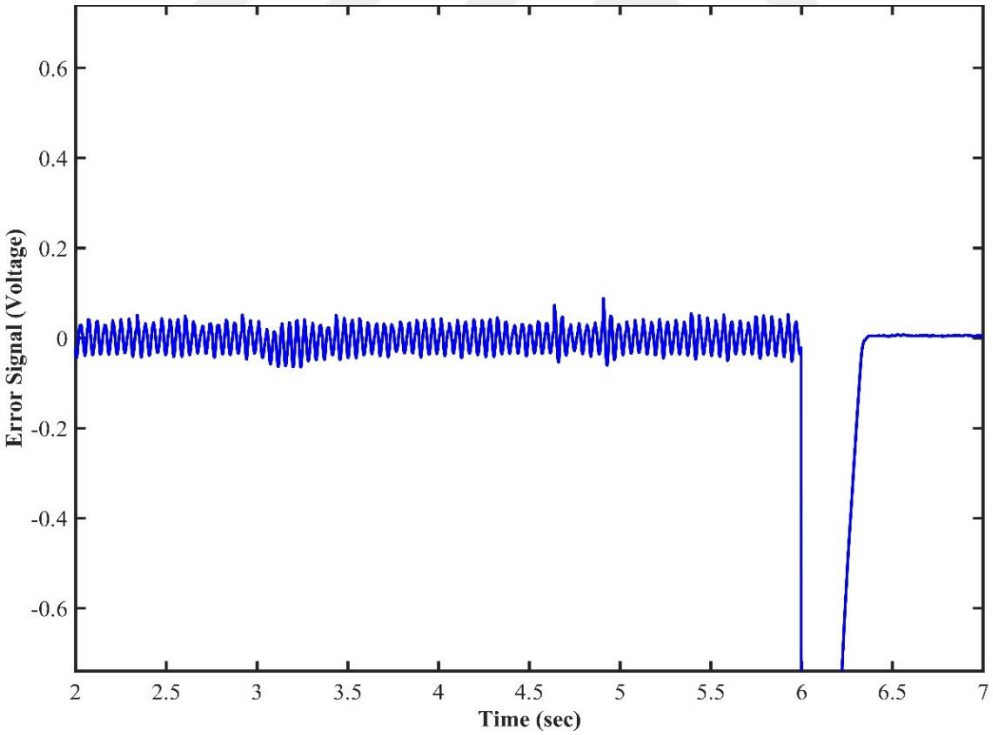

Figure 5.17. The Control Signal of ELADRC While Input Disturbance Exists

5.2.3. Tracking Test

Tracking performance can be denoted as the capability of the controlled system to follow the changable set point reference signals. For this study, the reference set point signals vary for certain durations between 1000 rpm and 1400 rpm. The results of the tracking performance of ELADRC is shown in the Figure 5.18 with control signal in the Figure 5.19 and error signal in the Figure 5.20. At 1000 rpm and 1400 rpm, the output deviation is reduced to ± 5.2 rpm.

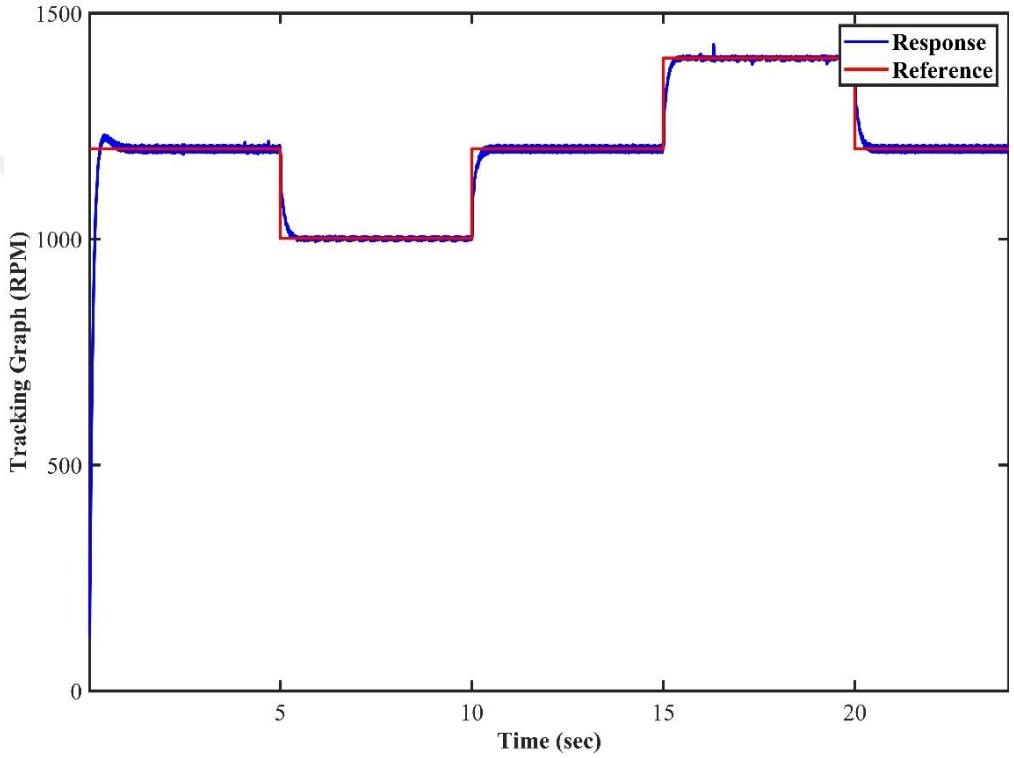

Figure 5.18. The Tracking Performance of ELADRC

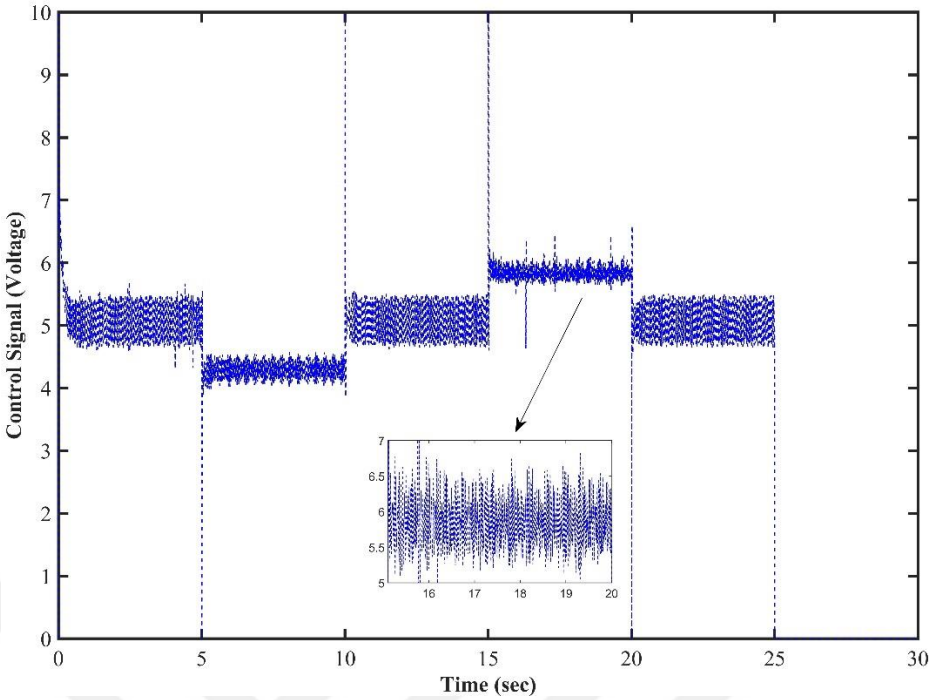

Figure 5.19. The Control Signal of Tracking Test of ELADRC

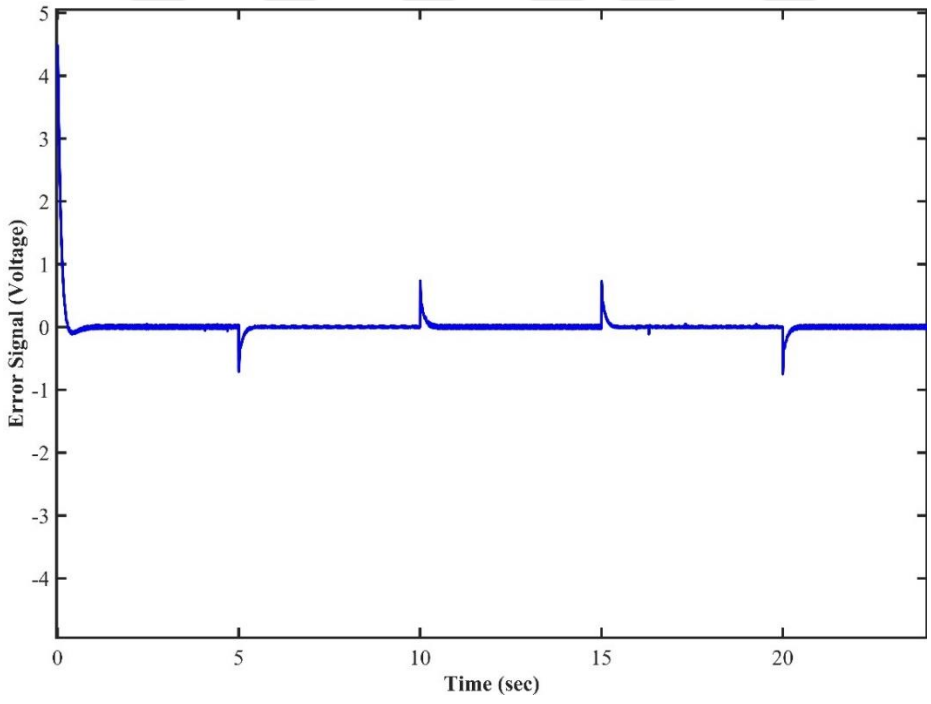

Figure 5.20. The Error Signal of Tracking Test of ELADRC

5.3. LADRC with IMC Applications and Results

The LADRC with IMC was chosen as third algorithm to apply to the system. The algorithm possesses the same parameters as mentioned before which are λ_d, λ, and β . These parameters were determined first then applied to the electromechanical system. The calculation of the parameters was carried out just before the experiment, and the experimental process was carried out with these parameters.

5.3.1. Step Test

The parameters are calculated to be $\lambda_d = 0.05, \lambda = 0.01, \beta = 400$. A low pass filter is used at the output of the system to be controlled in order to constitute the feedback signal. The result of transient response is shown in the Figure 5.21 and the whole response signal is shown in Figure 5.22. Also, the control signal in corformity with the total step response is given in the Figure 5.23 and the error signal that corresponds with the total step response is given in the Figure 5.24.

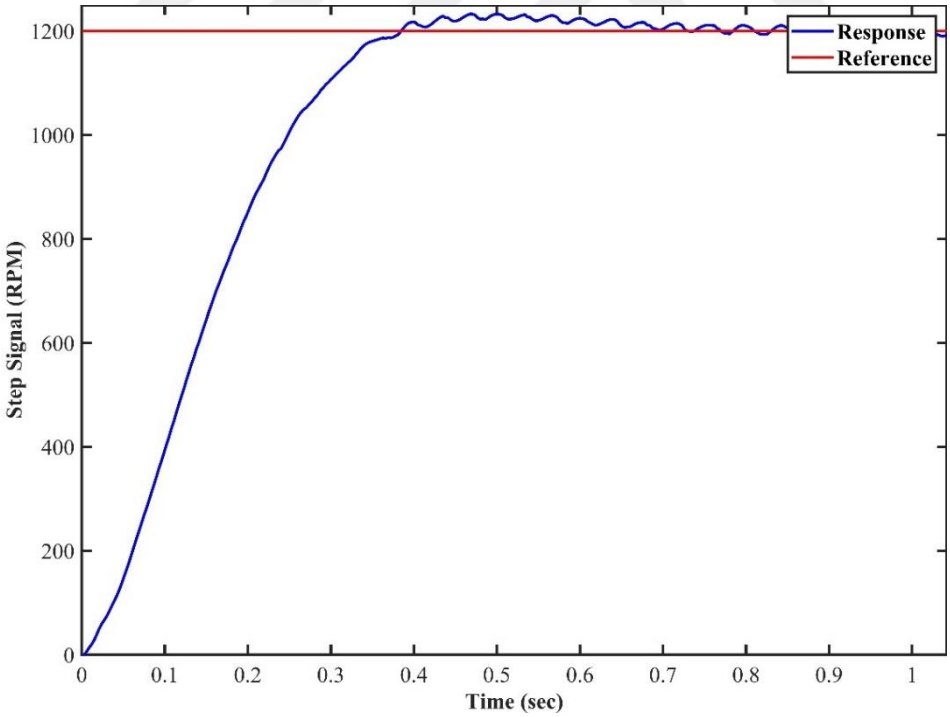

Figure 5.21. The Transient Response of LADRC with IMC

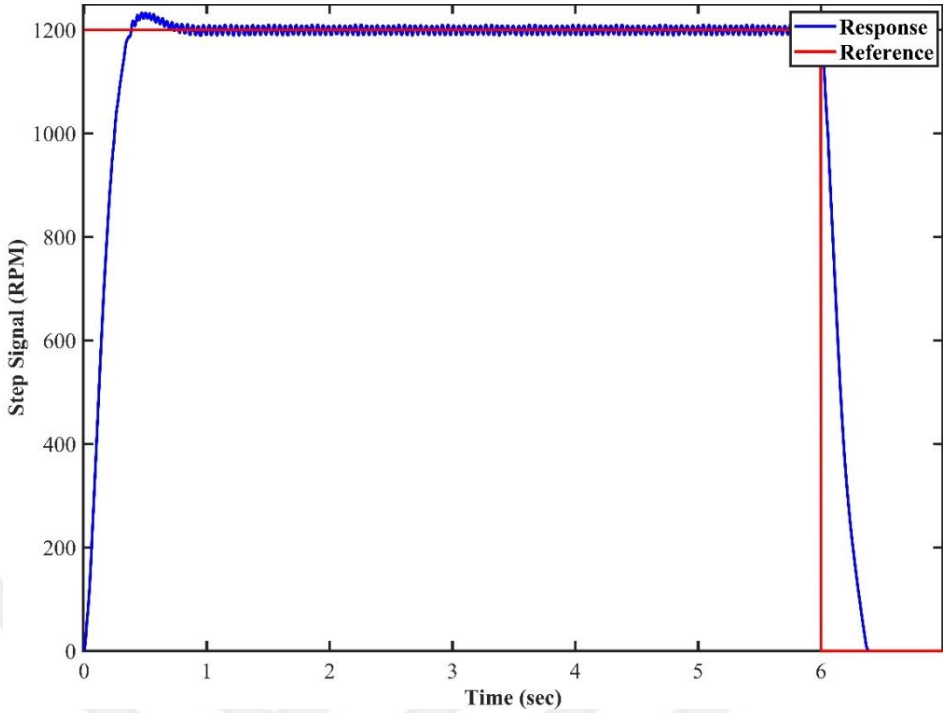

Figure 5.22. The Step Response of LADRC with IMC

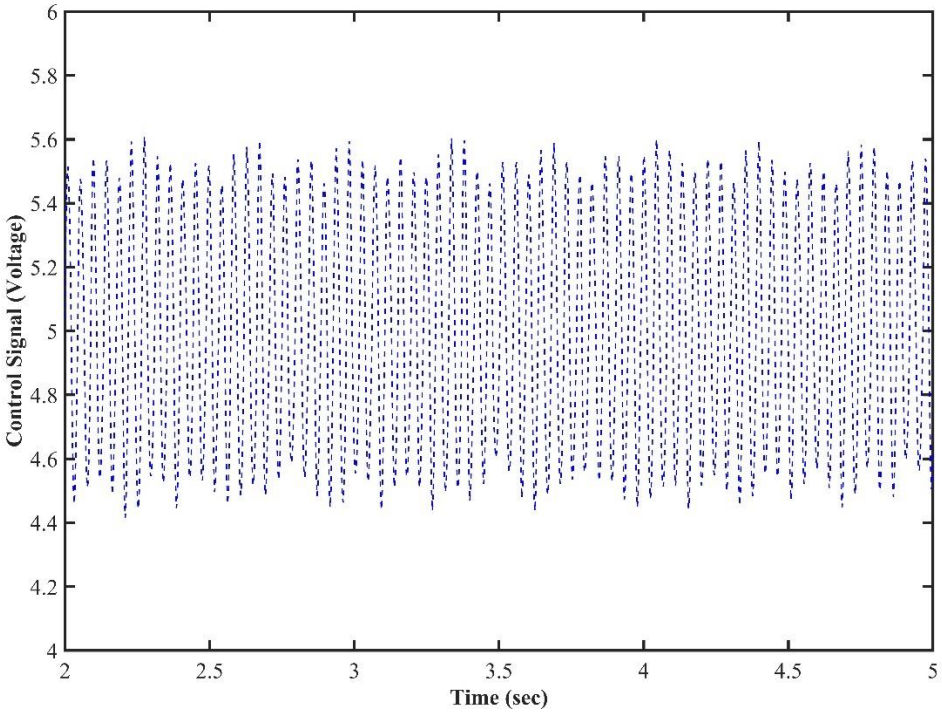

Figure 5.23. The Control Signal of LADRC with IMC

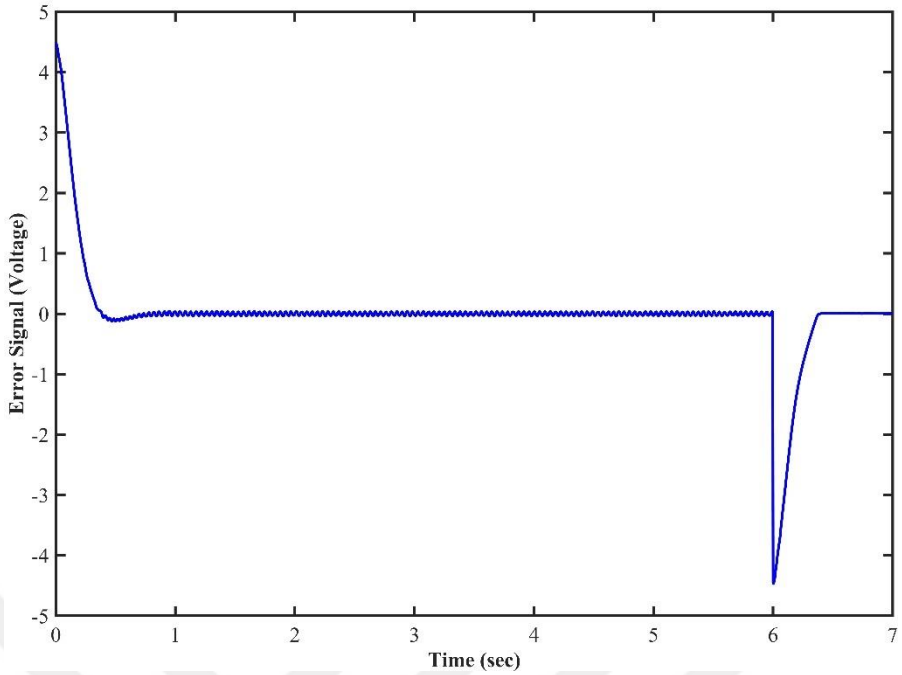

Figure 5.24. The Error Signal of LADRC with IMC

In compliance with the transient of response graph of LADRC with IMC, a small overshoot is observed. The datas for the transient profile is given in Table 5.3.

Table 5.3. The transient values correspond to LADRC with IMC

	Rise Time	Settling Time	Overshoot	Output Deviation
LADRC with IMC	0.28 sec	0.597 sec	% 2.66	±8.1 rpm

5.3.2. Disturbance Rejection Test

Input disturbance was applied to the system as an addition of 0.22 V, which is 5% of 4.48 V, from the control input channel. As a result, the performance graph of disturbance rejection capability of LADRC with IMC was observed. A voltage of 0.22V is applied to the system for a duration of 3 seconds, starting at 3 seconds. The result are shown in the Figure 5.25 with the control signal in the Figure 5.26 and error signal in the Figure 5.27.

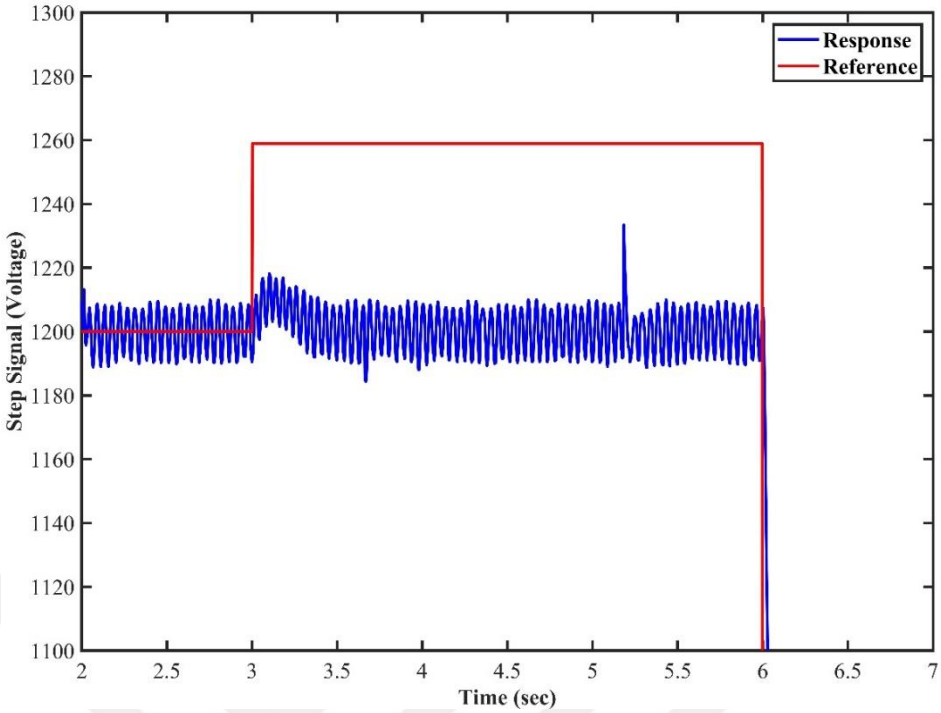

Figure 5.25. The Step Signal of LADRC With IMC While Input Disturbance Exists.

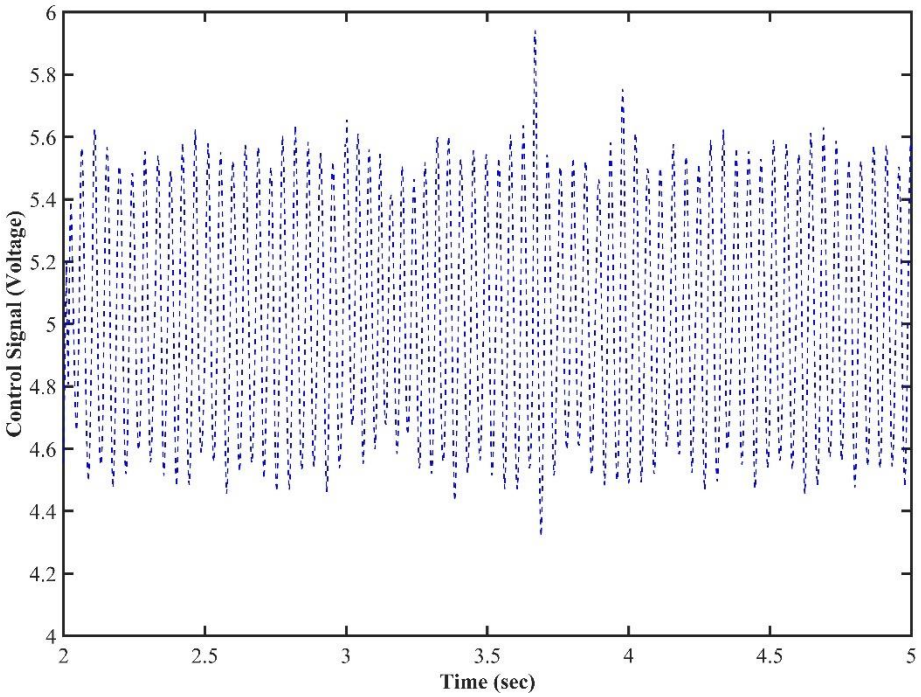

Figure 5.26. The Control Signal of LADRC With IMC While Input Disturbance Exists.

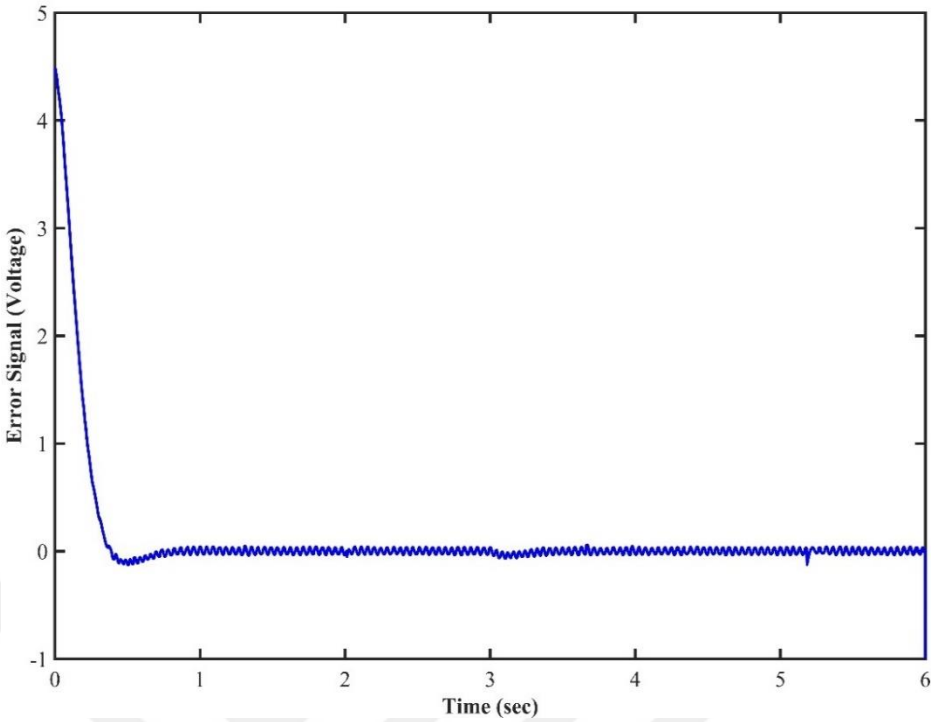

Figure 5.27. The Error Signal of LADRC With IMC While Input Disturbance Exists.

5.3.3. Tracking Test

For this study, the reference set point signals vary for certain durations between 1000 rpm and 1400 rpm. The results of the tracking performance of LADRC with IMC is shown in the Figure 5.28 with control signal in the Figure 5.29 and error signal in the Figure 5.30. At 1000 rpm and 1400 rpm, the output deviation is reduced to $\pm$4.1 rpm.

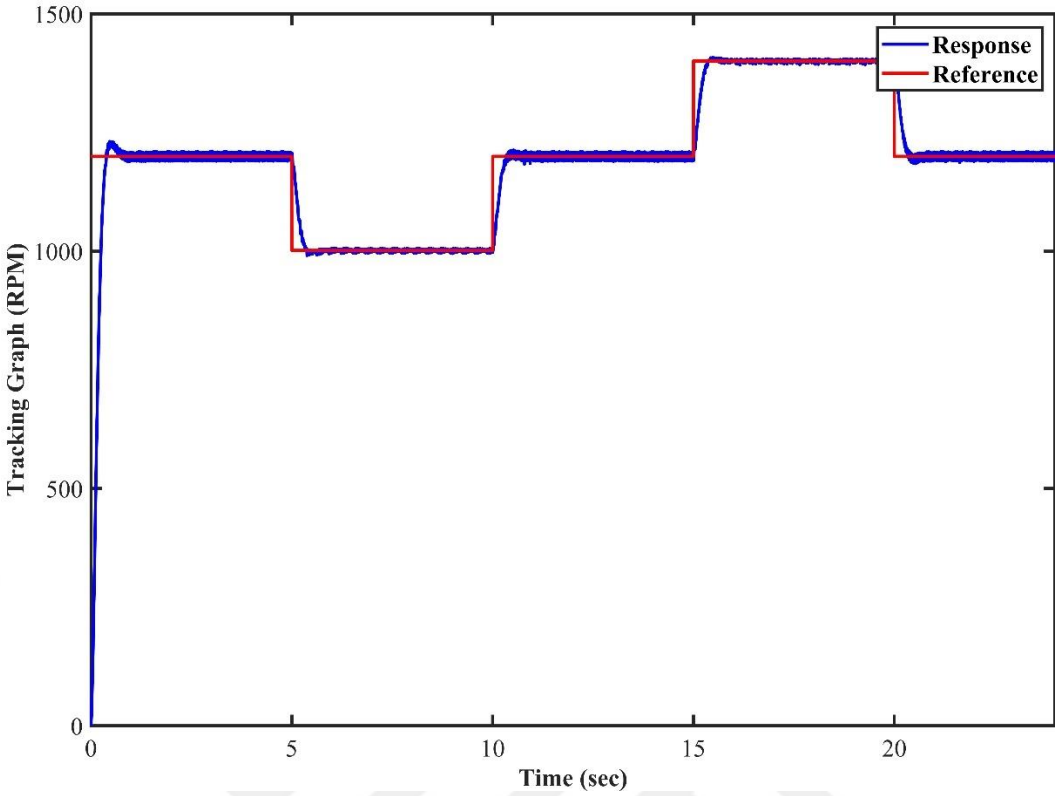

Figure 5.28. The Tracking Performance of LADRC With IMC

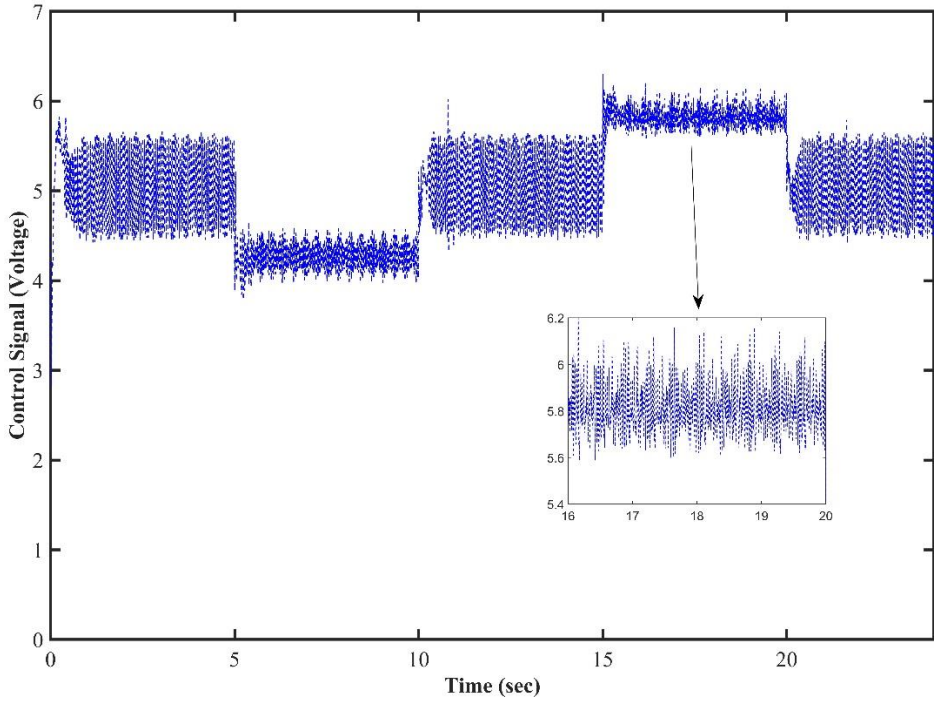

Figure 5.29. The Control Signal of LADRC With IMC

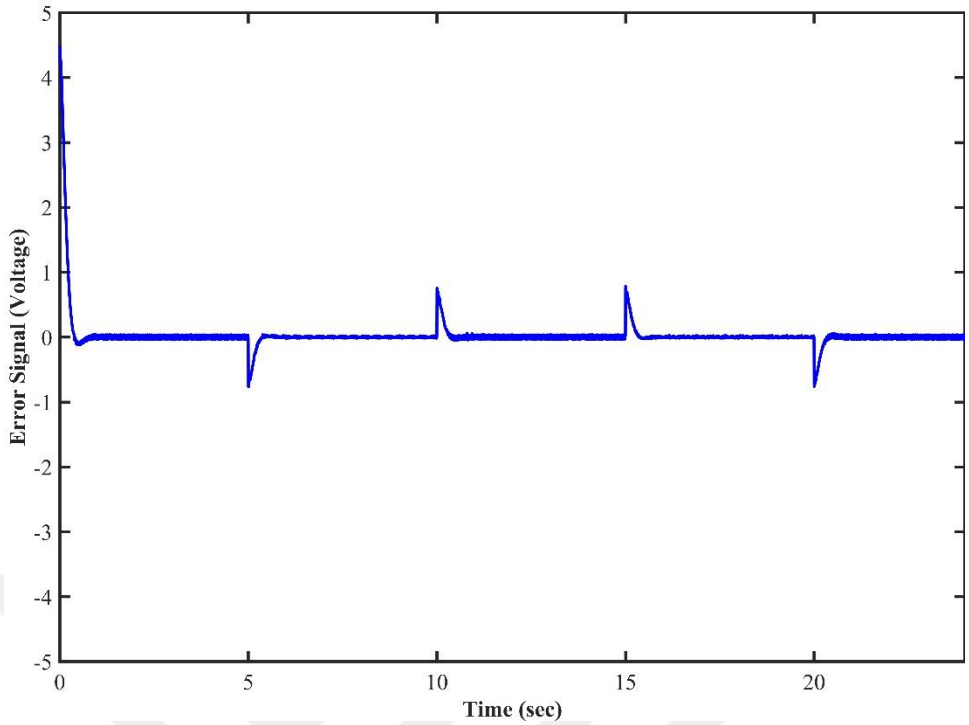

Figure 5.30. The Error Signal of LADRC With IMC

5.4. LADRC with Fractional Order Observer Applications and Results

The FOLADRC was chosen as third algorithm to apply to the system. The observer of algorithm possesses the parameters which are k, V, n and $Bandwidth$. These parameters were determined first then applied to the electromechanical system. The determination of the parameters was carried out just before the experiment, and the experimental process was carried out with these parameters. The toolbox for fractional order systems named as "nint" is used to realize the experiment. The rest of the parameters are the same as LADRC, denoted as T_s, w_C, w_O, β, K_P and K_D.

5.4.1. Step Test

The observer of FOLADRC parameters are chosen as follows:

- $k = 1.1$

- $V = -0.98$
- $Bandwidth = [0\ 0{,}1\ 100]$
- $n = 5$

The rest of the parameters are chosen as as $T_s = 0.5\ sec,\ \ w_C = 12,\ \ w_O = 120,\ \ \beta = 210,$ $K_P = 144$ and $K_D = 24$.

A low pass filter is used at the output of the system to be controlled in order to constitute the feedback signal. The result of transient response is shown in the Figure 5.31 and the whole response signal is shown in Figure 5.32. Also, the control signal in corformity with the total step response is given in the Figure 5.33 and the error signal that corresponds with the total step response is given in the Figure 5.34.

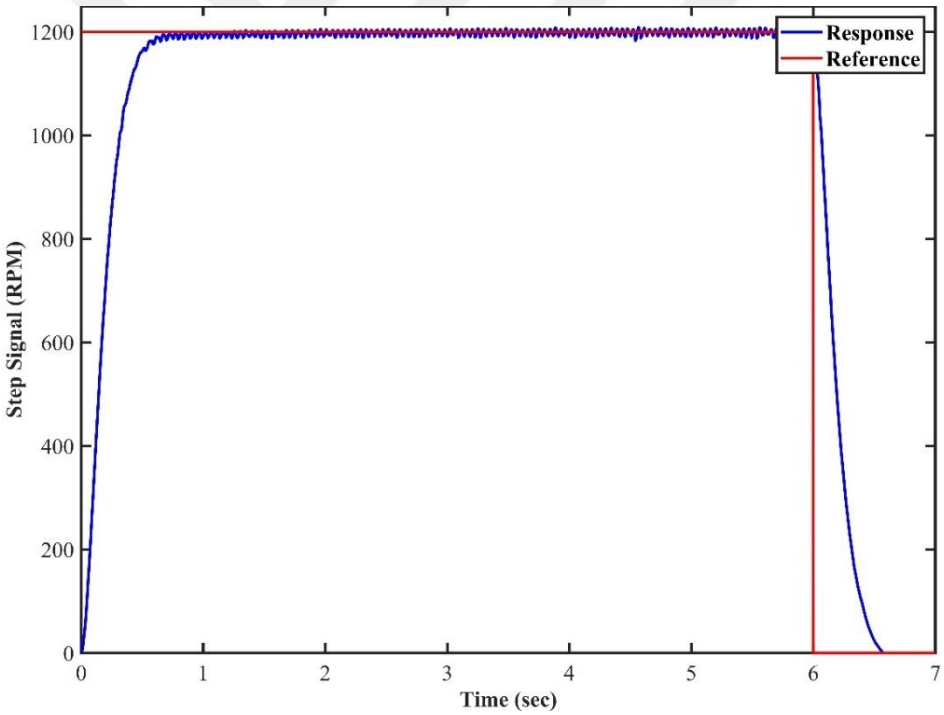

Figure 5.31. The Step Response of FOLADRC

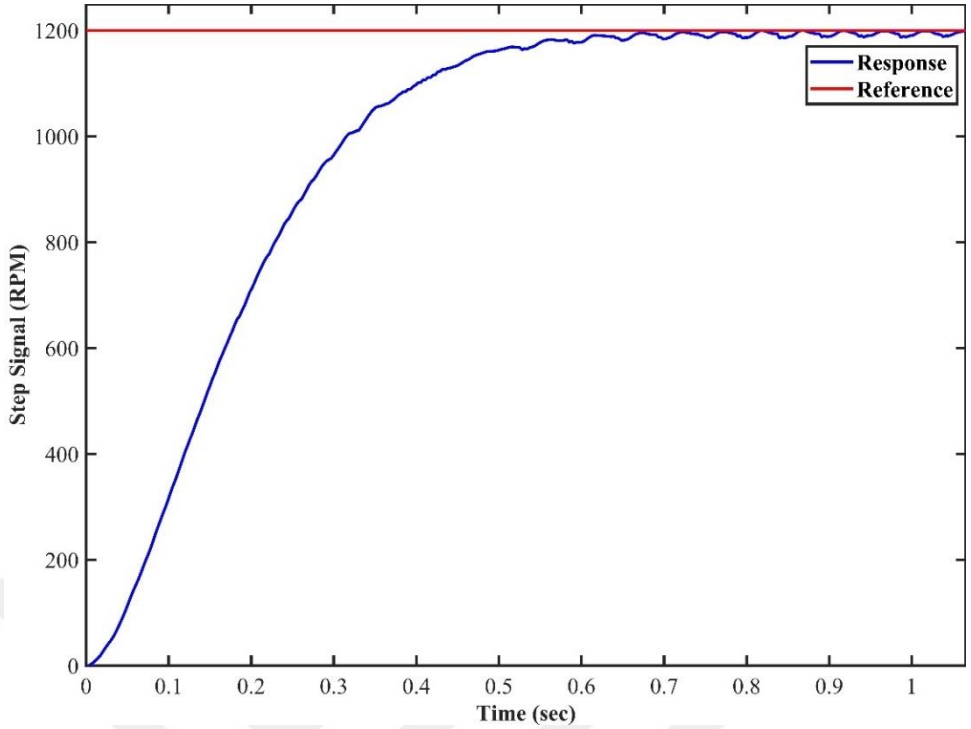

Figure 5.32. The Transient Profile of FOLADRC

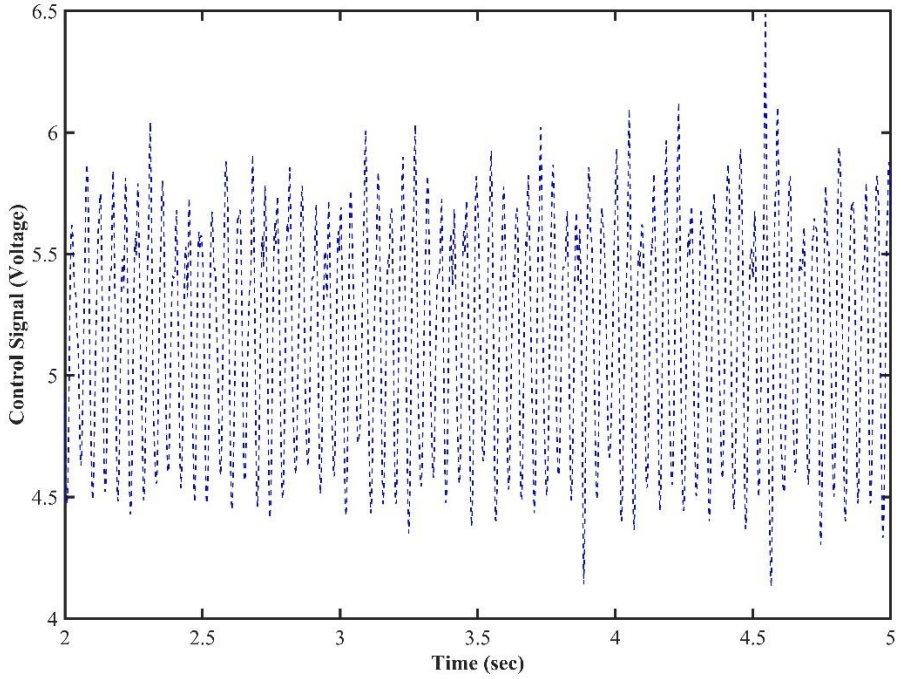

Figure 5.33. The Control Signal of FOLADRC

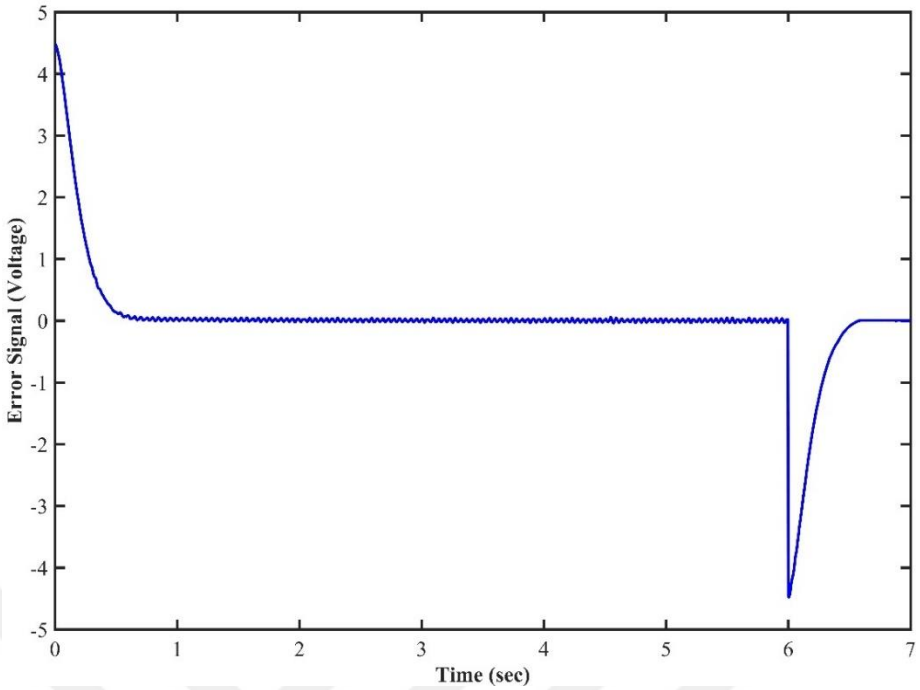

Figure 5.34. The Error Signal of FOLADRC

No overshoot is observed at the output of system. The transient values for FOLADRC are presented in Table 5.4.

Table 5.4. The transient values correspond to FOLADRC

	Rise Time	Settling Time	Overshoot	Output Deviation
FOLADRC	0.336 sec	0.573 sec	No Overshoot	±6 rpm

5.4.2. Disturbance Rejection Test

Input disturbance was applied to the system as an addition of 0.22 V, which is 5% of 4.48 V, from the control input channel. As a result, the performance graph of disturbance rejection capability of FOLADRC was observed. A voltage of 0.22V is applied to the system for a duration of 3 seconds, starting at 3 seconds. The result are shown in the Figure 5.35 with the control signal in the Figure 5.36 and error signal in the Figure 5.37.

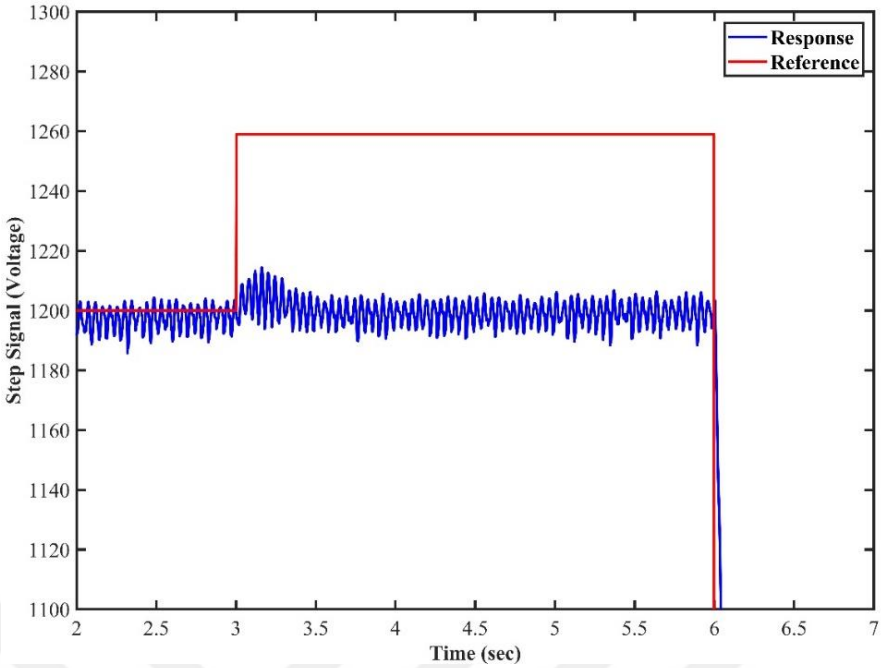

Figure 5.35. The Step Signal of FOLADRC While Input Disturbance Exists.

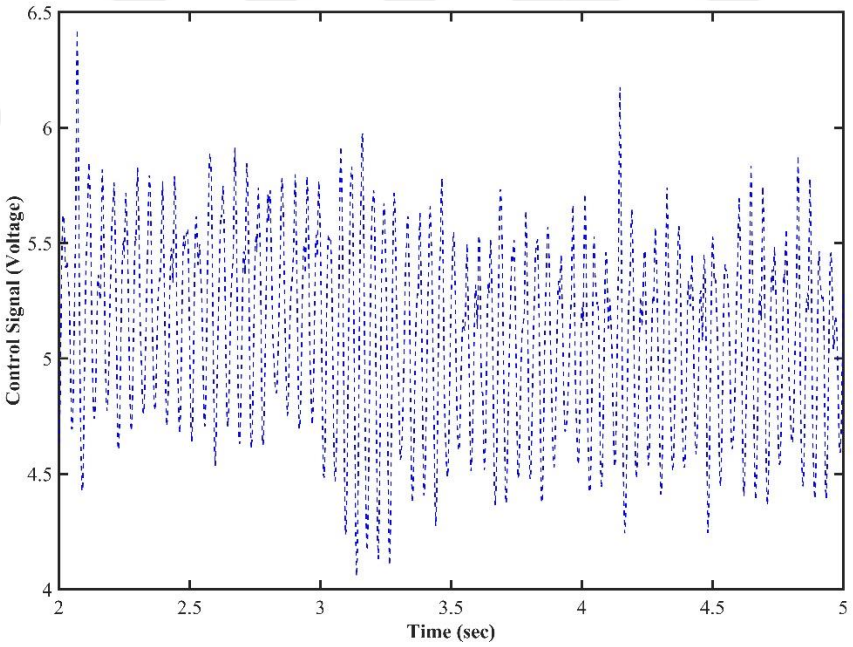

Figure 5.36. The Control Signal of FOLADRC While Input Disturbance Exists.

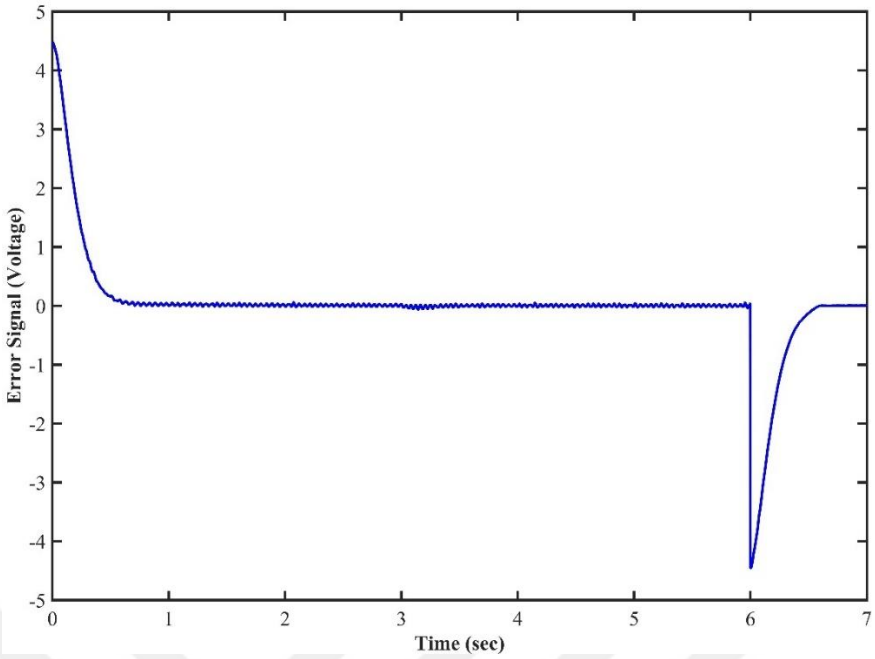

Figure 5.37. The Error Signal of FOLADRC While Input Disturbance Exists.

5.4.3. Tracking Test

For this study, the reference set point signals vary for certain durations between 1000 rpm and 1400 rpm. The results of the tracking performance of FOLADRC is shown in the Figure 5.38 with control signal in the Figure 5.39 and error signal in the Figure 5.40. At 1000 rpm and 1400 rpm, the output deviation is reduced to ± 4 rpm.

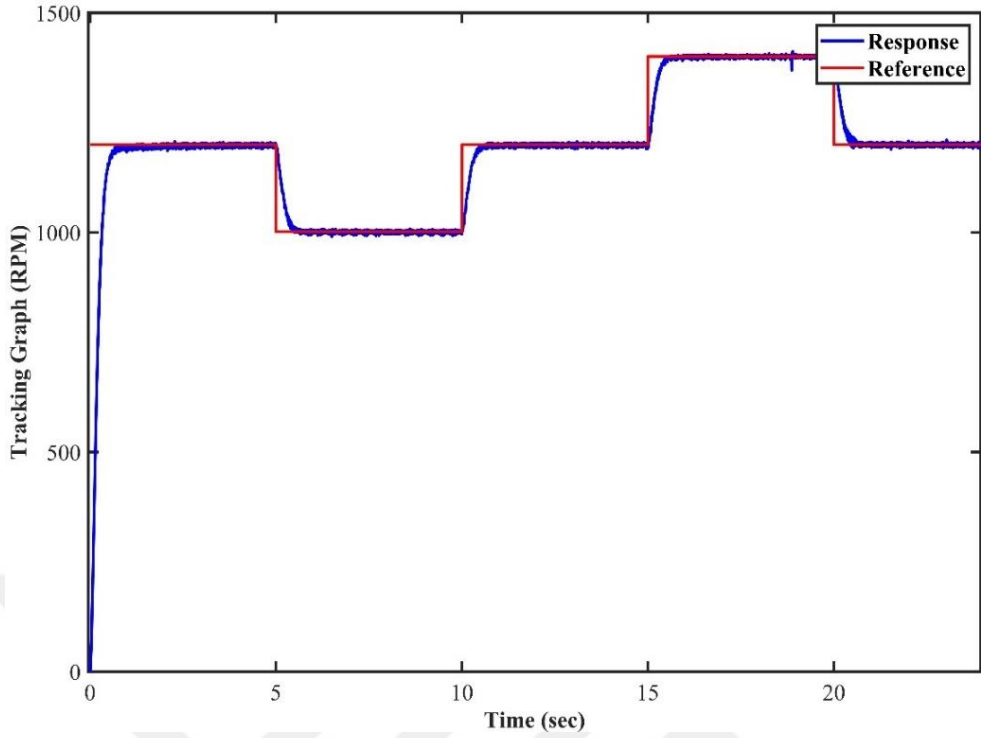

Figure 5.38. The Tracking Performance of FOLADRC

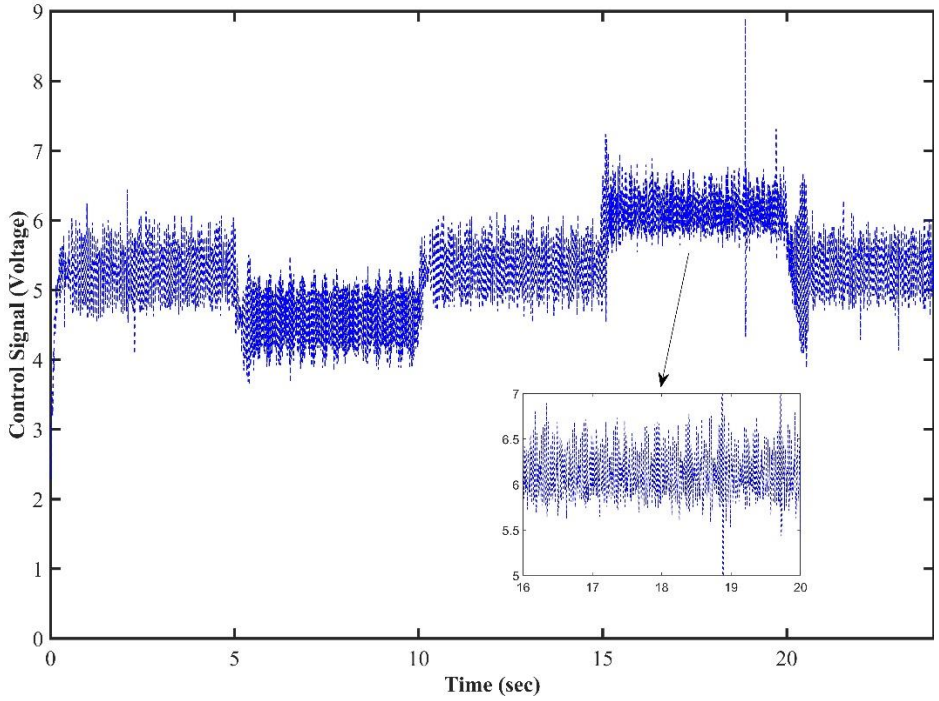

Figure 5.39. The Control Signal of Tracking Performance of FOLADRC

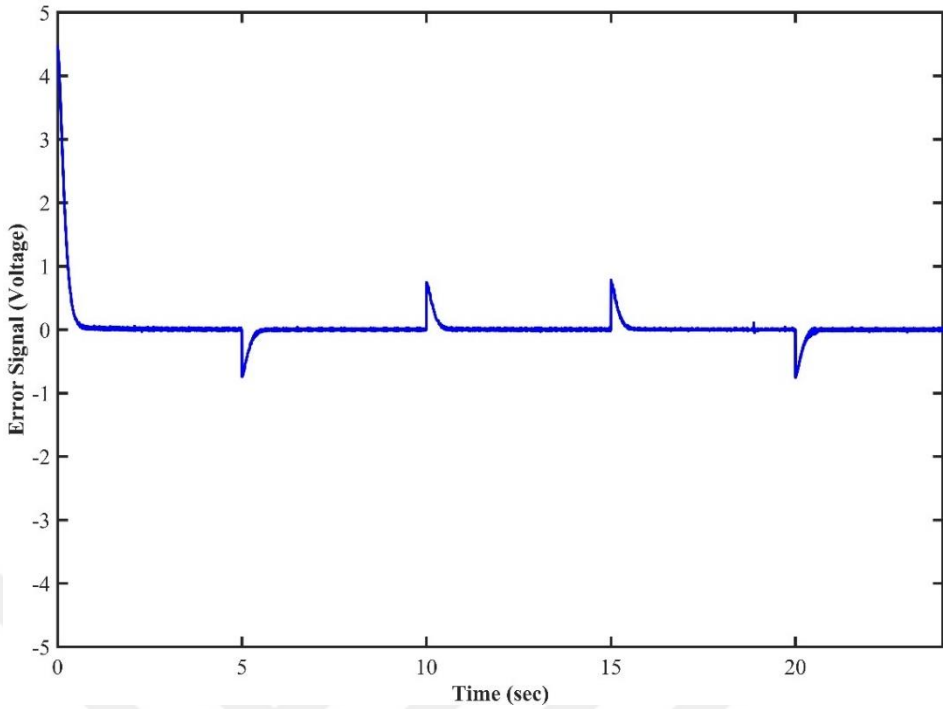

Figure 5.40. The Error Signal of Tracking Performance of FOLADRC

5.5. Performance Comparison of the Studied Control Methods

The performance indices are applied to the error and control signals to the each control methods for step response during 2-6 seconds and results are tabulated in Table 5.5.

Certain performance criteria are selected, in order to make comparisons between the aforementioned control methods. These criteria are listed as follows:

- Integral of absolute error (IAE)

$$IAE = \int |e(t)| dt \tag{5.1}$$

- Integral of square error (ISE)

$$ISE = \int e^2(t)dt \tag{5.2}$$

- Integral of time absolute error (ITAE)

$$ITAE = \int t|e(t)|dt \tag{5.3}$$

- Integral time squared error (ITSE)

$$ITSE = \int te^2(t)dt \tag{5.4}$$

- Integral squared control input (ISCI)

$$ISCI = \int u^2(t)dt \tag{5.5}$$

The performance indices regarding to the the studied control methods are given in Table 5.5

The least ISCI value is 80.25 which belongs to LADRC with IMC method. It shows the LADRC with IMC method has forced the control signal least in terms of voltage variation. This situation deduced that the method is the most energy saving among the others.

Table 5.5. The table of performance indices

(2-6 seconds)	**IAE**	**ISE**	**ITAE**	**ITSE**	**ISCI**
LADRC	0.5118	0.0351	0.1248	0.2018	105.58
ELADRC	0.4063	0.0333	0.0982	0.1946	105.39
LADRC (IMC)	0.3908	0.0321	0.0945	0.1878	80.25
FOLADRC	0.3259	0.0316	0.0776	0.1862	107.81

The least IAE, ISE, ITAE, ITSE values belongs to the FOLADRC method. IAE is 0.3259, ISE is 0.0316, ITAE is 0.0776 and ITSE is 0.1862 respectively in FOLADRC. The method possesses the least amount of error values except ISCI according to the Table 5.1. Because of the representation of physical systems with fractional order systems is more precise, it can validated that the utilization of fractional order observer has made a difference. The difference is to maintain the error less than that in rest of methods and it shows its efficacy over the other methods.

The disturbance rejection performance of the all four methods are quite satisfactory and similar. Approximately 0.27 seconds after the the input disturbance injected, the electromechanical system recovers itself and follows the reference signal again.

Table 5.6. The rise time, settling time and overshoot with output deviation

	Rise Time	Settling Time	Overshoot	Output Deviation
LADRC	0.363 sec	0.561 sec	No overshoot	±8.0 rpm
ELADRC	0.09 sec	0.561sec	% 11.5	±8.4 rpm
LADRC with IMC	0.28 sec	0.597 sec	% 2.66	±8.1 rpm
FOLADRC	0.336 sec	0.573 sec	No Overshoot	±6 rpm

Although LADRC, ELADRC and FOLADRC posses the same tuning parameters, the transient values are different from each other. FOLADRC has shown its superiority over the other methods in terms of output deviation with no overshoot at the output of system. For LADRC and ELADRC, the difference between overshoot and output deviation values are expected as in stated (Madonski et al., 2023). LADRC gave the response with no overshoot while ELADRC caused the output of the system with an acceptable overshoot as in Table 5.6.

The tuning LADRC with IMC method has been proved its usefullness while comparing the LADRC method. 0.1 rpm difference demonstrated the both methods are good alternatives for the steady state condition as in Table 5.6.

All four methods have been designed based on specific settling time value and it can be remarked that with efficient designing procedure, their consistency is proved with experimentally in Table 5.6.

The tracking performance of studied control methods are quite satisfactory. Under the different reference signals changing instantly, the controllers are adapted in order to maintain the system robustness.

According to the rise time values in Table. 5.6, ELADRC completed the transient time 0.09 seconds, which demonstrates the least transient period when compared with other methods. It is an elegant method in the need of faster response time. However, the overshoot of ELADRC should be taken into consideration.

6. CONCLUSION AND FUTURE WORKS

In this thesis, observer-based control methodologies are explained briefly. The general theoretical background apart from ADRC has explained and demonstrated their necessity in the control engineering field. The vision of the of observer-based control methods are introduced.

The compliance of ADRC method with existing methods such as SMC and Fuzzy Control are investigated. The findings deduced that ADRC is key element to reduce and suppress the unwanted dynamics and signals from the system to be controlled while utilizing with the control methods which the efficiency and performance are proved in the literature.

The detailed explanation about four variants of LADRC was given expressively. By taking into account the key studies, first time in the literature, it is aimed to light these four methods for further use and study.

Consecutively, the four variants of LADRC methods have been examined with experimental applications. The experimental applications are utilized with the usage of DC Motor which belongs to DIGIAC 1750. The system identification is used to extract the model of the plant by several test procedures.

One the aim of this thesis, to observe the variants of LADRC methods under the same parameters. The variants of LADRC which examined in this thesis are as follows:

- LADRC
- ELADRC
- LADRC with IMC
- FOLADRC

All methods are successfully implemented to the electromechanical system after the simulation studies. The performance analysis of has been done based on the experimental results. Those

four methods are tested first time on a specific electromechanical system and comparison is made among them. It is demonstrated that the FOLADRC is more superior then the rest of the methods in terms of the tests applied to the system to be controlled.

For future works, the adaptive based LADRC control method will be utilized and studied for the electromechanical system. The parameter optimization is another field for ADRC methods and will be studied both experimentally and theoretically. The original ADRC method contains nonlinearity and will be studied on the nonlinear modeled system such as quadrotor, pendulum system models to demonstrate its usefulness.

REFERENCES

Alonge, F., Cirrincione, M., D'Ippolito, F., Pucci, M., & Sferlazza, A. (2017). Robust Active Disturbance Rejection Control of Induction Motor Systems Based on Additional Sliding-Mode Component. *IEEE Transactions on Industrial Electronics*, *64*(7), 5608–5621. https://doi.org/10.1109/TIE.2017.2677298

Chen, C. F., Du, Z. J., He, L., Wang, J. Q., Wu, D. M., & Dong, W. (2019). Active Disturbance Rejection with Fast Terminal Sliding Mode Control for a Lower Limb Exoskeleton in Swing Phase. *IEEE Access*, *7*, 72343–72357. https://doi.org/10.1109/ACCESS.2019.2918721

Chen, X., Liu, Z., Hu, H., Wang, L., & Dong, J. (2017). Backstepping Adaptive Sliding Mode Control for the USV Course Tracking System. *2017 9th International Conference on Advanced Infocomm Technology*, 265–269. Wuhan.

Cui, W., Tan, W., Li, D., Wang, Y., & Wang, S. (2020). A Relay Feedback Method for the Tuning of Linear Active Disturbance Rejection Controllers. *IEEE Access*, *8*, 4542–4550. https://doi.org/10.1109/ACCESS.2019.2963419

Djeghali, N., Bettayeb, M., & Djennoune, S. (2021). Sliding mode active disturbance rejection control for uncertain nonlinear fractional-order systems. *European Journal of Control*, *57*, 54–67. https://doi.org/10.1016/j.ejcon.2020.03.008

Dong, H., Huang, H., & Zhuang, Y. (2020). Heading Angle Controller Design of USV Based on Improved Sliding Mode Active Disturbance Rejection Control. *Proceedings - 2020 Chinese Automation Congress, CAC 2020*, (2), 3547–3551. https://doi.org/10.1109/CAC51589.2020.9326809

Du, Y., Cao, W., She, J., & Fang, M. (2020). A Comparison Study of Three Active Disturbance Rejection Methods. *Proceedings of the 39th Chinese Control Conference*, 135–139.

Eker, D., & Özbek, N. S. (2021). An Assessment of Active Disturbance Rejection Technique From a Theoretical Perspective. *European Journal of Science and Technology*, (29), 284–291. https://doi.org/10.31590/ejosat.1024241

Eker, D., Özbek, N. S., & Çelik, Ö. (2022). An Alternative Approach of Disturbance Rejection Control Methodology to DC-DC Boost Converte. *European Journal of Science and Technology Special Issue*, (37), 108–112. https://doi.org/10.31590/ejosat

Eker, İ. (2004). Experimental on-line identification of an electromechanical system. *ISA Transactions*, *43*, 13–32.

Feng, H., & Guo, B. Z. (2017). Active disturbance rejection control: Old and new results. *Annual Reviews in Control*, *44*, 238–248. https://doi.org/10.1016/j.arcontrol.2017.05.003

Fu, C., & Tan, W. (2020). Parameters Tuning of Reduced-Order Active Disturbance Rejection Control. *IEEE Access*, *8*, 72528–72536. https://doi.org/10.1109/ACCESS.2020.2987398

Fu, C., & Tan, W. (2021). Analysis and tuning of reduced-order active disturbance rejection control. *Journal of the Franklin Institute*, *358*(1), 339–362. https://doi.org/10.1016/j.jfranklin.2020.10.017

Gao, Z. (2003). Scaling and Bandwidth-Parameterization Based Controller Tuning. *Proceedings of the 2003 American Control Conference*, 4989–4996. Denver, CO, USA: IEEE. https://doi.org/10.1109/ACC.2003.1242516

Han, J. (2009). From PID to active disturbance rejection control. *IEEE Transactions on Industrial Electronics*, *56*(3), 900–906. https://doi.org/10.1109/TIE.2008.2011621

Herbst, G. (2013). A simulative study on active disturbance rejection control (ADRC) as a control tool for practitioners. *Electronics* , *2*(3), 246–279. https://doi.org/10.3390/electronics2030246

Kara, T., & Eker, I. (2004). Nonlinear modeling and identification of a DC motor for bidirectional operation with real time experiments. *Energy Conversion and Management*, *45*(7–8), 1087–1106. https://doi.org/10.1016/j.enconman.2003.08.005

Li, A., Ye, L., Yanqing, J., Yueming, L., Jian, C., & Jiayu, H. (2019). Soft-Switching Proximate Time Optimal Heading Control for Underactuated Autonomous Underwater Vehicle. *IEEE Access*, *7*, 143233–143249. https://doi.org/10.1109/ACCESS.2019.2945162

Li, R., Li, T., Li, X., & Shen, H. (2016). Path following for underactuated ships control and simulation based on active disturbance rejection with sliding mode control. *ICIC Express Letters*, *10*(6), 1415–1420.

Li, S., Yang, J., Chen, W.-H., & Xisong, C. (2014). *Disturbance Observer-Based Control Methods and Applications*. CRC Press.

Li, X. A., Sun, K., Guo, C., & Liu, H. (2021). Hybrid adaptive disturbance rejection control for inflatable robotic arms. *ISA Transactions*. https://doi.org/10.1016/j.isatra.2021.08.016

Li, Z., Guan, X., Li, Y., & Xu, C. (2020). Fuzzy Active Disturbance Rejection Control for Direct Driven Exoskeleton of Swing Leg. *2020 5th International Conference on Advanced Robotics and Mechatronics (ICARM))*, 234–239.

Madonski, R., Herbst, G., & Stankovic, M. (2023). ADRC in output and error form: connection, equivalence, performance. *Control Theory and Technology*. https://doi.org/10.1007/s11768-023-00129-y

Ouyang, Q., Fan, K., Liu, Y., & Li, N. (2021). Adaptive LADRC Parameter Optimization in Magnetic Levitation. *IEEE Access*, *9*, 36791–36801. https://doi.org/10.1109/ACCESS.2021.3062797

Özbek, N. S. (2018). *Control of Time-Delayed Systems with Experimental Applications* (PhD). Çukurova University, Adana.

Ozbek, N. S., & Eker, I. (2015). An interactive computer-aided instructional strategy and assessment methods for system identification and adaptive control laboratory. *IEEE Transactions on Education*, *58*(4), 297–302. https://doi.org/10.1109/TE.2015.2412512

Pacheco, C., Duarte-Mermoud, M. A., Aguila-Camacho, N., & Castro-Linares, R. (2017). Fractional-order state observers for integer-order linear systems. *Journal of Applied Nonlinear Dynamics*, *6*(2), 251–264. https://doi.org/10.5890/JAND.2017.06.010

Pu, C., Ren, J., & Su, J. (2019). The sliding mode control of the drum water level based on extended state observer. *IEEE Access*, *7*, 135942–135948. https://doi.org/10.1109/ACCESS.2019.2940056

Qiu, Z., Xiao, J., & Wang, S. (2015). Active-disturbance rejection control based on a novel sliding mode observer for PMSM speed and rotor position. *Journal of Vibroengineering*, *17*(8), 4603–4617.

Qu, L., Qiao, W., & Qu, L. (2021). Active-Disturbance-Rejection-Based Sliding-Mode Current Control for Permanent-Magnet Synchronous Motors. *IEEE Transactions on Power Electronics*, *36*(1), 751–760.

She, J. H., Fang, M., Ohyama, Y., Hashimoto, H., & Wu, M. (2008). Improving disturbance-rejection performance based on an equivalent-input-disturbance approach. *IEEE Transactions on Industrial Electronics*, *55*(1), 380–389. https://doi.org/10.1109/TIE.2007.905976

She, J. H., Xin, X., & Pan, Y. (2011). Equivalent-input-disturbance approachanalysis and application to disturbance rejection in dual-stage feed drive control system. *IEEE/ASME*

Transactions on Mechatronics, *16*(2), 330–340. https://doi.org/10.1109/TMECH.2010.2043258

Shi, H., Li, R., Bai, X., Zhang, Y., Min, L., Wang, D., … Lei, Y. (2023). A review for control theory and condition monitoring on construction robots. *Journal of Field Robotics*, *40*(4), 934–954. https://doi.org/10.1002/rob.22156

Tan, W., & Fu, C. (2016). Linear Active Disturbance-Rejection Control: Analysis and Tuning via IMC. *IEEE Transactions on Industrial Electronics*, *63*(4), 2350–2359. https://doi.org/10.1109/TIE.2015.2505668

Wang, R., Wang, S., Wang, Y., Tang, C., & Tan, M. (2018). Three-Dimensional Helical Path Following of an Underwater Biomimetic Vehicle-Manipulator System. *IEEE Journal of Oceanic Engineering*, *43*(2), 391–401. https://doi.org/10.1109/JOE.2017.2762498

Wang, Y. W., Zhang, W. A., Dong, H., & Yu, L. (2020). A LADRC based fuzzy PID approach to contour error control of networked motion control system with time-varying delays. *Asian Journal of Control*, *22*(5), 1973–1985. https://doi.org/10.1002/asjc.2080

Wang, Z., & Zhao, T. (2022). Adaptive-based linear active disturbance rejection attitude control for quadrotor with external disturbances. *Transactions of the Institute of Measurement and Control*, *44*(2), 286–298. https://doi.org/10.1177/01423312211031781

Zhang, B., Tan, W., & Li, J. (2020). Tuning of Smith predictor based generalized ADRC for time-delayed processes via IMC. *ISA Transactions*, *99*, 159–166. https://doi.org/10.1016/j.isatra.2019.11.002

Zhang, H. (2017). *Information Driven Control Design: A Case for PMSM Control* (Cleveland State University). Cleveland State University. Retrieved from https://engagedscholarship.csuohio.edu/etdarchivehttps://engagedscholarship.csuohio.edu/etdarchive/1026

Zhang, X., Hou, B., & Mei, Y. (2017). Deadbeat Predictive Current Control of Permanent-Magnet Synchronous Motors with Stator Current and Disturbance Observer. *IEEE Transactions on Power Electronics*, *32*(5), 3818–3834. https://doi.org/10.1109/TPEL.2016.2592534

Zhang, Z., Yang, Z., Zhou, G., Liu, S., Zhou, D., Chen, S., & Zhang, X. (2021). Adaptive fuzzy active-disturbance rejection control-based reconfiguration controller design for aircraft anti-skid braking system. *Actuators*, *10*(8). https://doi.org/10.3390/act10080201

Zhou, R., Fu, C., & Tan, W. (2021). Implementation of linear controllers via active disturbance rejection control structure. *IEEE Transactions on Industrial Electronics*, *68*(7), 6217–6226. https://doi.org/10.1109/TIE.2020.2992951

Zhou, R., & Tan, W. (2015). A Generalized Active Disturbance Rejection Control Approach for Linear Systems. *IEEE 10th Conference on Industrial Electronics and Applicatons*, 248–255.

Zhou, Xiangyang, Wang, T., & Diallo, D. (2022). An active disturbance rejection sensorless control strategy based on sliding mode observer for marine current turbine. *ISA Transactions*, *124*, 403–410. https://doi.org/10.1016/j.isatra.2020.05.027

Zhou, Xuesong, Cui, Y., & Ma, Y. (2021). Fuzzy Linear Active Disturbance Rejection Control of Injection Hybrid Active Power Filter for Medium and High Voltage Distribution Network. *IEEE Access*, *9*, 8421–8432. https://doi.org/10.1109/ACCESS.2021.3049832

APPENDIX

Appendix A: Control Bandwidth Coefficient

The desired transfer function for LADRC denoted as:

$$G_{cl}(s) = \frac{{w_C}^2}{(s + w_C)^2} \quad \text{(A 1.1)}$$

where w_c is denoted as control bandwidth. If step signal is applied to the closed loop transfer function and expand with partial fraction expansion:

$$Y(s) = \frac{{w_C}^2}{s(s + w_C)^2} = \frac{1}{s} - \frac{{w_C}^2}{(s + w_C)^2} - \frac{1}{s + w_C} \quad \text{(A 1.2)}$$

Using the inverse laplace transform of $Y(s)$:

$$y(t) = 1 - w_C t e^{-w_C t} - e^{-w_C t} = 1 - (1 + w_C t)e^{-w_C t} \quad \text{(A 1.3)}$$

At the infinity, the output of the system is expected to become unity. So, the differemce the output at a particular time and the output at the infinity can be decided 2%:

$$|y(t_s) - y(\infty)| = 0.02 \quad \text{(A 1.4)}$$

where $y(\infty) = 1$. Using the equation A 1.3:

$$(1 + w_C t_s)e^{-w_C t_s} = 0.02 \quad \text{(A 1.5)}$$

Let $w_C t_s = k$ then taking the logarithm:

$$(1+k)e^{-k} = 0.02 \quad \text{(A 1.6.a)}$$

$$\log(1+k) - k\log e = \log 0.02 \quad \text{(A 1.6.b)}$$

$$\log(1+k) - 0.43k = -1.69 \quad \text{(A 1.6.c)}$$

When the equation above is solved for k, two values can be obtained, which equals to 5.82 and -0.9. Positive value should be taken into account then:

$$w_C t_s = 5.82 \quad \text{(A 1.7.a)}$$

$$w_C = \frac{5.82}{t_s} \approx \frac{6}{t_s} \quad \text{(A 1.7.b)}$$

Appendix B: Linear ADRC with IMC Proof

The control signal of the aforementioned method equals:

$$U(s) = \frac{Q}{1 - P_0 Q Q_d} R(s) - \frac{Q Q_d}{1 - P_0 Q Q_d} Y(s) \quad \text{(B 1.1)}$$

It can be seen that the equation above possesses a resemblence with control signal which contains $C_1(s)$, $C_2(s)$ and $F_r(s)$. So, this can be eqaulized with equation (3.54) and expected to satisfied the following:

$$C_1(s)F_r(s) = \frac{Q}{1 - P_0 Q Q_d}$$
$$C_2(s) = \frac{Q Q_d}{1 - P_0 Q Q_d} \quad \text{(B 1.2)}$$

It should be extracted Q and Q_d from the equation above for the simplification. For Q_d:

$$\frac{C_2(s)}{Q_d} = C_1(s)F_r(s) = \frac{Q}{1 - P_0 Q Q_d}$$
$$C_2(s) = C_1(s)F_r(s)Q_d \quad \text{(B 1.3)}$$

Then disturbance rejection IMC controller can be concluded that:

$$Q_d = \frac{C_2(s)}{C_1(s)F_r(s)} \quad \text{(B 1.4)}$$

The next step is to determine the setpoint tracking IMC controller. With the usage of Q_d term:

$$C_2(s) = \frac{Q\dfrac{C_2(s)}{C_1(s)F_r(s)}}{1 - P_0 Q\dfrac{C_2(s)}{C_1(s)F_r(s)}} = \frac{QC_2(s)}{C_1(s)F_r(s) - P_0 Q C_2(s)} \quad \text{(B 1.5)}$$

Then, after the simplification of the equation above leads to:

$$Q = C_1(s)F_r(s) - P_0 Q C_2(s) \quad \text{(B 1.6)}$$

Taking the term starts with P_0 to the left hand side and taking the common paranthesis brings about:

$$Q(1 + P_0 C_2(s)) = C_1(s)F_r(s)$$
$$Q = \frac{C_1(s)F_r(s)}{1 + P_0 C_2(s)} \quad \text{(B 1.7)}$$

By using the P_0, C_1 and C_2 defined in (3.54) and substitute them into derived representation of IMC controller parameters, it is obvious to prove that the both controller have the form stated in (3.56)